Scanning Tunneling Microscopy

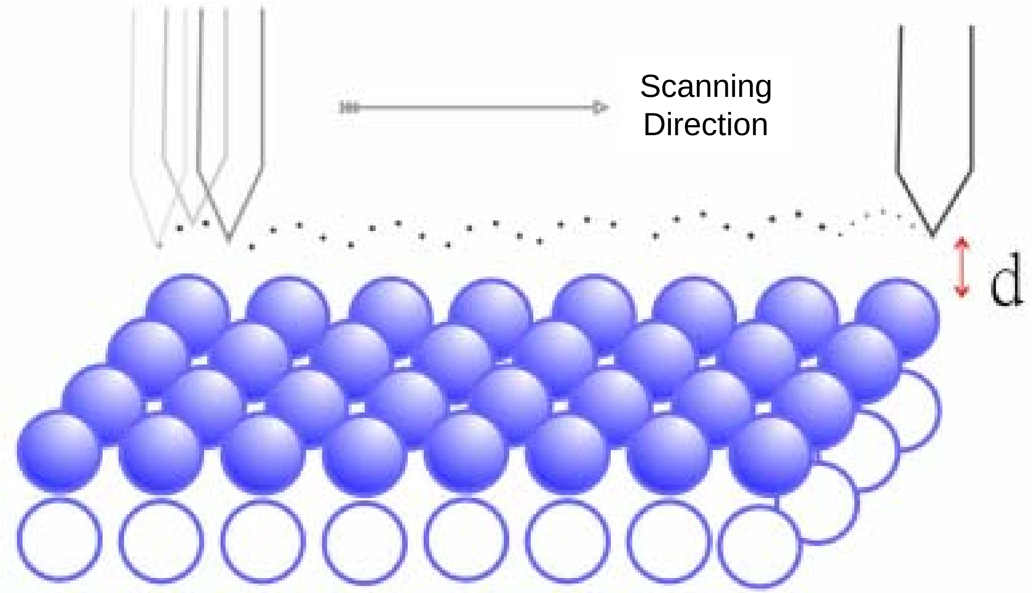

References:

1. G. Binnig, H. Rohrer, C. Gerber and Weibel, Phys. Rev. Lett. **49**, 57(1982); and ibid **50**,120(1983).
2. J. Chen, *Introduction to Scanning Tunneling Microscopy*, New York, Oxford Univ. Press(1993).

Concept: Eye and Finger

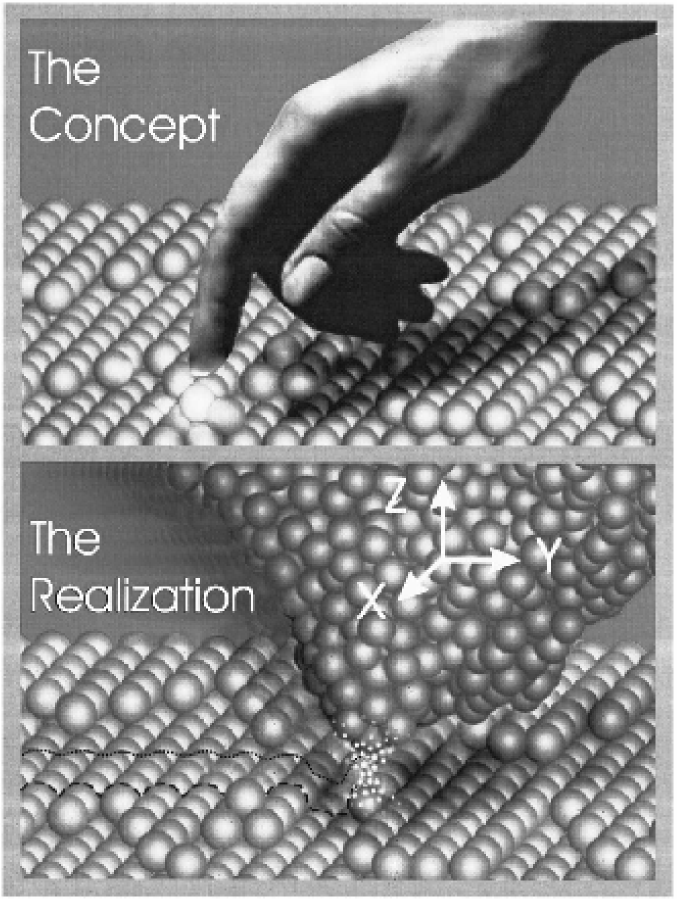

G. Binnig and and H. Rohrer, *Rev. of Mod. Phys.* **71**, S324-S330 (1999).

Theory of STM

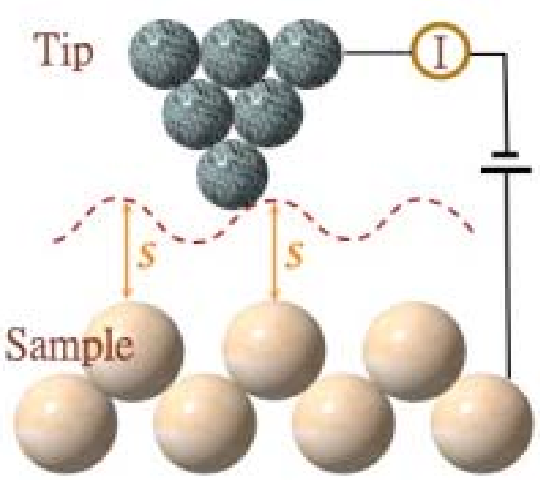

Constant Current Mode

Tunneling

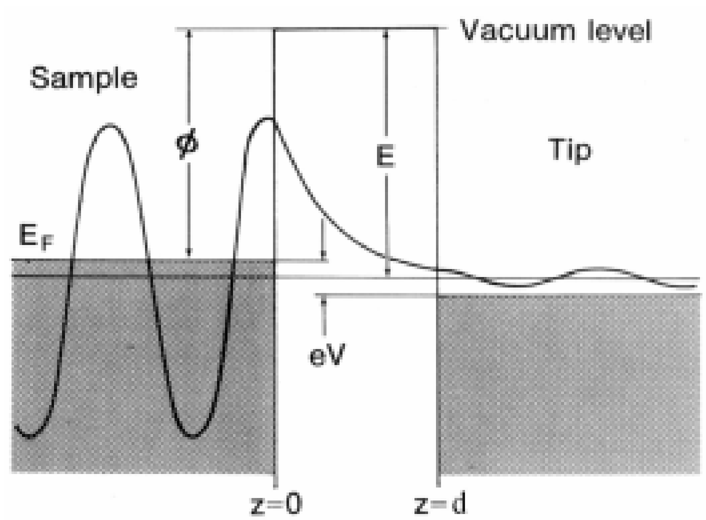

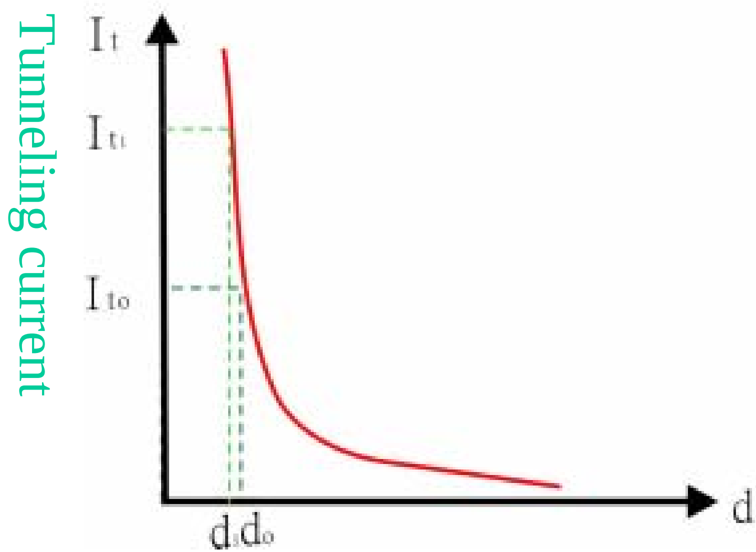

Tunneling current I_t

$I_t \propto (V/d)\exp(-A\phi^{1/2}d)$

$A = 1.025\ (\mathrm{eV})^{-1/2}\mathrm{Å}^{-1}$

$\phi \sim 4 - 5$ eV

d decreases by 1 Å,

I_t will be increased by ~10 times.

Schematics of STM

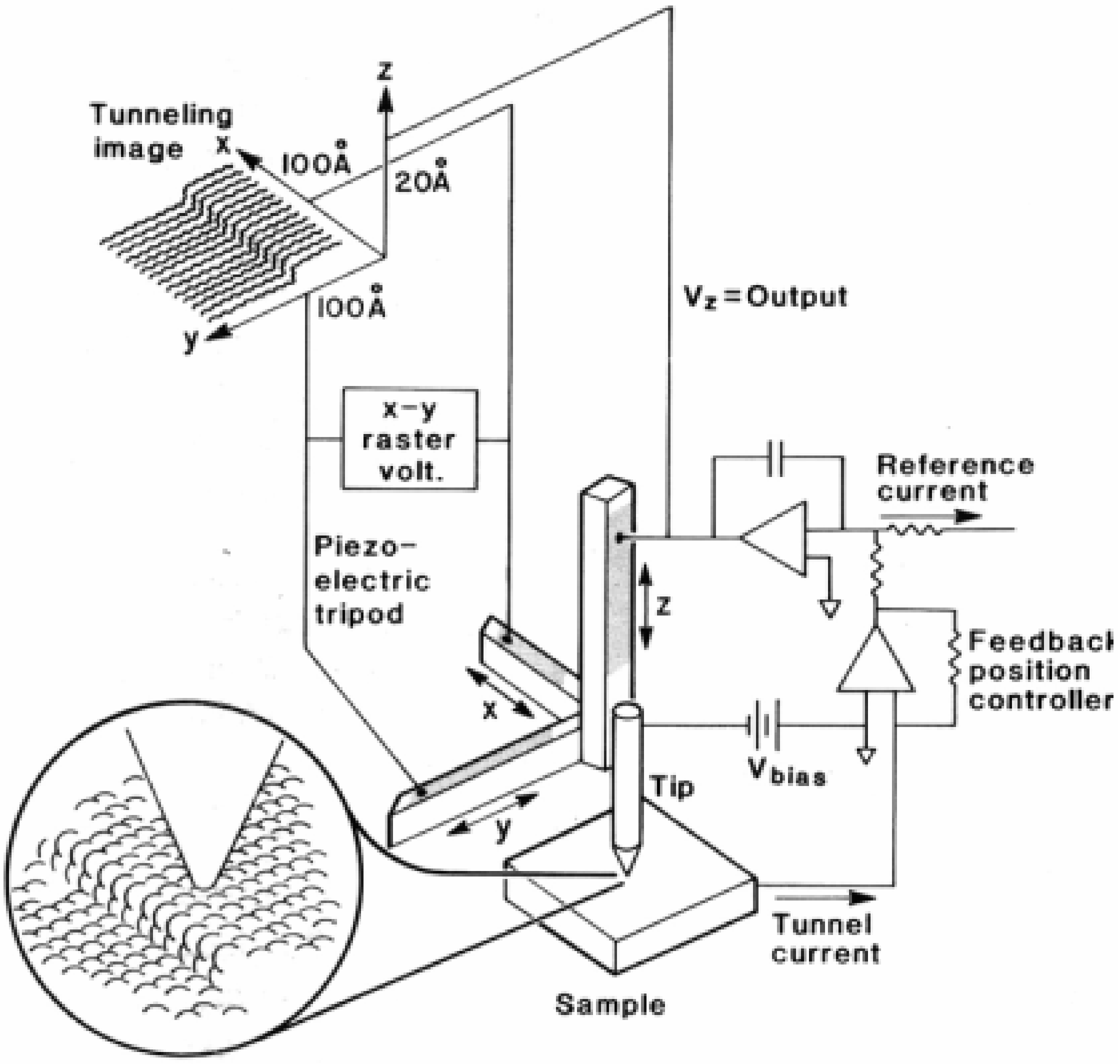

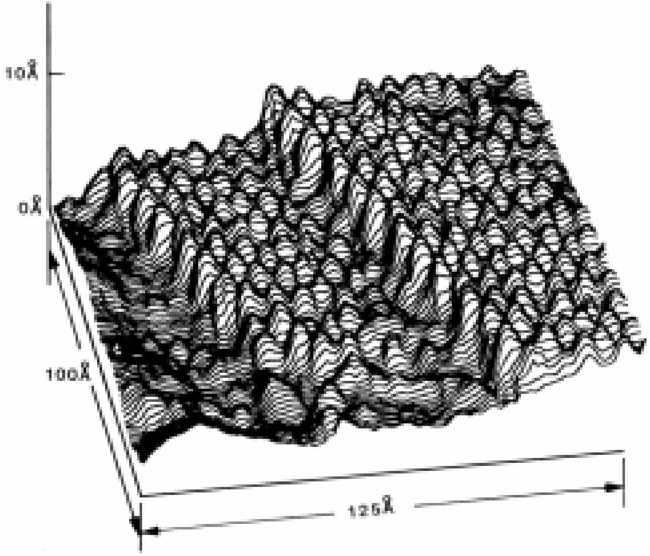

Piezoelectric Scanner

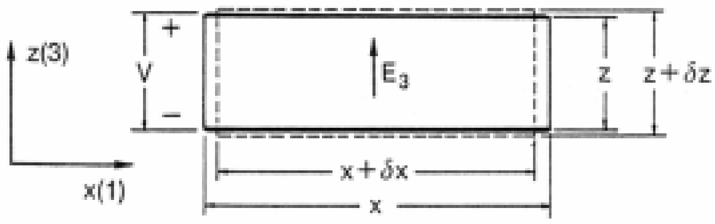

Strain: $S_1 = \delta x/x$, $S3 = \delta z/z$

Electric field: $E_3 = V/z$

Piezoelectric Coeff.: $d_{33} = S_3/E_3$, $d_{31} = S_1/E_3$

Variation of piezoelectric coefficient with temperature.

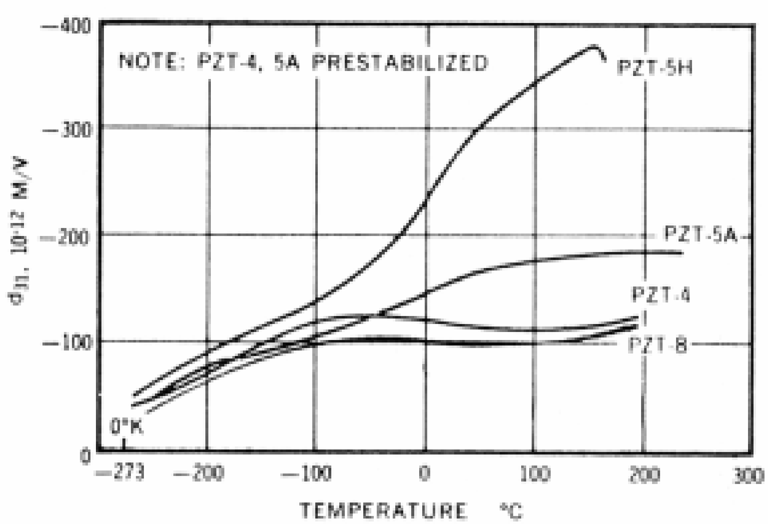

Tripod scanner

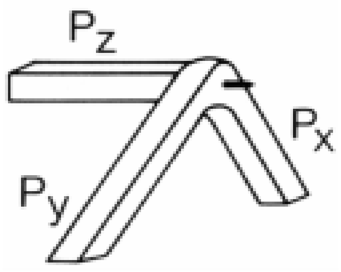

Tube scanner

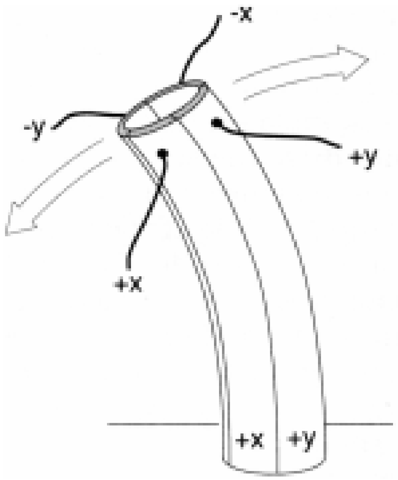

STM electronics and control

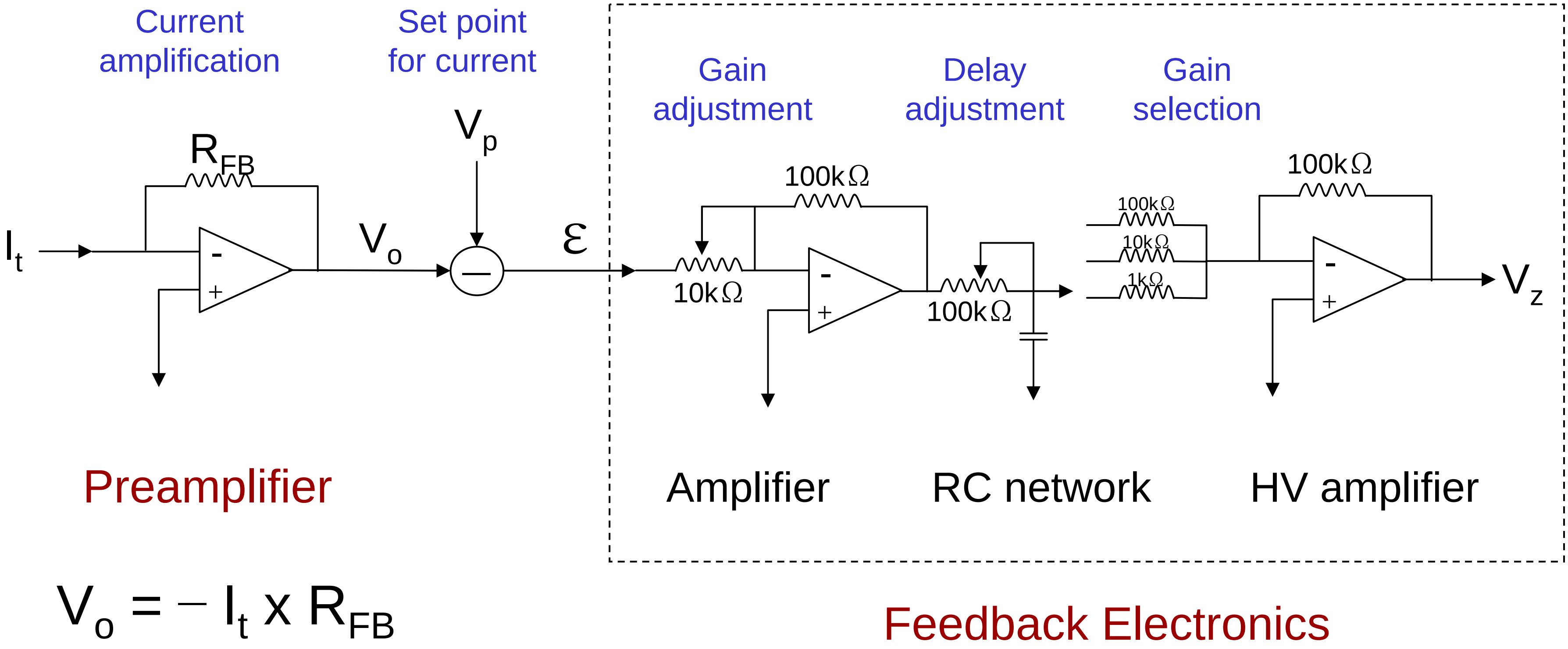

$$V_o = -I_t \times R_{FB}$$

$$R_{FB} = 100\ M\Omega$$

Ultra-High Vacuum Scanning Tunneling Microscope

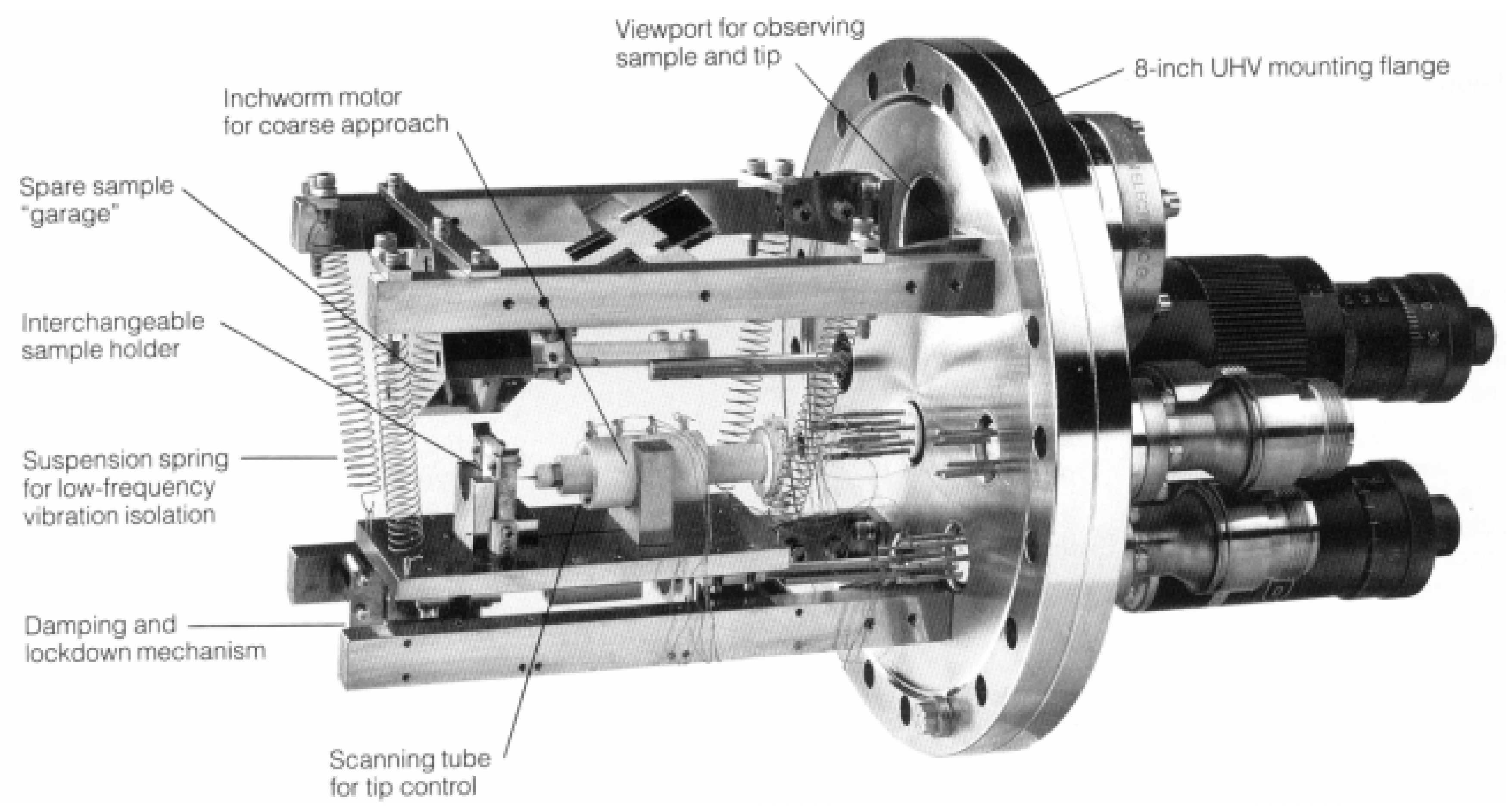

Atomic Structure of the Pt(001) Surface

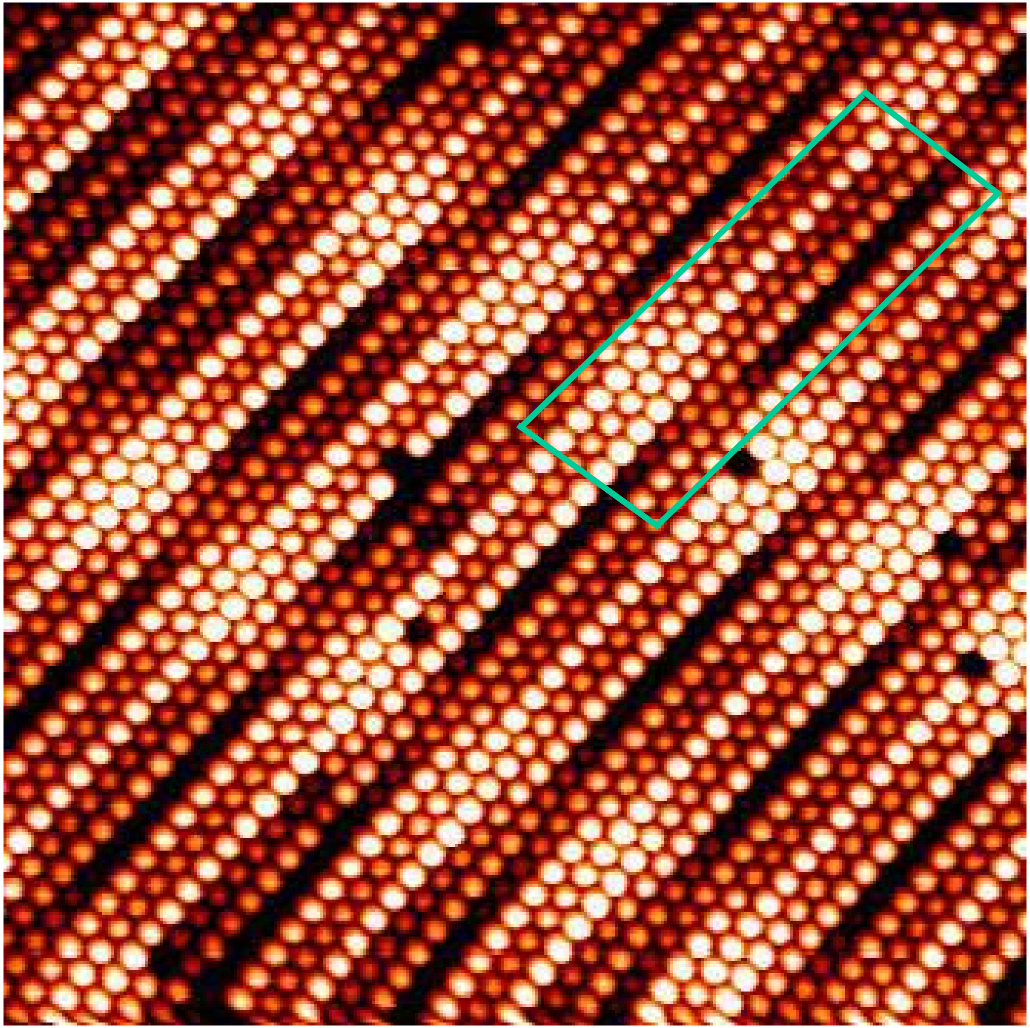

Surface Science **306**, 10 (1994).

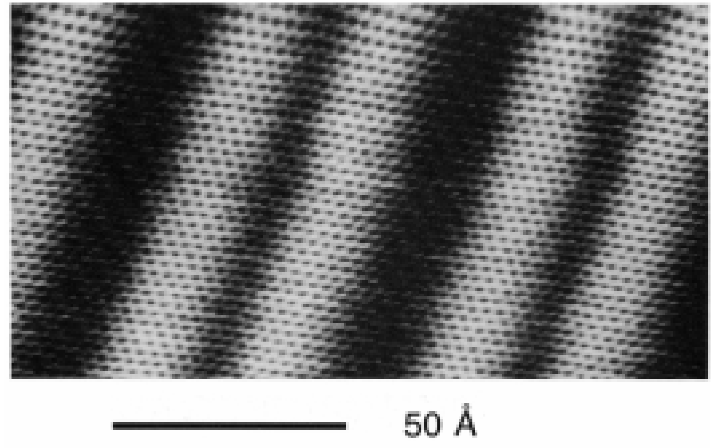

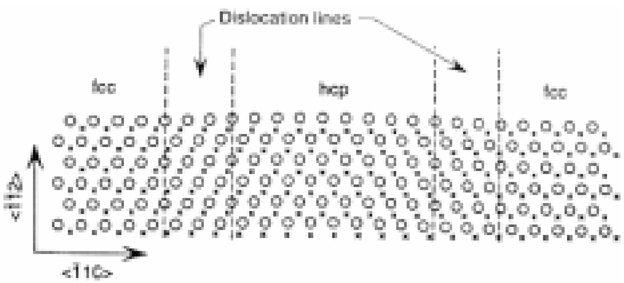

Fig. 1. In-plane structure of the Au(111) surface with a $22 \times \sqrt{3}$ reconstruction. The circles and crosses correspond to atoms in the first and second surface layers, respectively. Surface atoms in both sides of the figure lie on fcc sites, whereas atoms in the center of the figure lie on hcp sites. The domain walls (dislocation lines) involve atoms in bridge sites.

Large-scale image of the Au(111)-$22\times\sqrt{3}$ reconstruction. The Au(111) surface reconstructs at room temperature to form a $22\times\sqrt{3}$ structure, which has a two-fold symmetry. On a large scale, three equivalent orientations for this reconstruction coexist on the surface. Furthermore, on an intermediate scale, a herring-bone pattern is formed.

Science 258, 1763 (1992).

STM Images of Si(111)-(7×7)

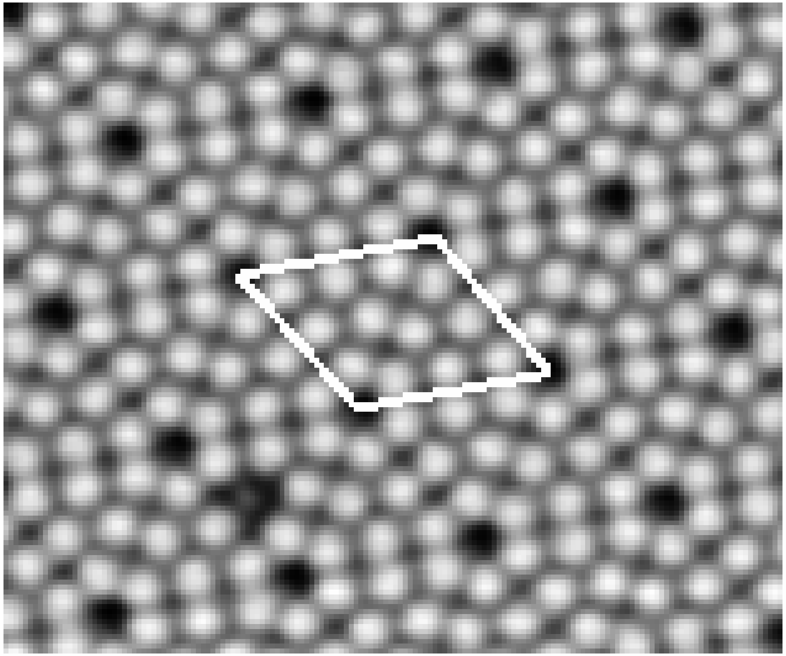

Empty-state image

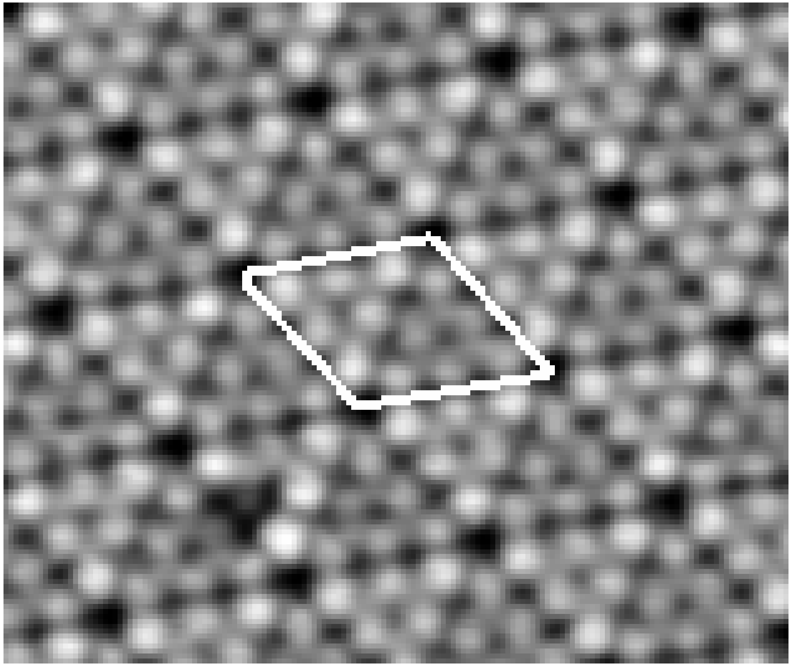

Filled-state image

Atomic Model of Si(111)-(7×7)

Top view

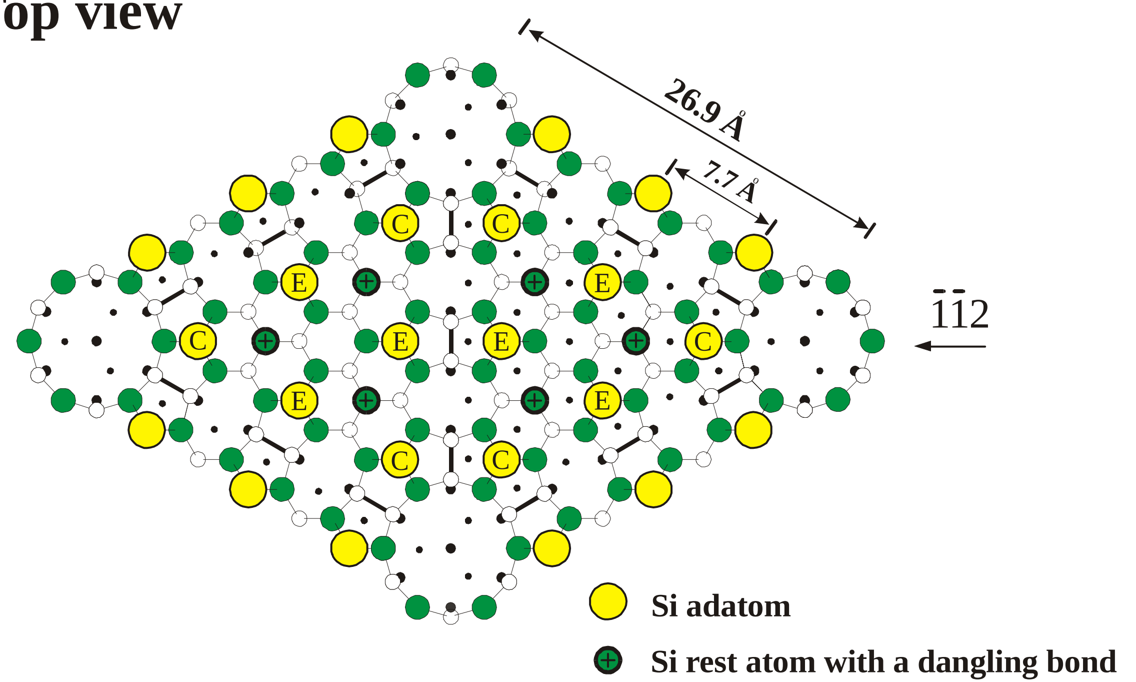

Side view

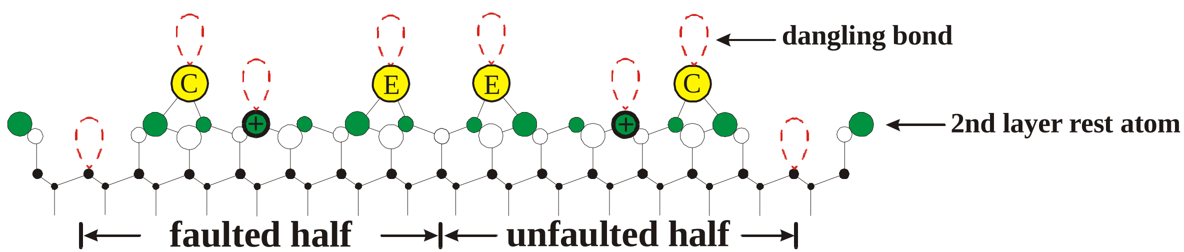

Si(111)-(7x7)

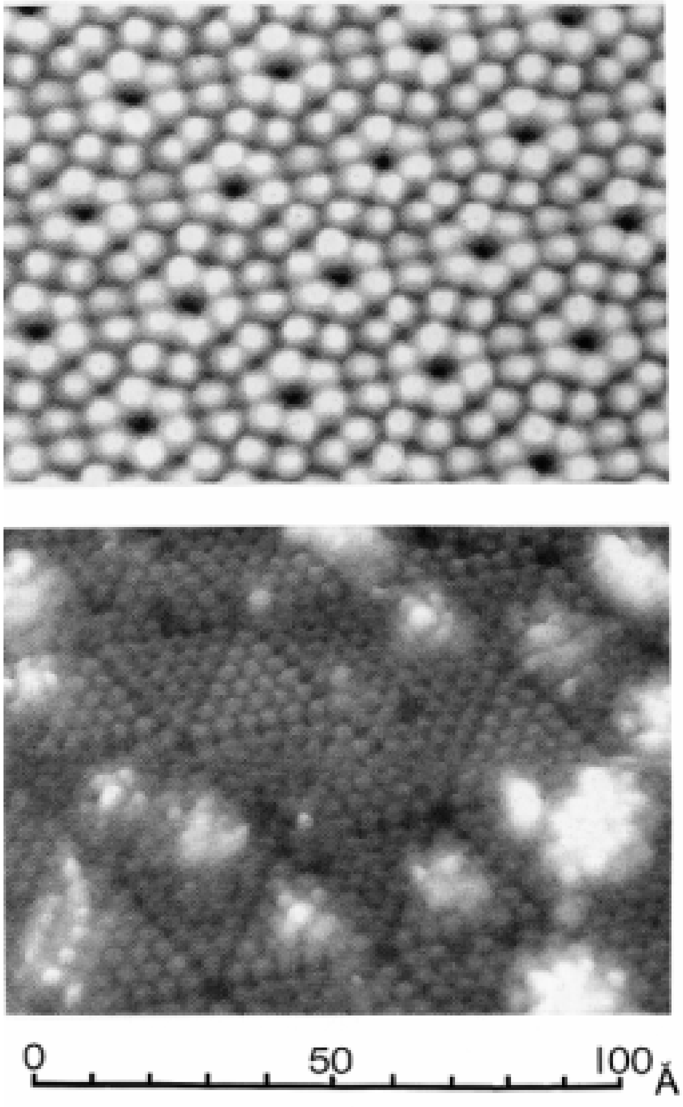

Si(111)-2x1

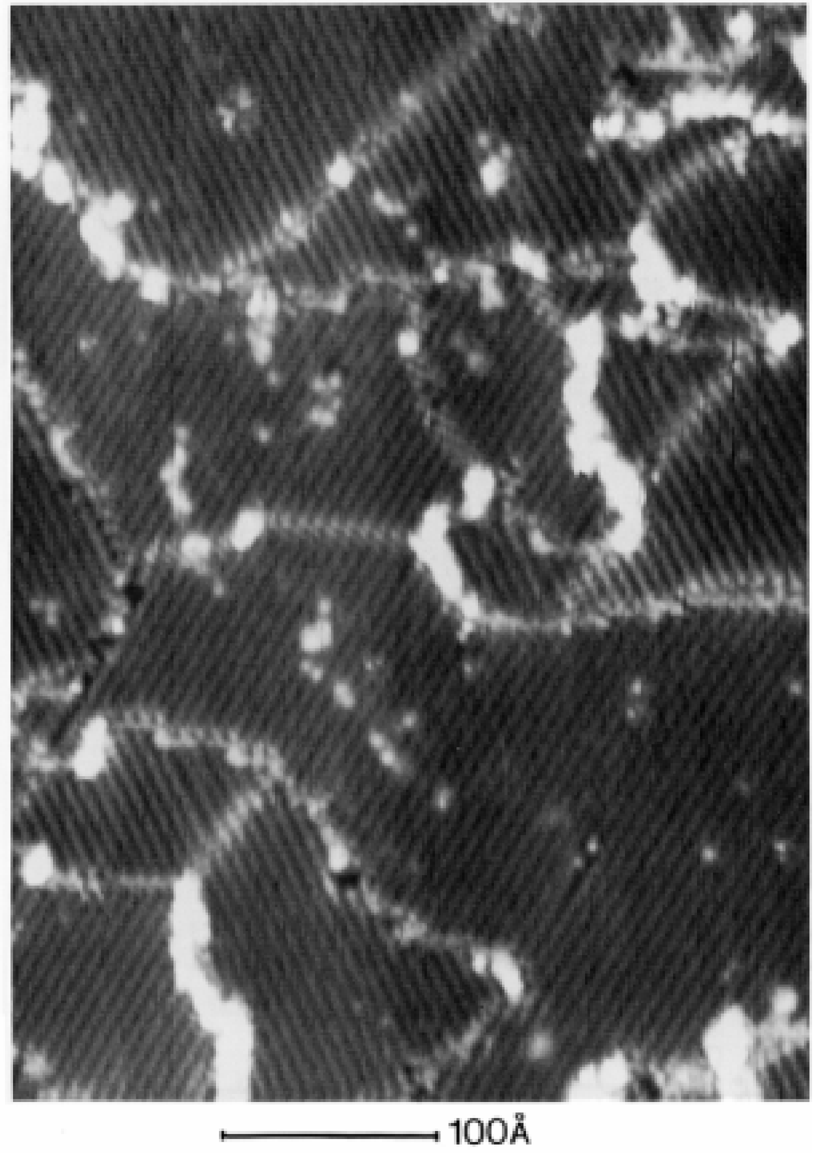

Atomic Structure of the Si(001) Surface

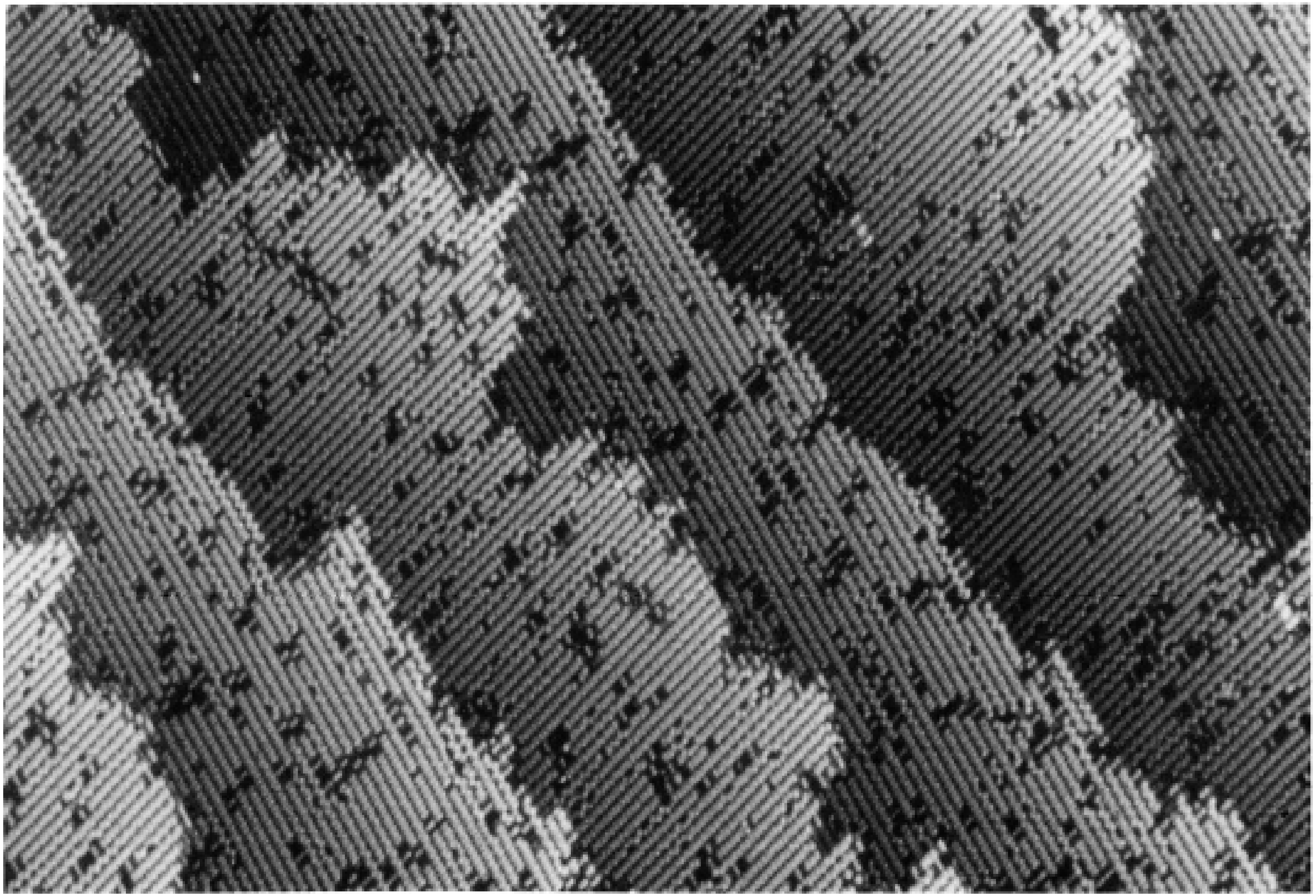

Si(001)-2x1 and 1x2

Si(001)-c(4x2)

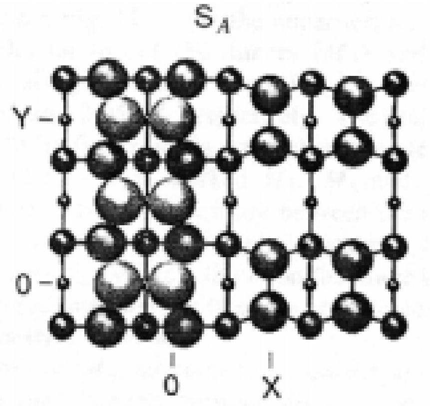

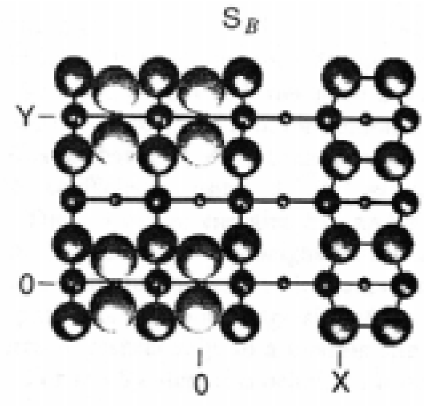

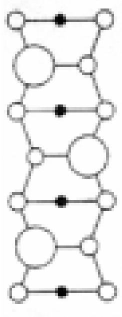

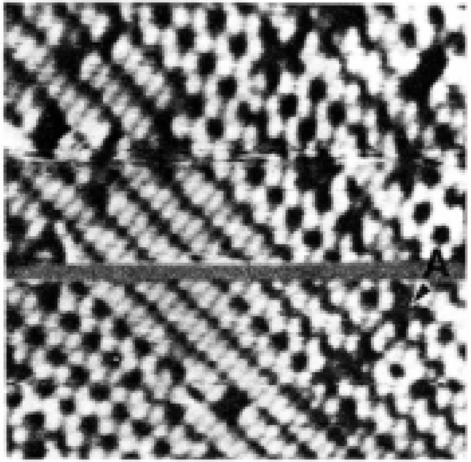

Si(111)-(2x1)

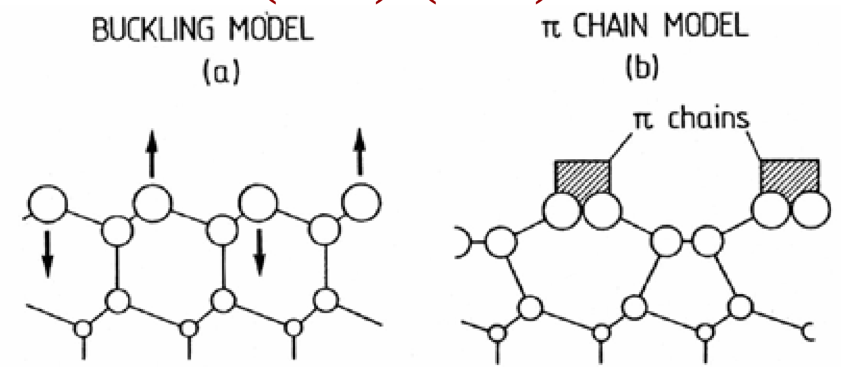

Atomic Structure of the Ge(111) Surface

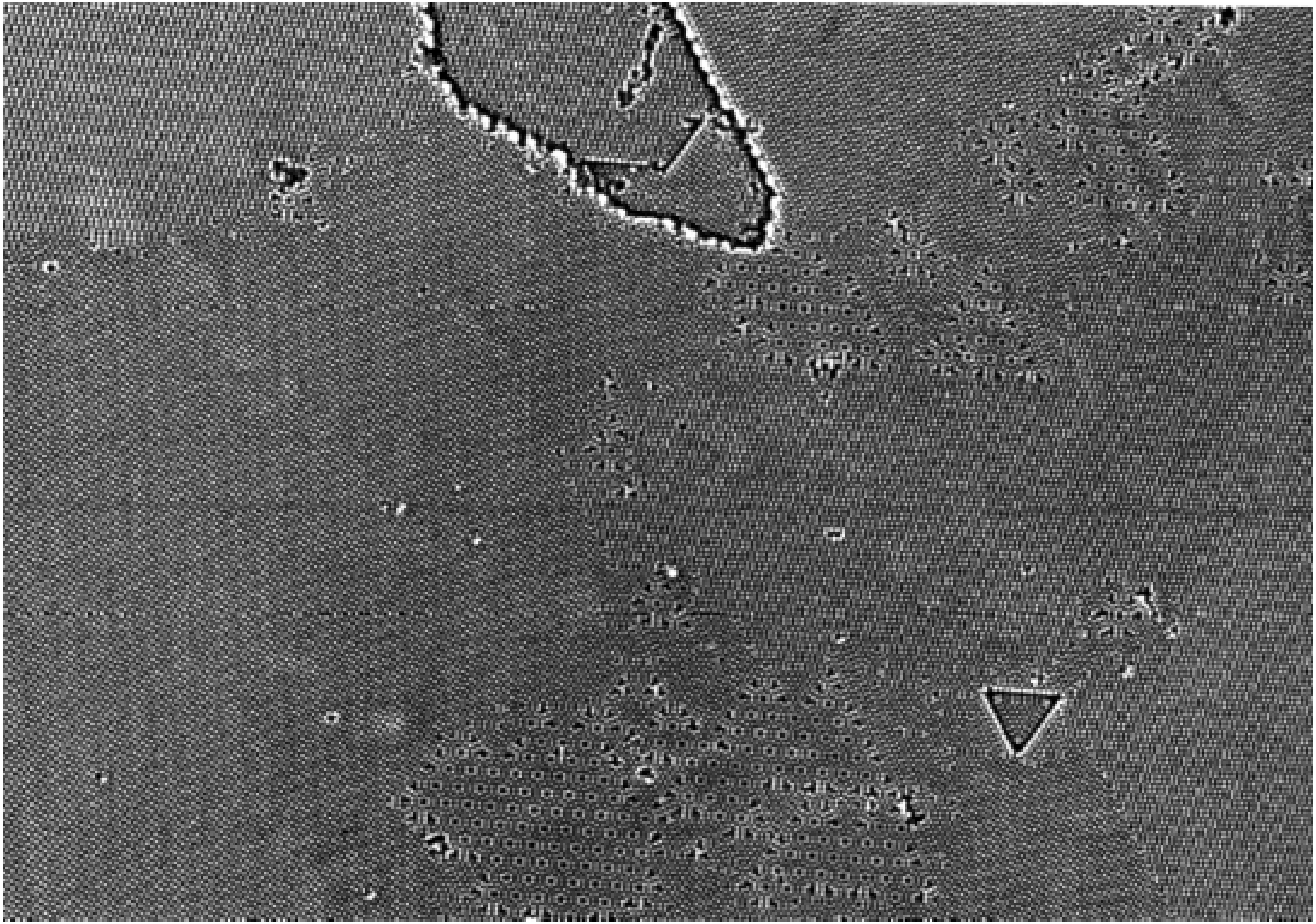

Site Hopping of O_2 on Si(111)-7x7

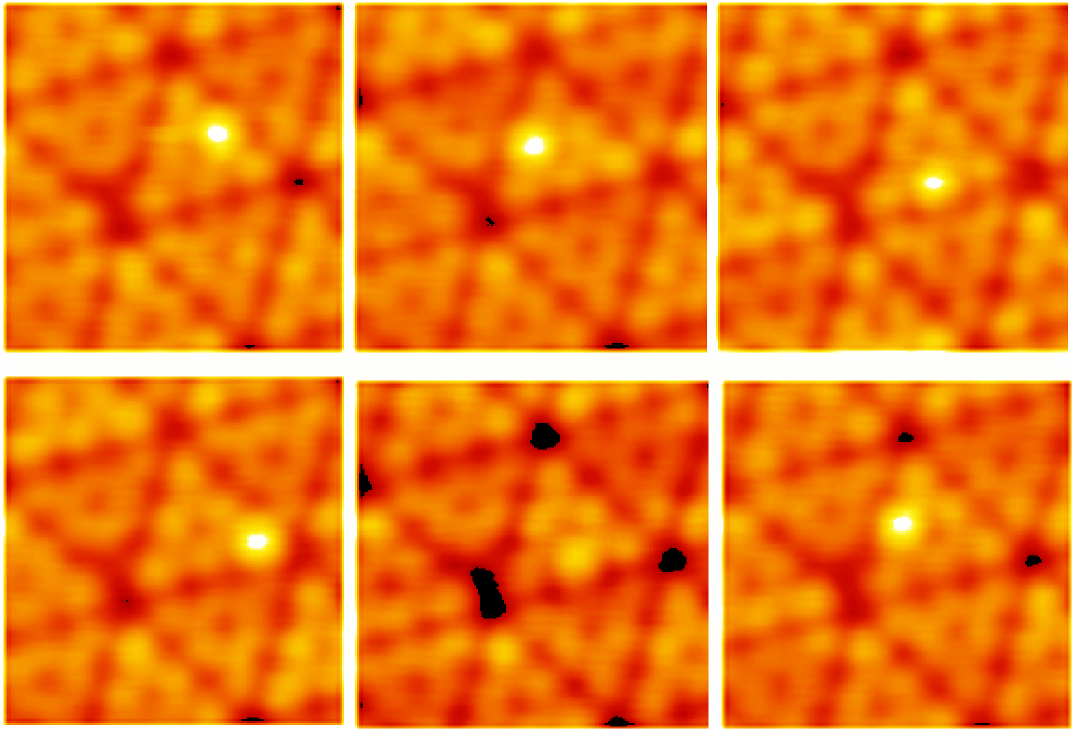

O_2 molecule starts to hop between neighboring adatom sites at temperature about 300ºC.

1. I.-S. Hwang, R.-L. Lo, and T.T. Tsong, Physical Review Letters **78**, 4797 (1997).
2. I.-S. Hwang, R.-L. Lo, and T.T. Tsong, Surface Science **399**, 173 (1998).

Site Hopping of O_2 Molecule on Si(111)-(7x7)

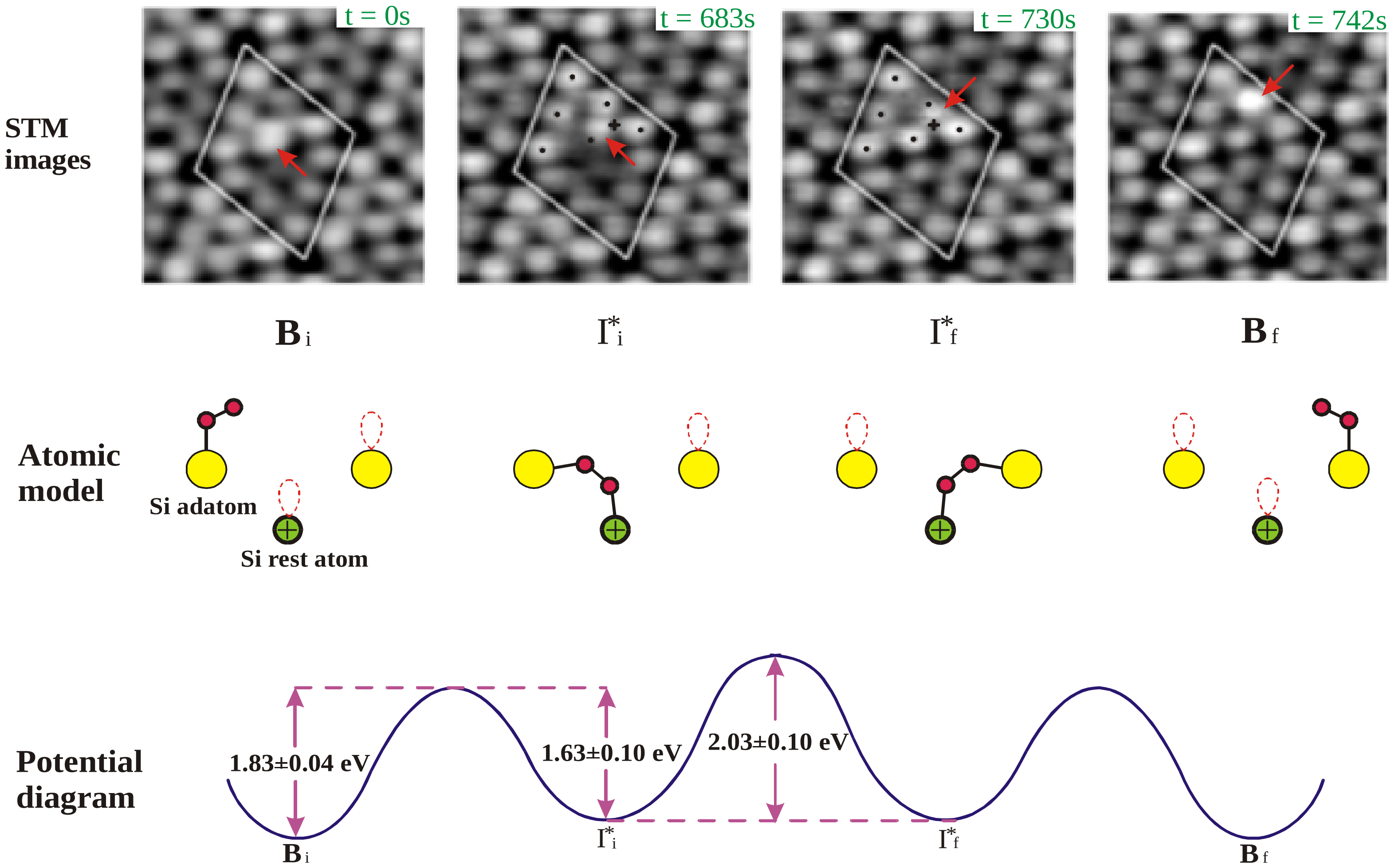

Tunneling current

$$I_{T\to S} = \frac{2\pi e}{\hbar}\sum_{\mu\nu} f(E_\mu)[1 - f(E_\nu + eV)]|M_{\mu\nu}|^2 \delta(E_\mu - E_\nu - eV)$$

where $f(E)$ is Fermi function

E_μ is the energy of state μ ,where μ and ν run over all the states of the tip and surface , respectively.

$M_{\mu\nu}$ is tunneling matrix element

$$M_{\mu\nu} \equiv \frac{\hbar^2}{2m}\int d\vec{s}\left(\psi_\mu^* \nabla \psi_\nu - \psi_\nu \nabla \psi_\mu^*\right)$$

where ψ_μ is the wave function, and the integral is over any plane in the barrier region.

$$I = I_{T\to S} - I_{S\to T}$$

$$= A'\int_{-\infty}^{\infty} \rho_T(E)\rho_S(E+eV)|M(E)|^2 [f(E) - f(E+eV)]dE$$

where ρ_S and ρ_T are the densities of states in the sample and the tip, respectively.

Tunneling current

$$I \equiv A' \int_{-\infty}^{\infty} \rho_T(E)\rho_S(E+eV)|M(E)|^2[f(E)-f(E+eV)]dE$$

Transmission probability of the electron

$$M(E) = \exp\left[-A\phi^{\frac{1}{2}}S\right]$$

Usually, we assume ρ_T is featureless (ie. $\rho_T \approx const.$), and the sample electronics states dominate the tunnel spectra.

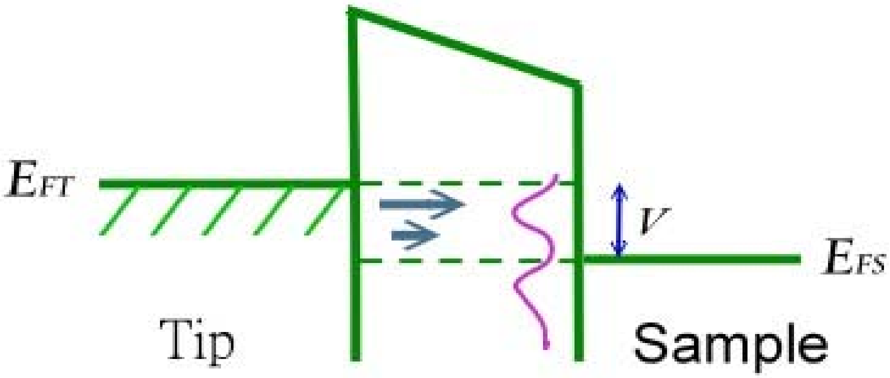

However, the tips might have effect on the tunnel spectra, if

1. we have atomically sharp tips ,or
2. the tip has picked up a foreign atom.

Case Ⅰ -----metals

In the low-voltage limit

$$I \propto V\rho_S(\tilde{r}_t;E_F)\rho_t(E_F)$$

where $\rho_S(\tilde{r}_t;E_F)$ is the surface density of states of the sample at the center of the tip($\tilde{r}_t$),

$$\rho_S(\tilde{r};E) \equiv \sum_\nu |\psi_\nu(\tilde{r})|^2 \delta(E_\nu - E)$$

$\rho_t(E_F)$ is the density of states of the tip at the Fermi level and is often regarded as a constant.

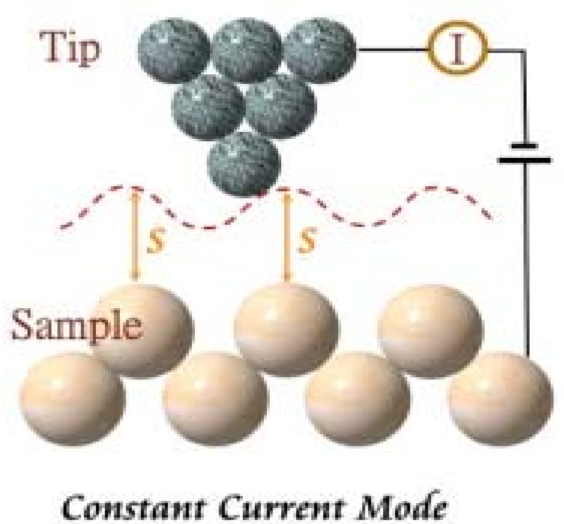

Electronic Structures at Surfaces

Not Tunneling

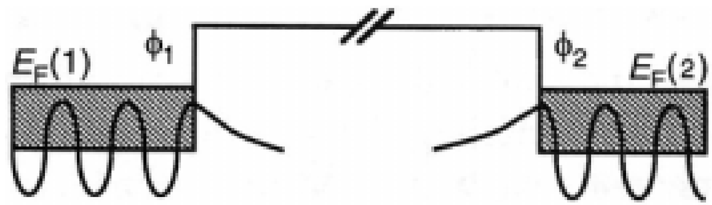

Empty-State Imaging

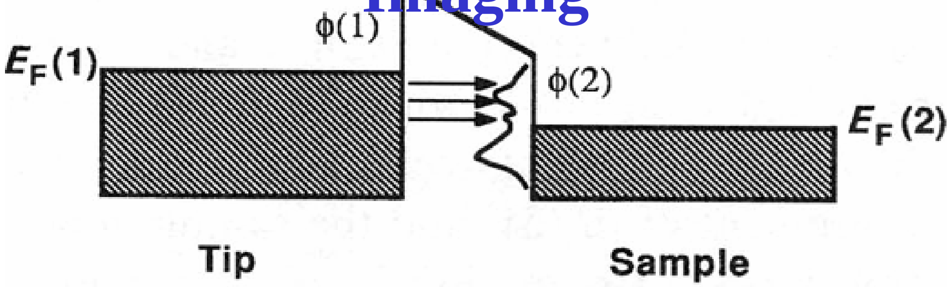

Tunneling

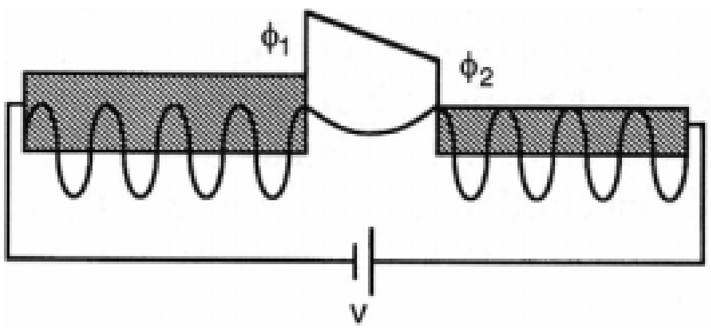

Filled-State Imaging

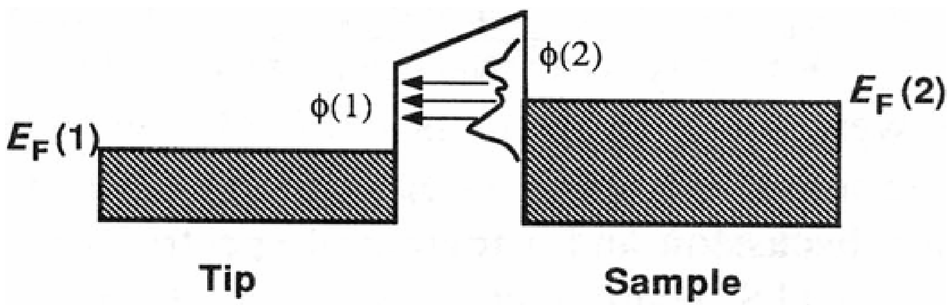

Surface States at Cu(111)

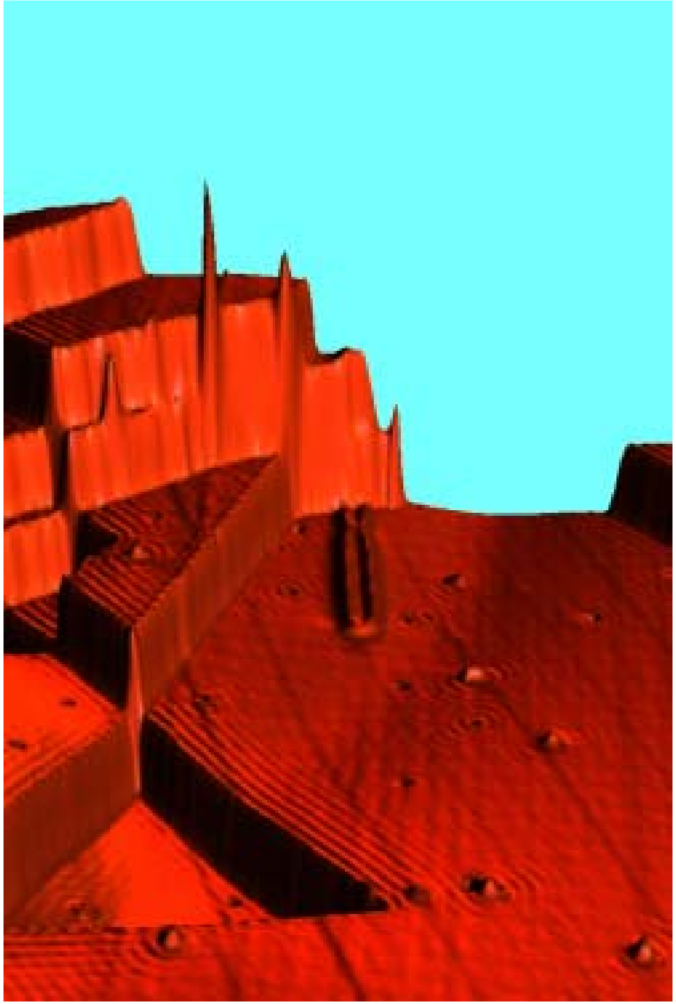

Nature **363**, 524 (1993).

Example -----Semiconductor

1.Tip-negativ

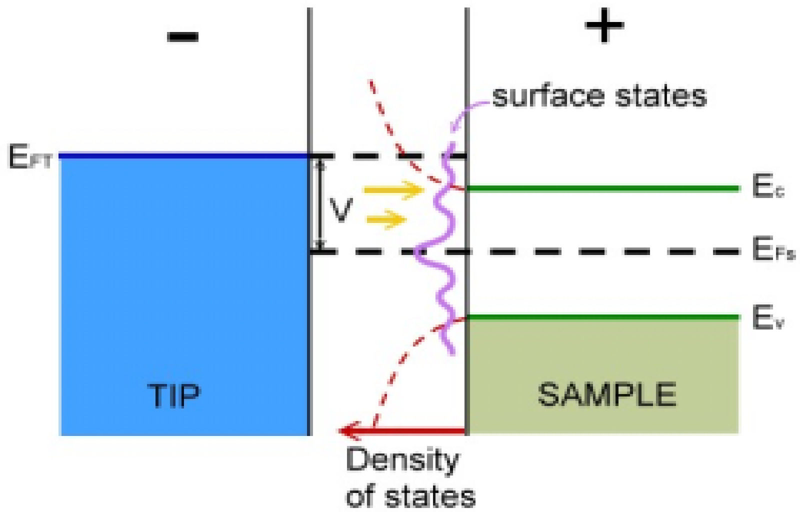

Science **234**, 304 (1986).

2.Tip -positiv

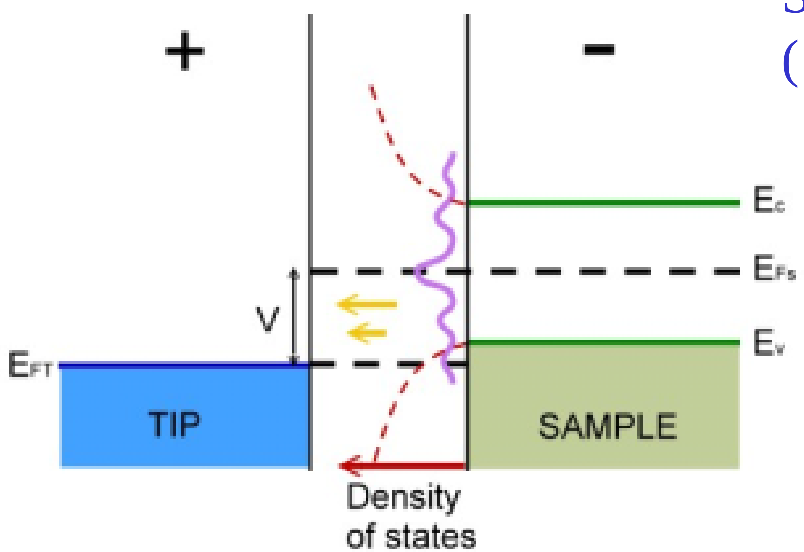

Scanning Tunneling Spectroscopy

STM provides atomic-scale topographic information, and atomic-scale electronic information. However, the mixture of geometric and electronic structure information often complicates interpretation of observed feature. Several spectroscopic modes:

1. Voltage-dependent STM imaging.
2. Tunneling I-V curves, current-imaging-tunneling spectroscopy (CITS).
3. Scanning tunneling spectroscopy (STS): dI/dV and topograph.

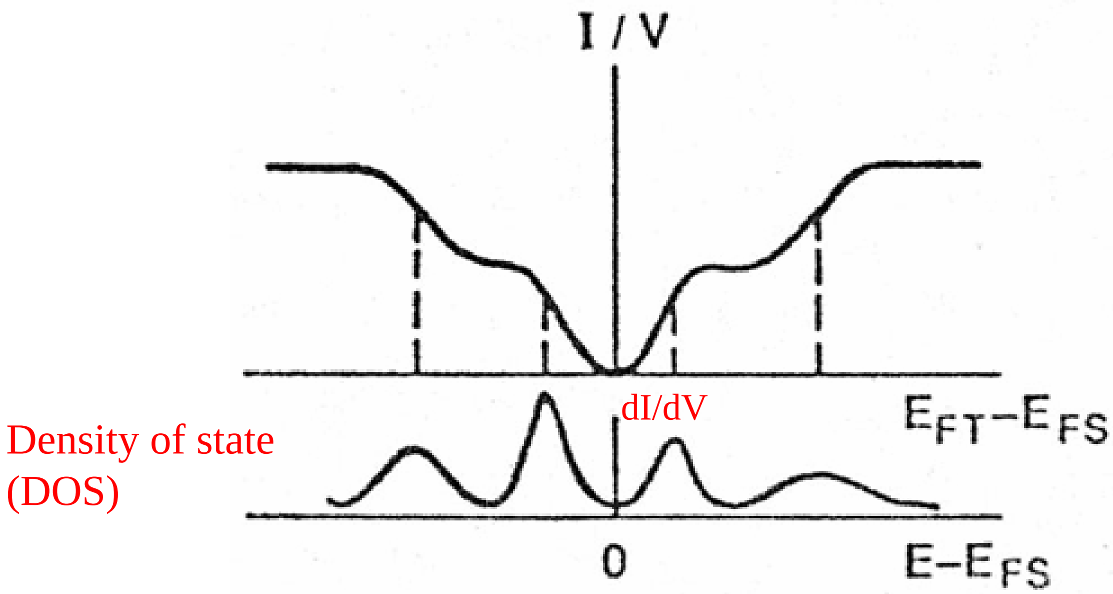

STS of Si(111)-(7x7)

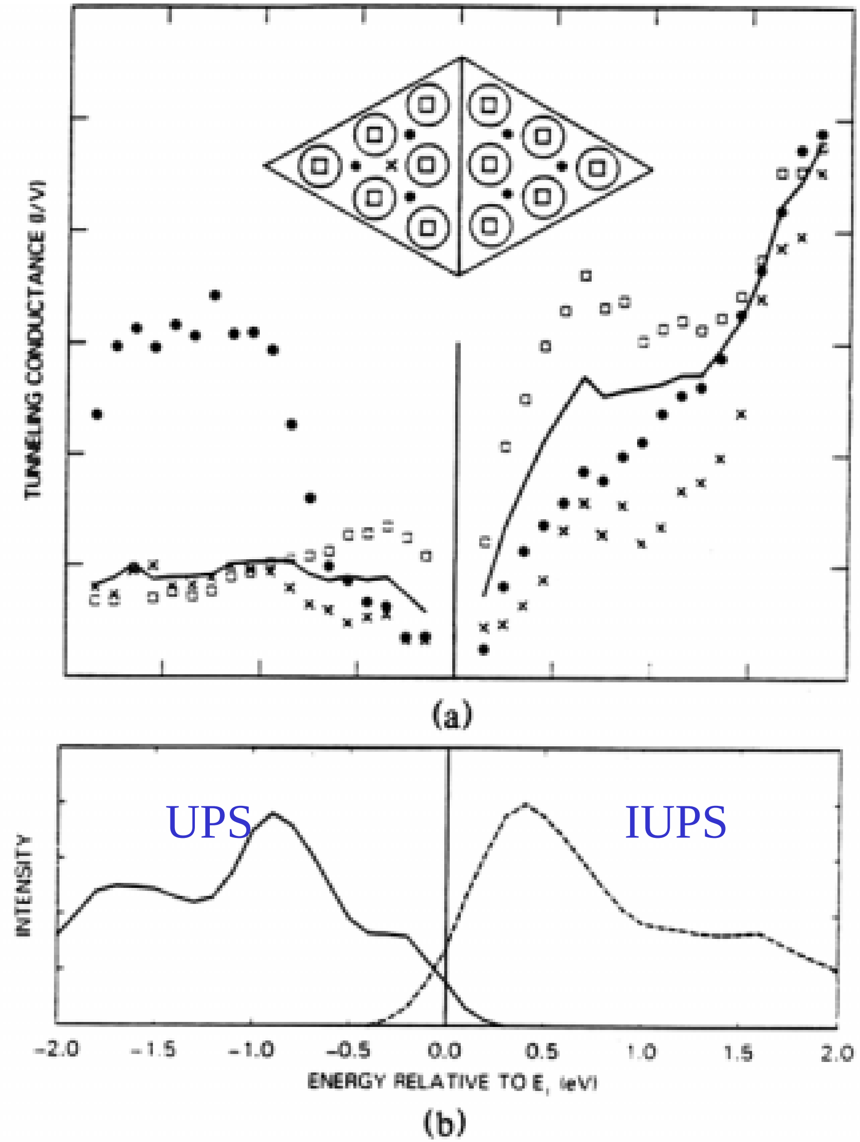

Science **234**, 304 (1986).

STS of Si(111)-(7x7)

topograph

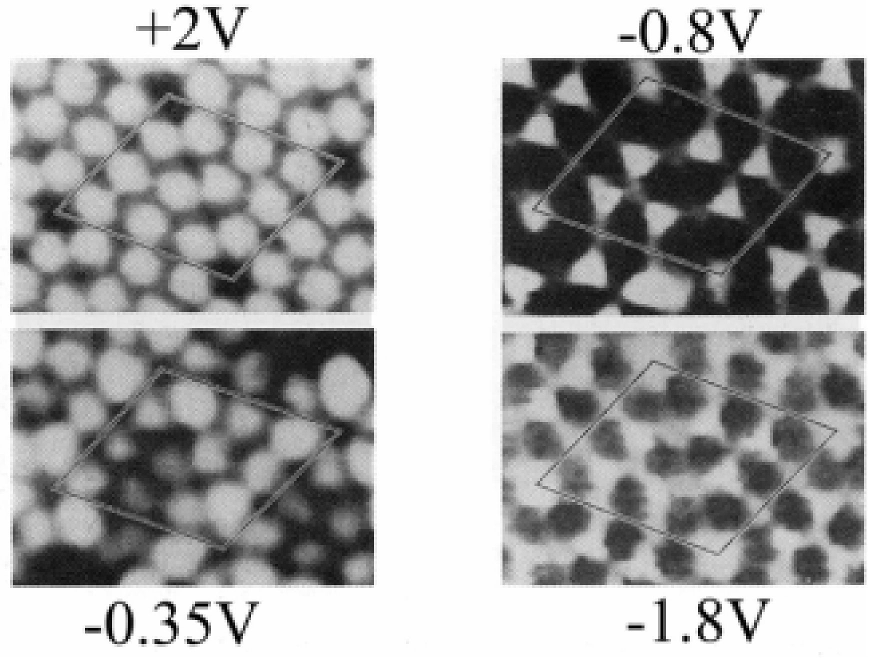

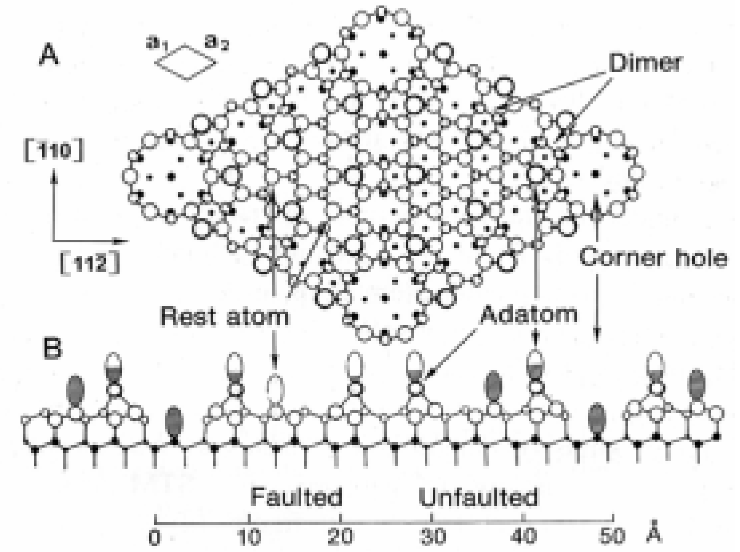

1. Science **234**, 304-309 (1986).
2. Phys. Rev. Lett. **56**, 1972-1975 (1986).

Single-Wall Carbon Nanotubes

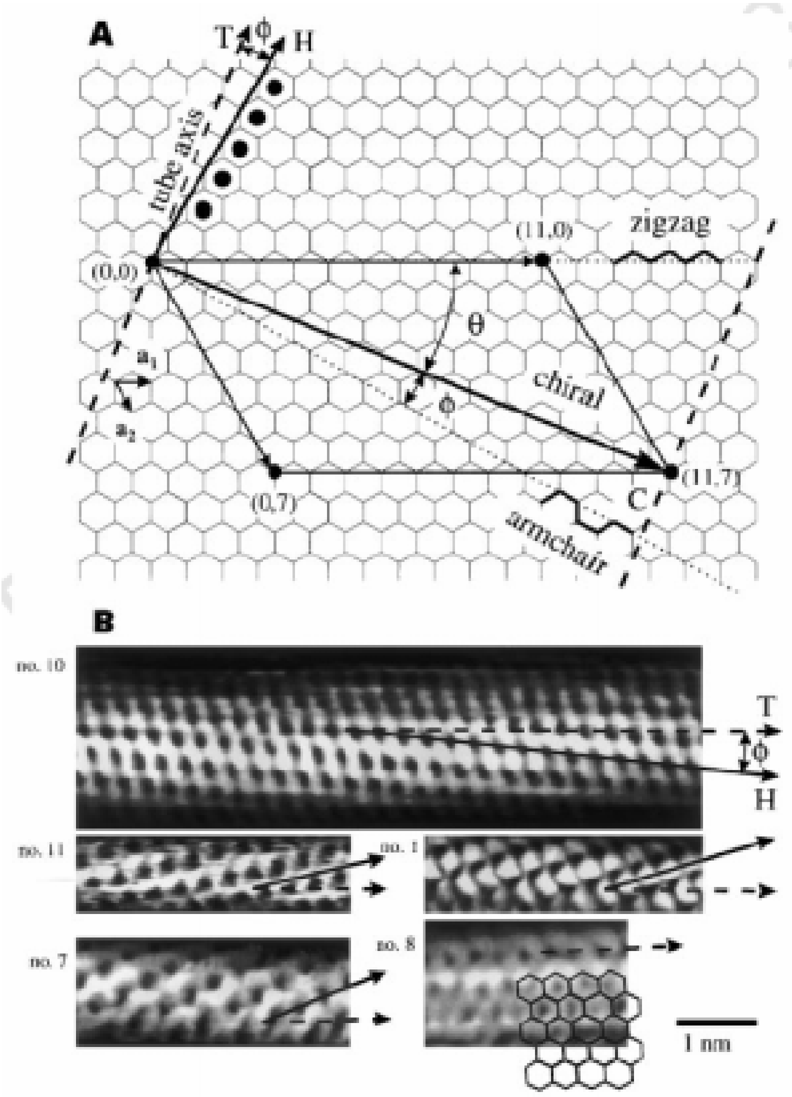

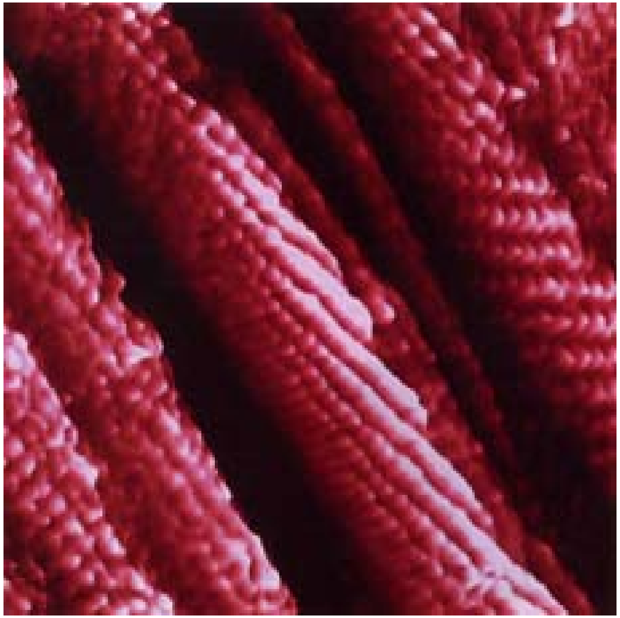

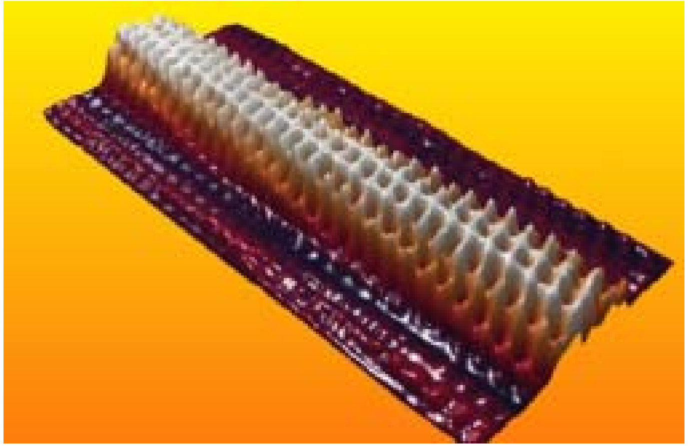

Electronic Structure of Single-Wall Nanotubes

1. Armchair nanotubes (n,n) → metallic

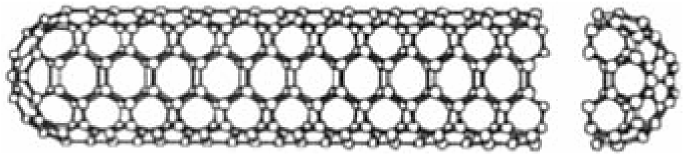

2. Zigzag nanotubes (n,0) → metallic, when n=3q

   → semiconducting, otherwise

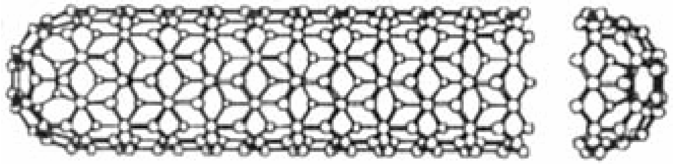

3. Chiral nanotubes (n,m) → metallic, when m=n+3q

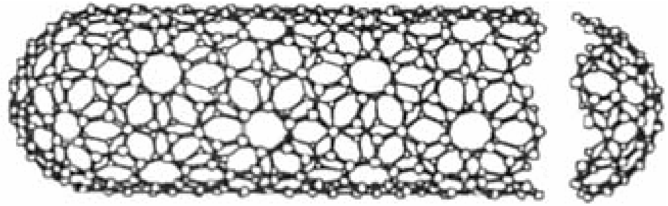

Electronic Structure of Single-wall Nanotubes

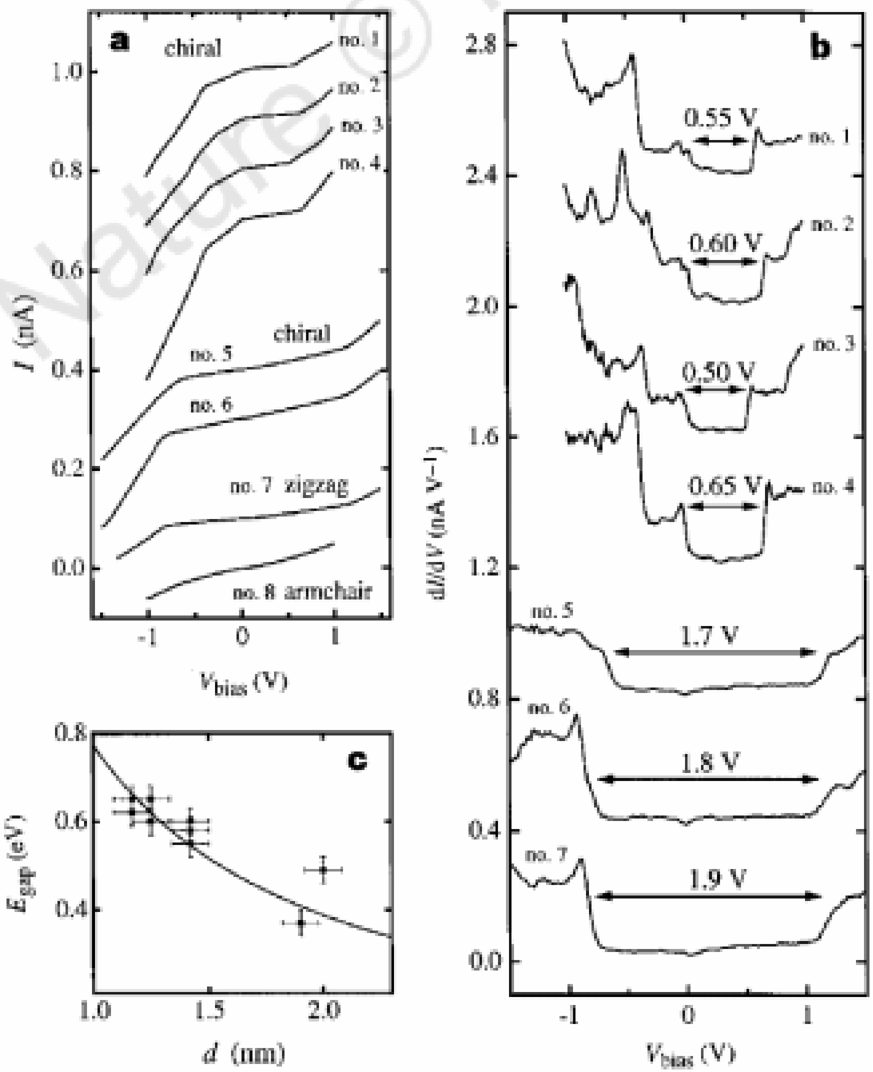

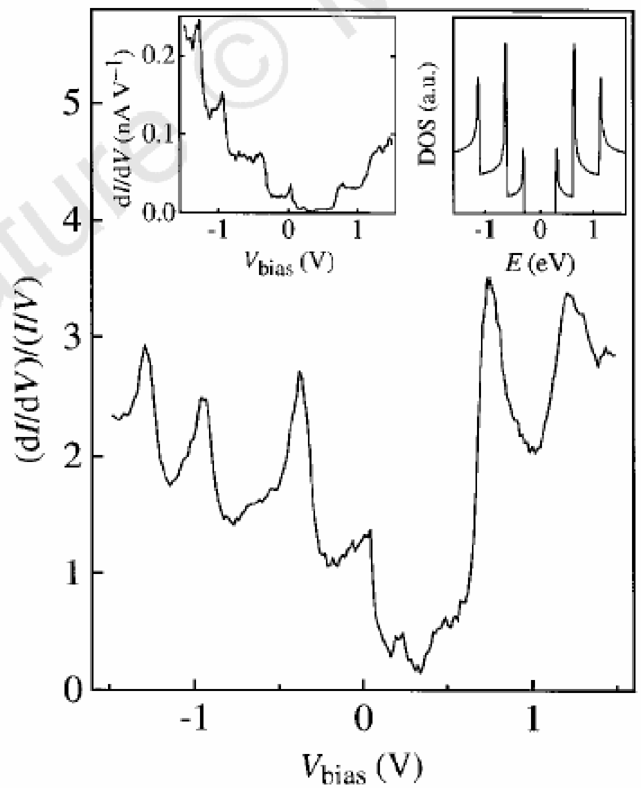

Nature **391**, 59 (1998).

Single-Wall Armchair Nanotube on Au(111)

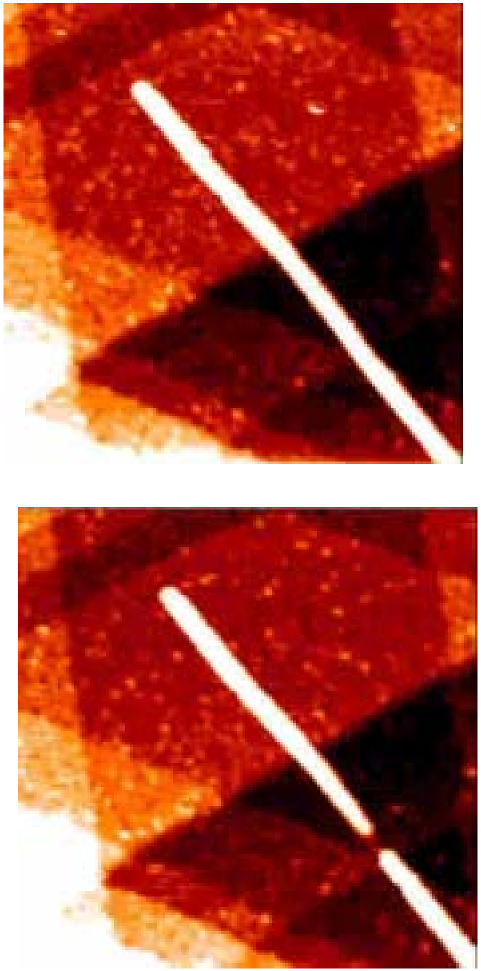

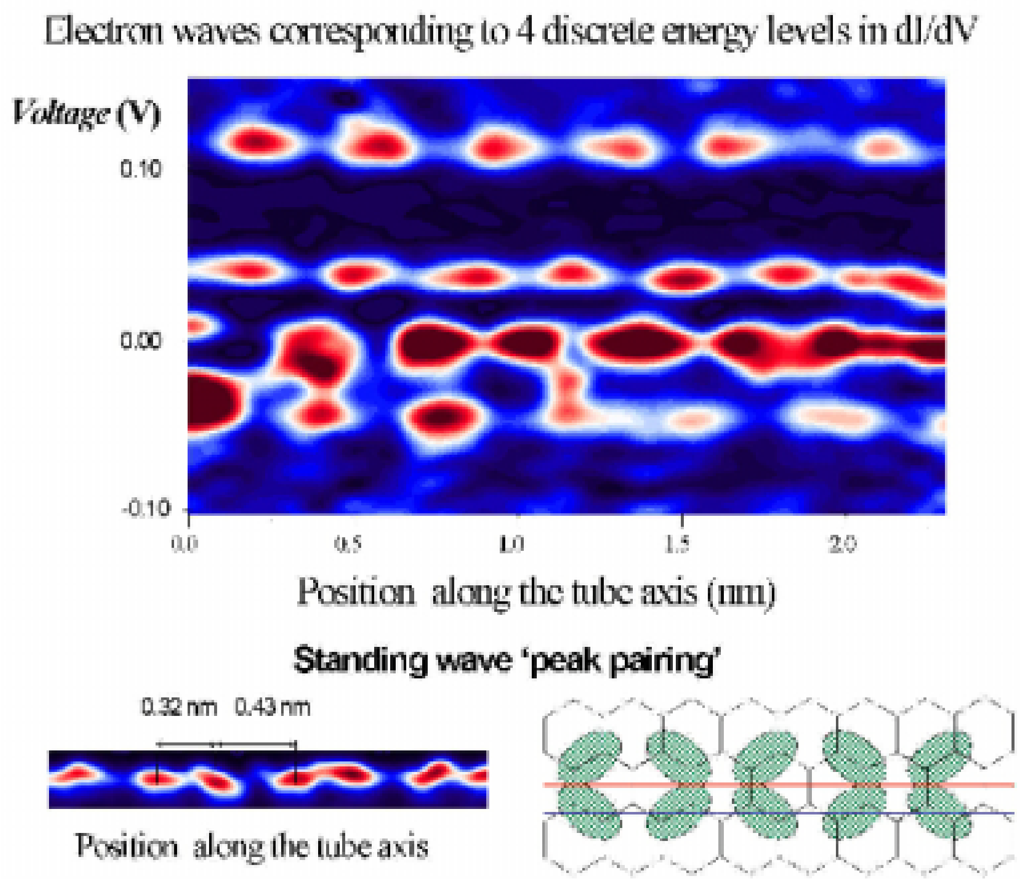

Science **283**, 52 (1999).

Superstructures of 2D islands

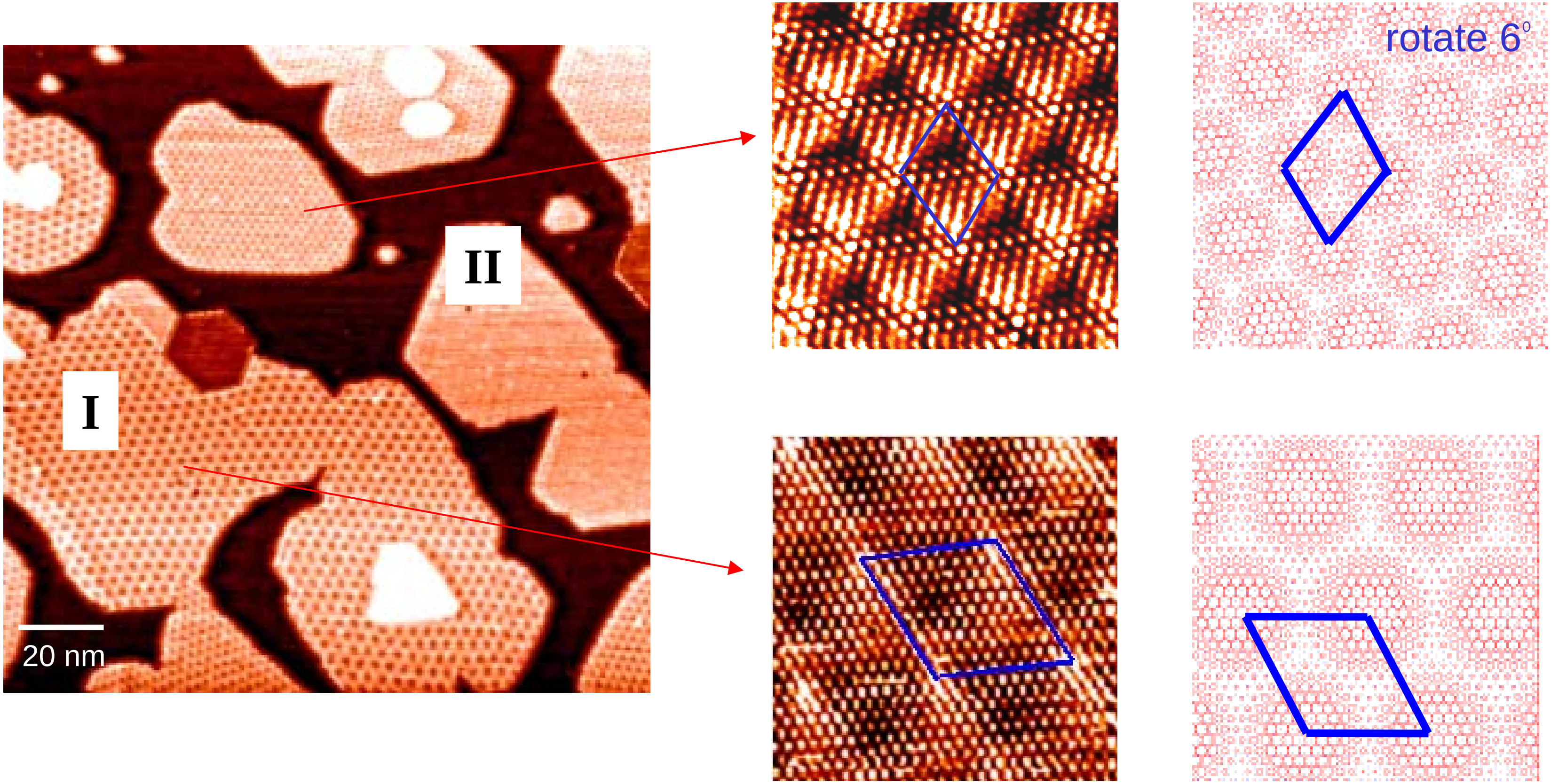

Characteristics of Pb islands---Bias-dependent imaging contrast

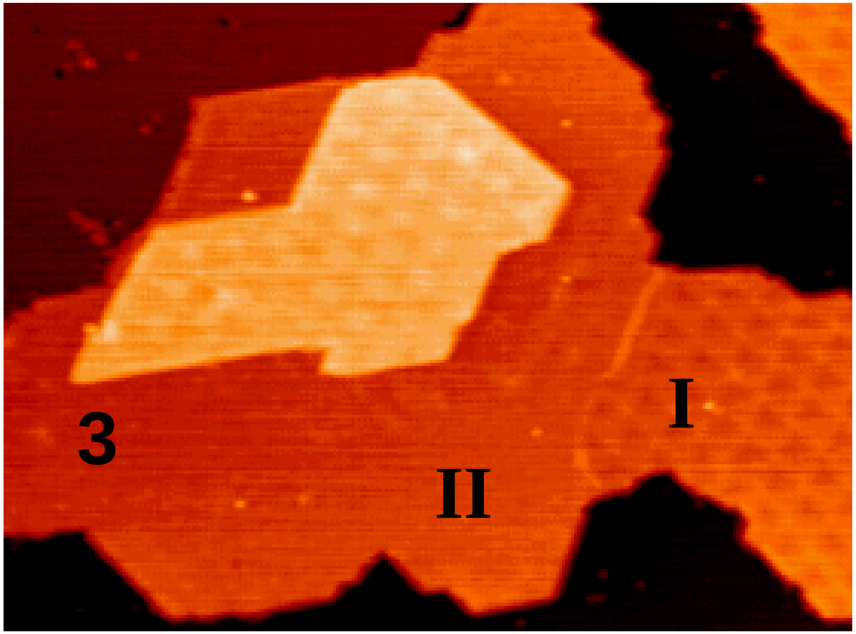

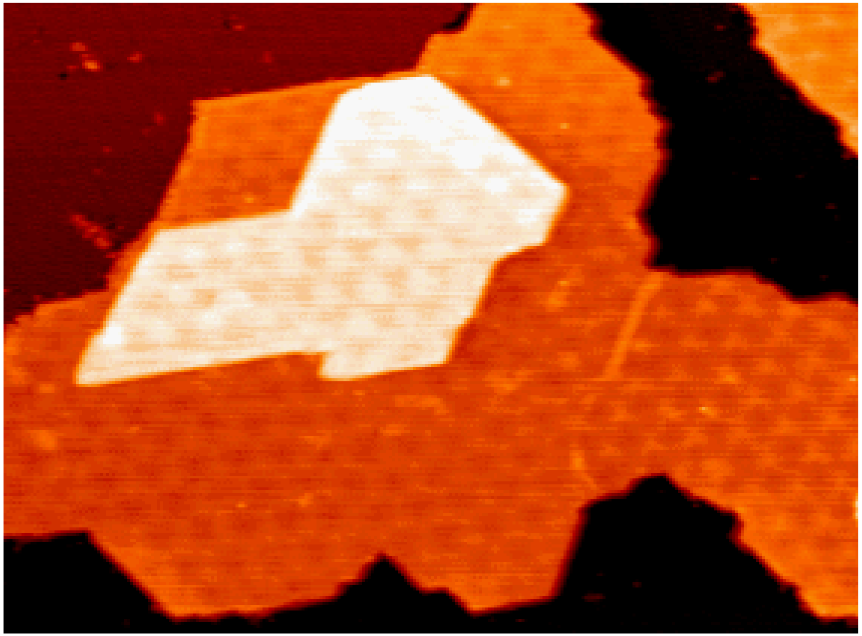

Sample bias :+2V

Sample bias :+0.4V

Characteristics of Pb island---oscillatory and complementary contrast

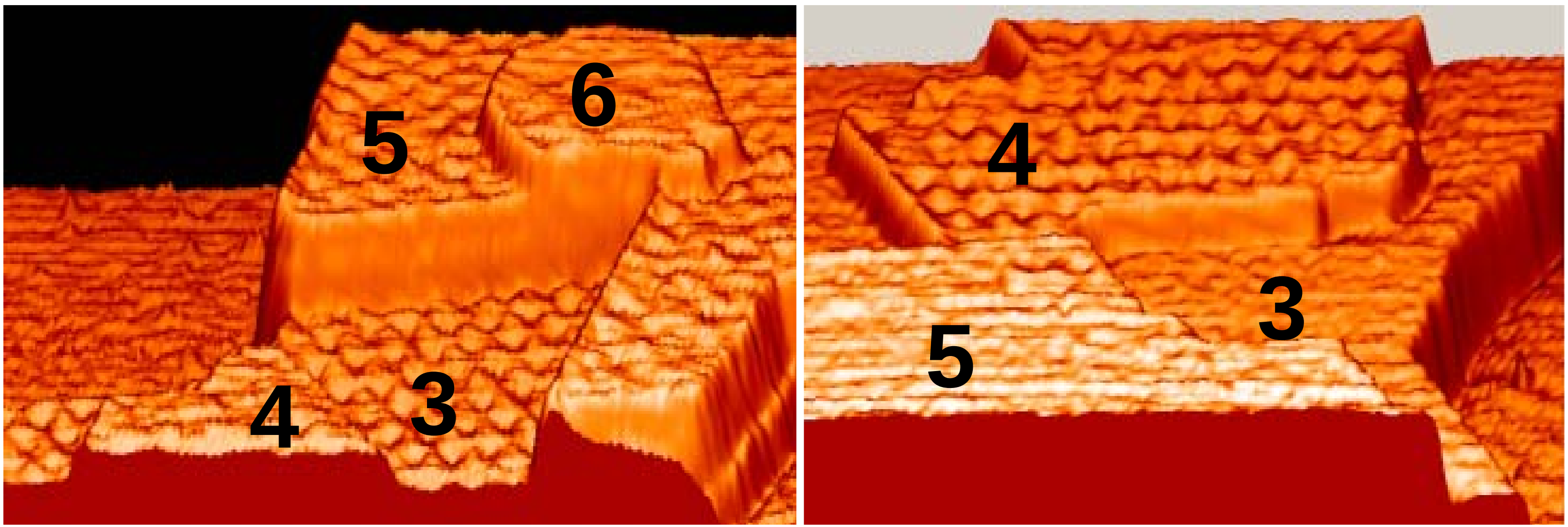

Type I **Type II**

Quantum size effect

λ = de Broglie wavelength of electron
a = thickness of metal film

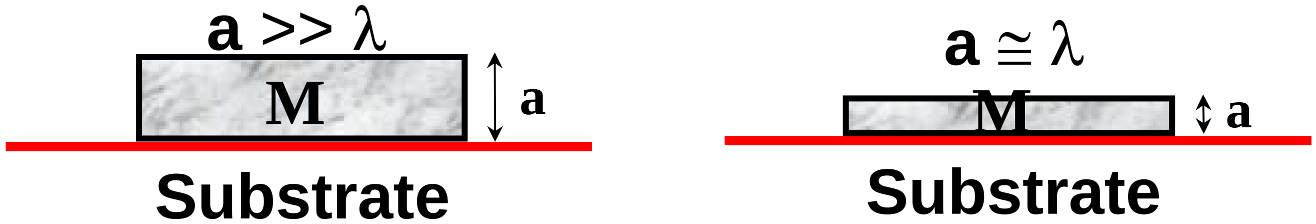

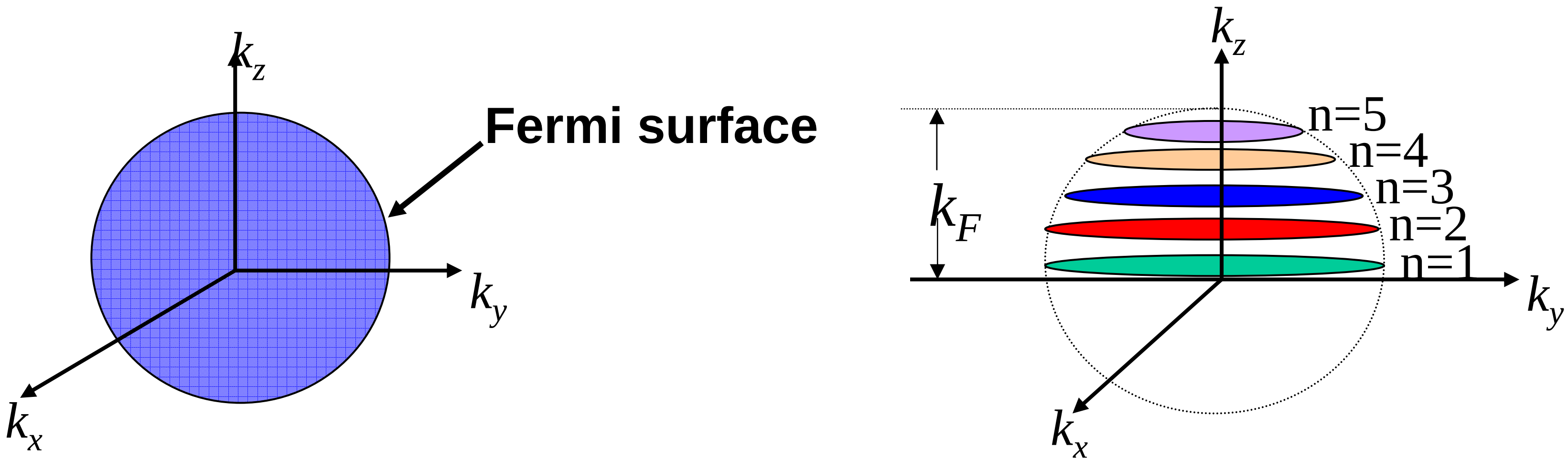

Spectra for Pb Films

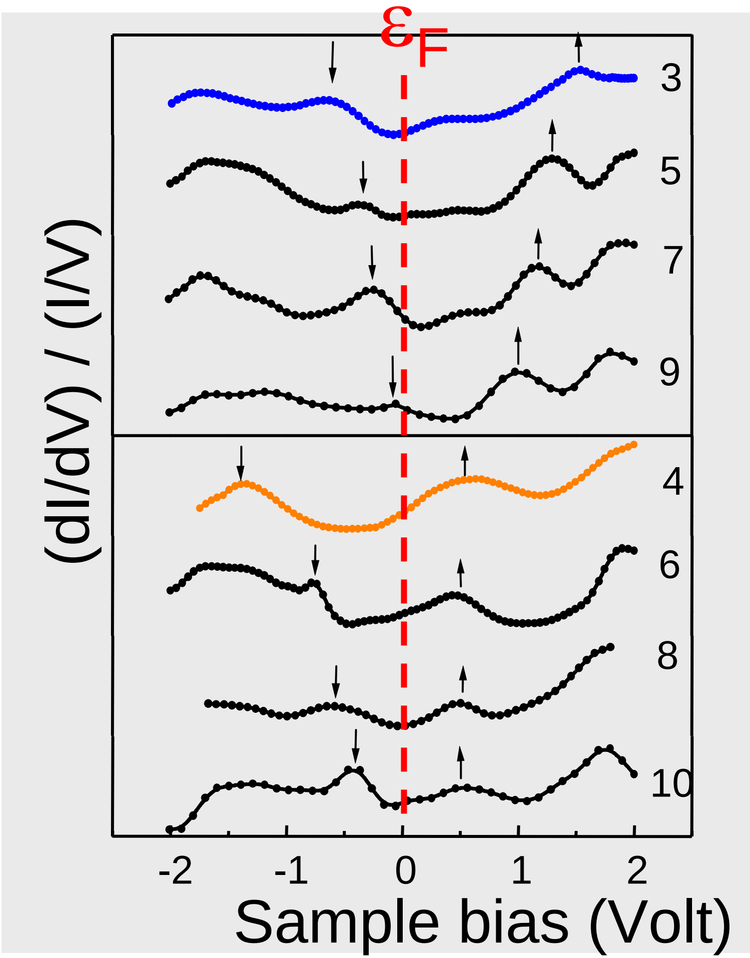

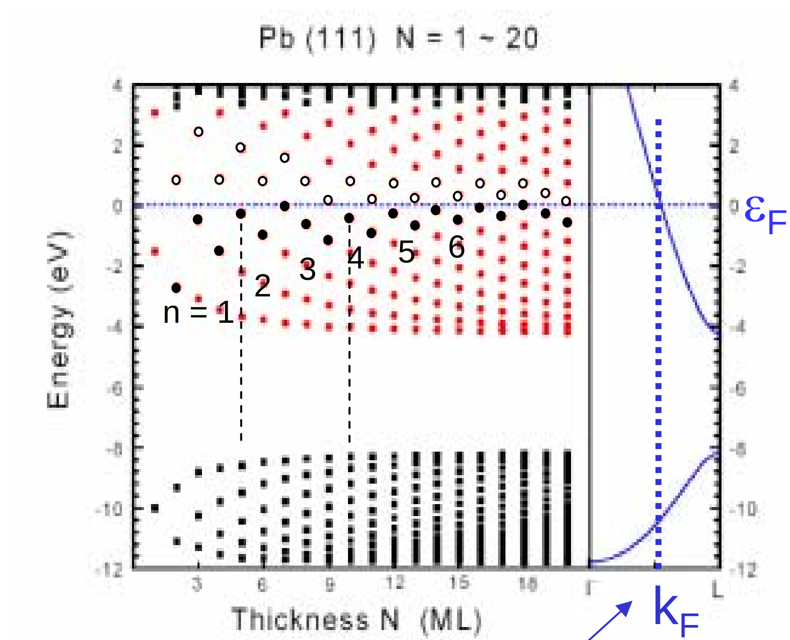

d_0 = 2.85 Å **λ_F = 3.94 Å**

$2d_0 \approx 3(\lambda_F/2)$

Atomic Manipulation with STM

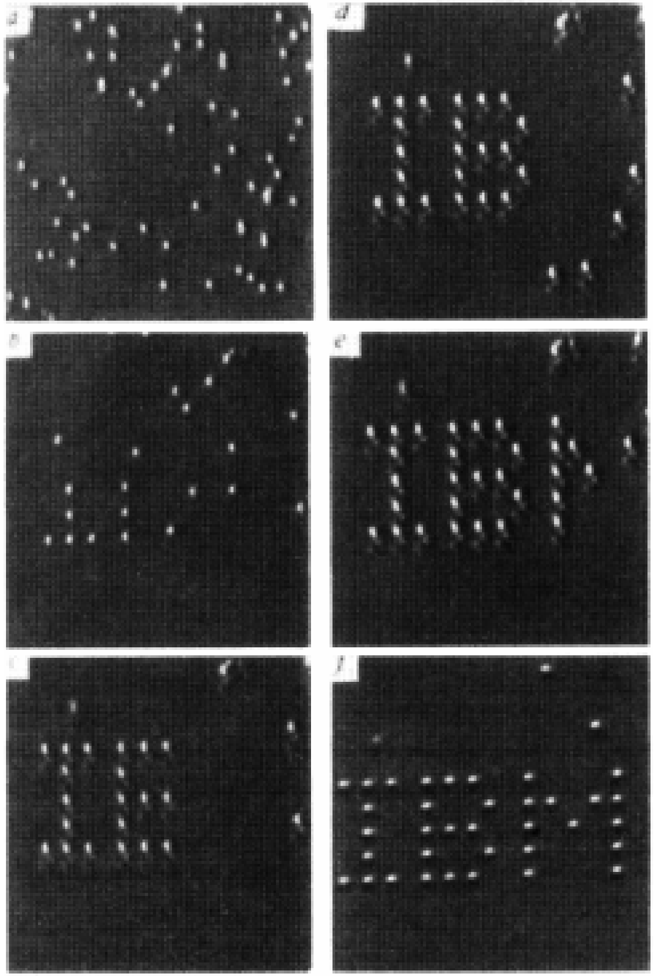

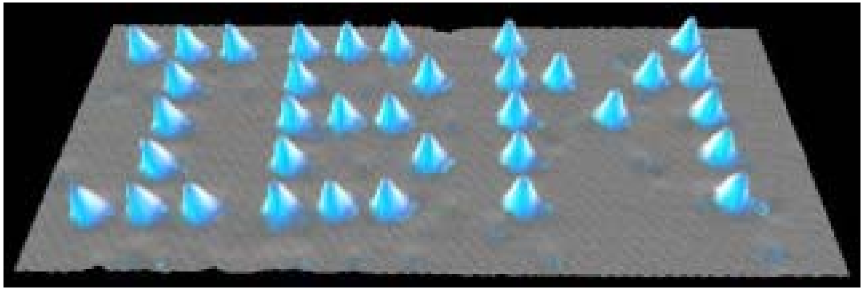

Nature **344**, 524 (1990)

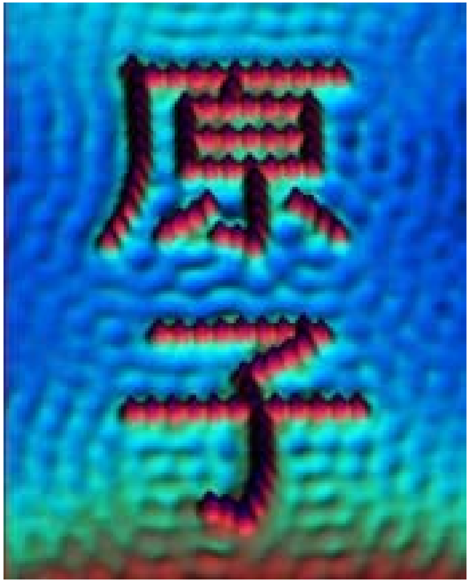

Positioning Atoms with an STM

D.M. Eigler & E.K. Schweizer Nature **344** 524 (1990)

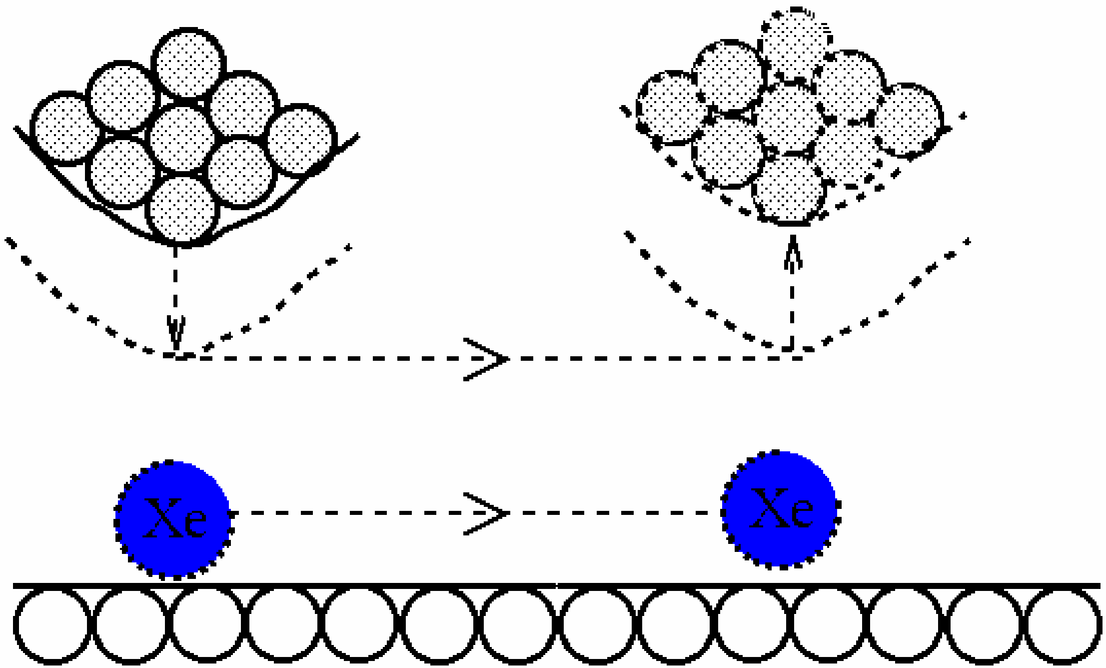

The STM tip is brought down near the atom, until the attraction is enough to hold it as the atom is dragged across the surface to a new position.

Quantum Corral

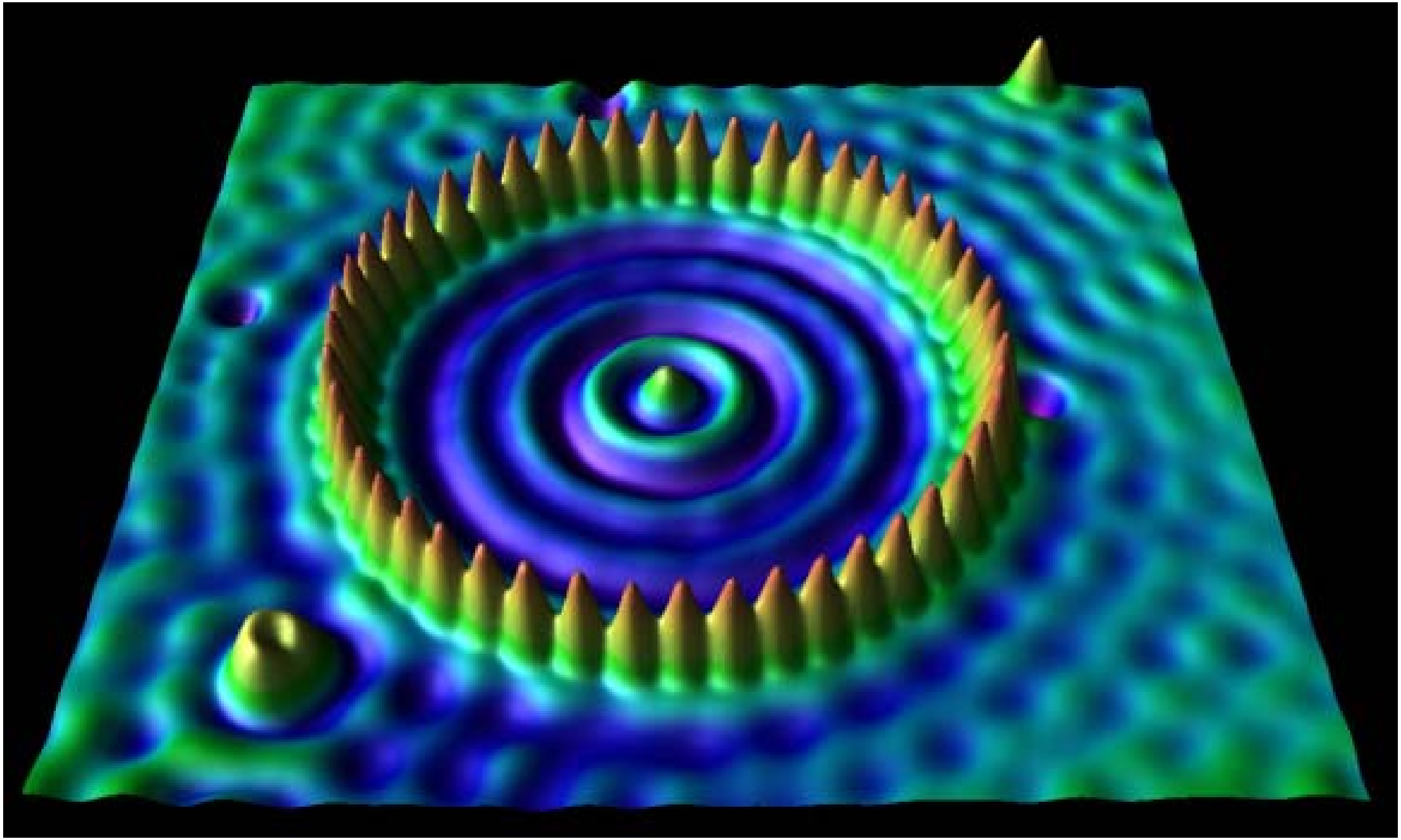

M.F. Crommie *et al., Science* 262, 218 (1993).

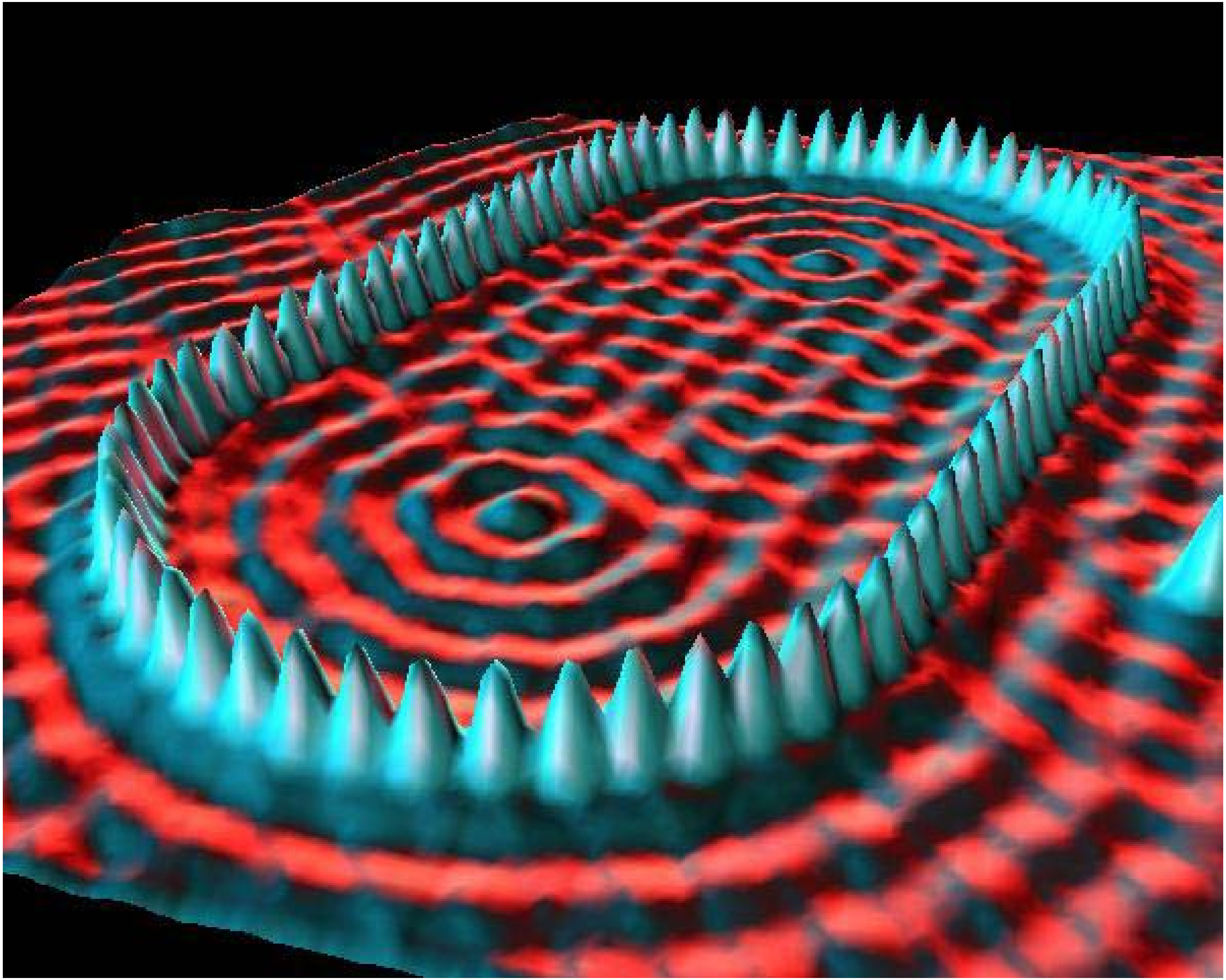

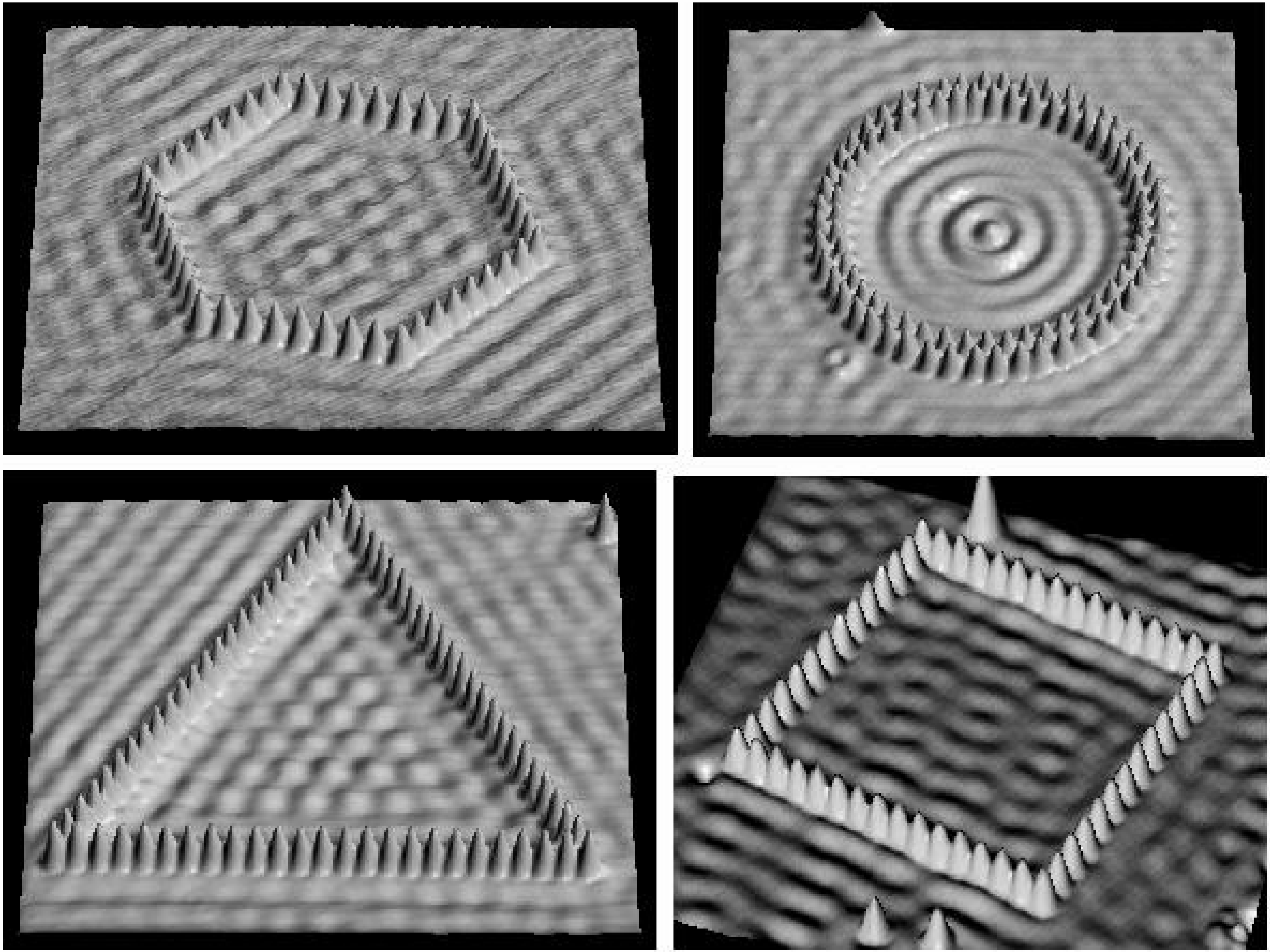

Quantum Mirage

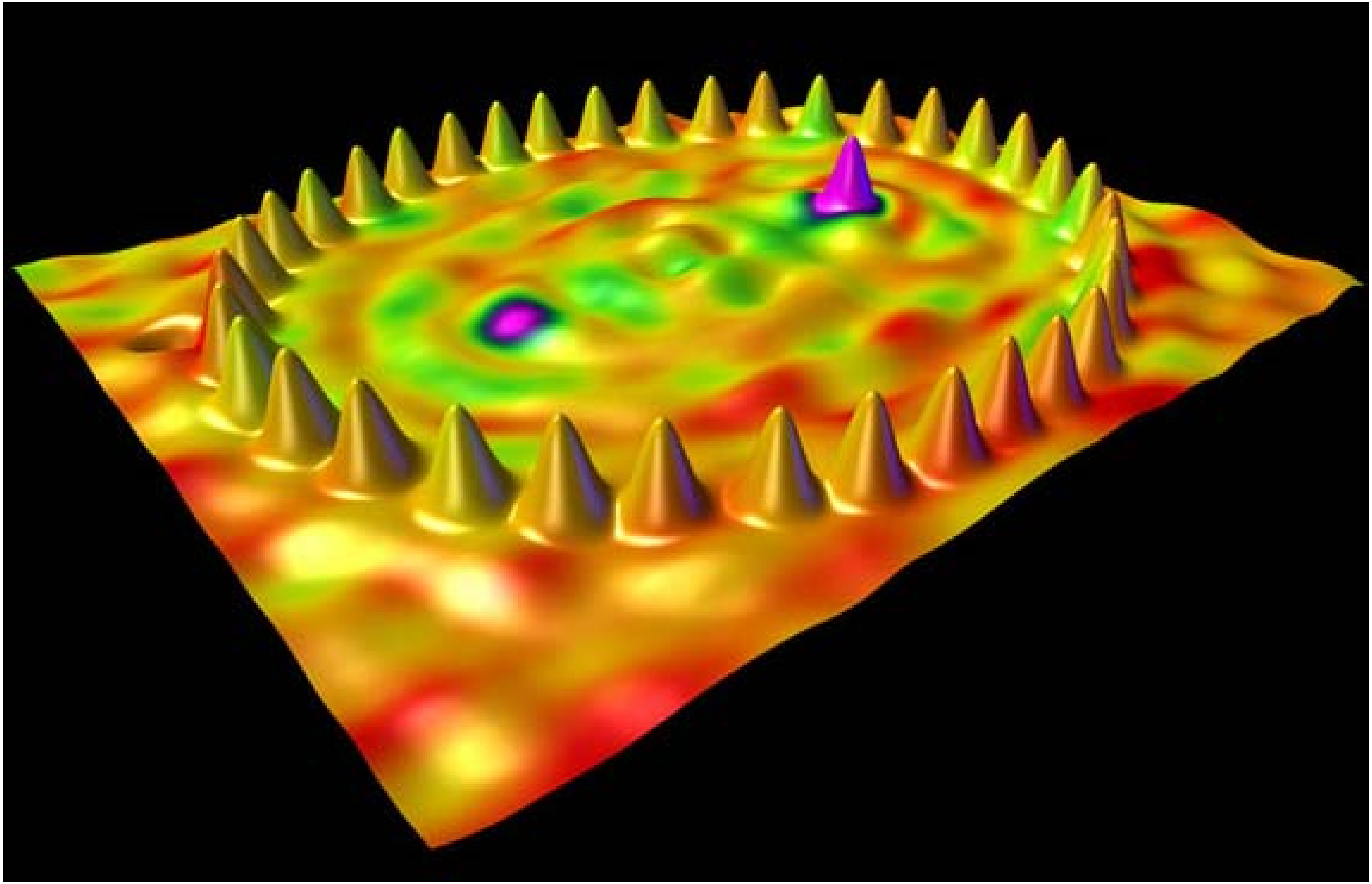

H. C. Manoharan *et al., Nature* 403, 512 (2000).

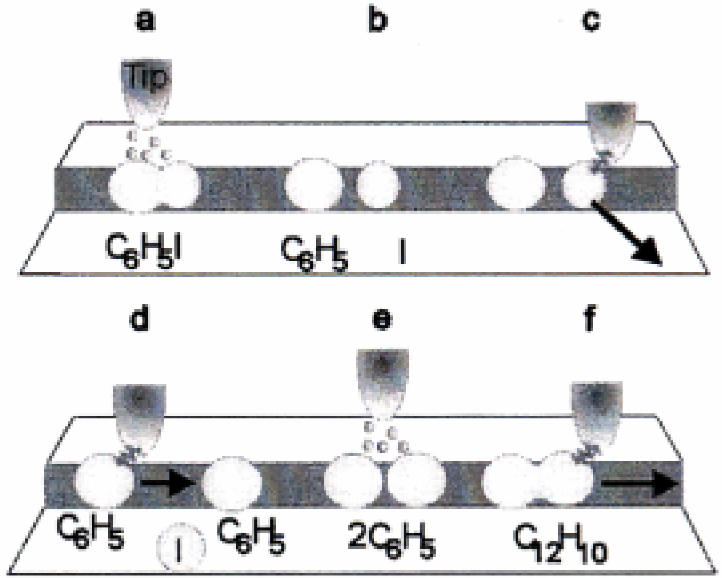

FIG. 1. Schematic illustration of the STM tip-induced synthesis steps of a biphenyl molecule. (a),(b) Electron-induced selective abstraction of iodine from iodobenzene. (c) Removal of the iodine atom to a terrace site by lateral manipulation. (d) Bringing together two phenyls by lateral manipulation. (e) Electron-induced chemical association of the phenyl couple to biphenyl. (f) Pulling the synthesized molecule by its front end with the STM tip to confirm the association.

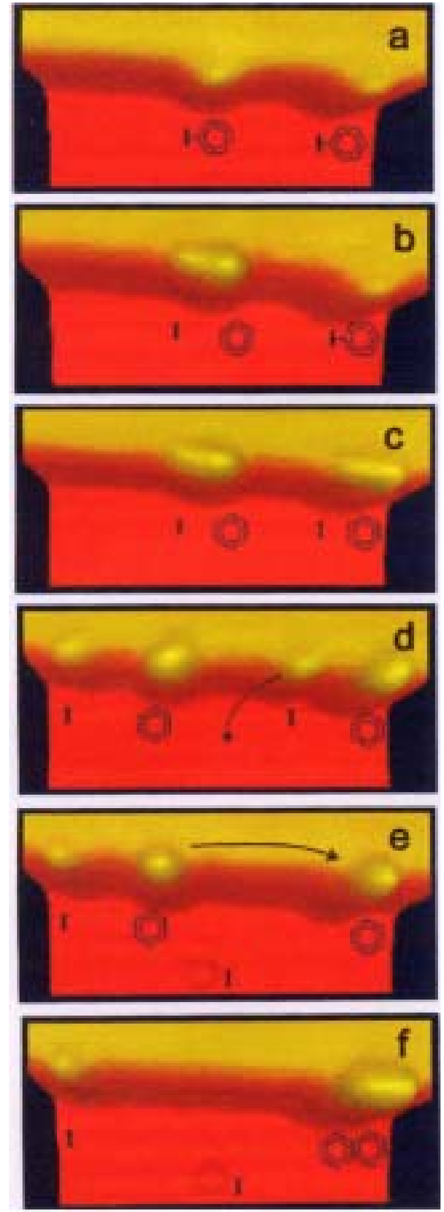

Phys. Rev. Lett. 85, 2777 (2000)

Atom Memory at Room Temperature
Au/Si(111)

Nanotechnology **13** (2002) 499–502

CD-ROM

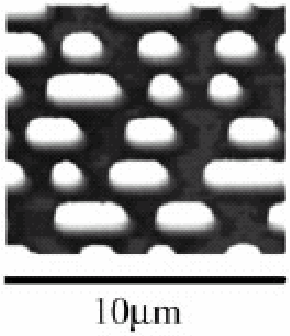

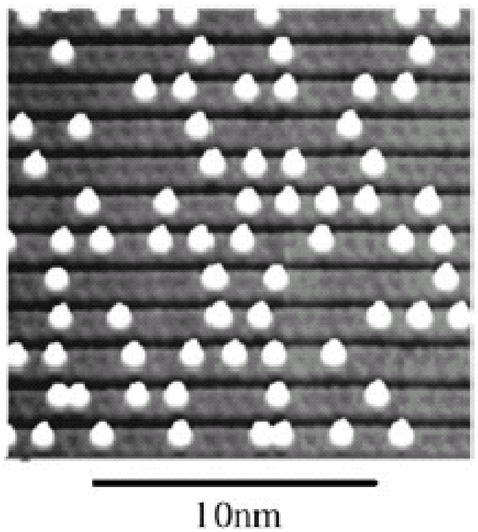

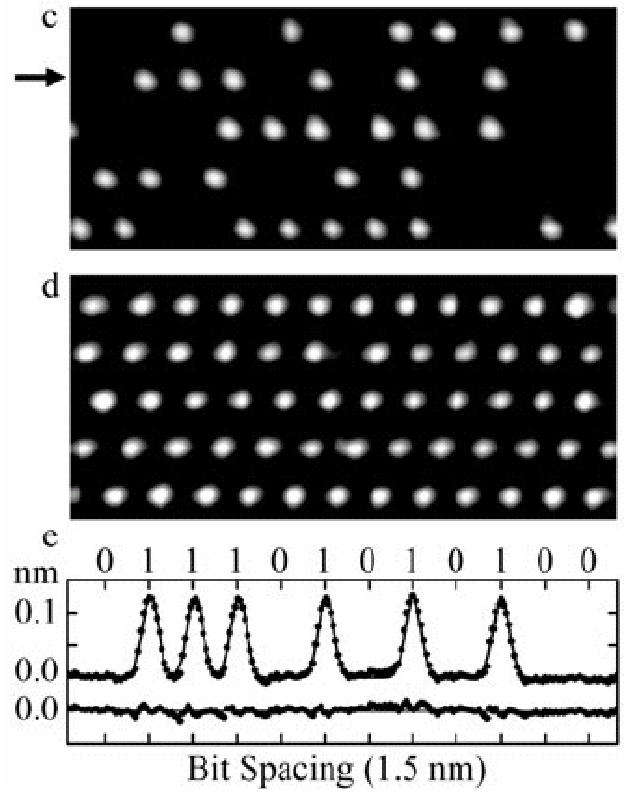

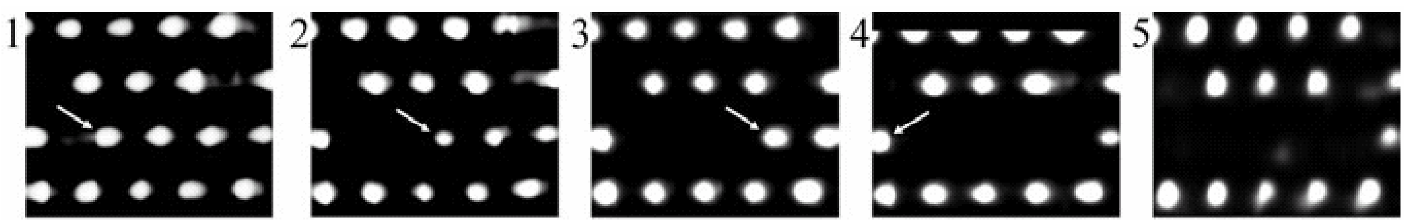


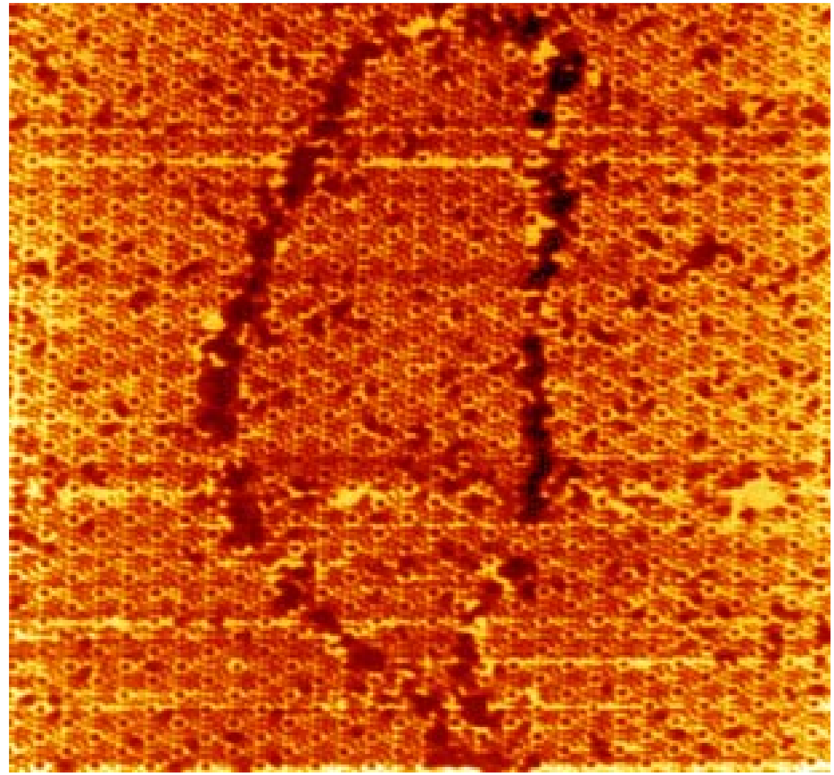

Atomic Force Microscopy (AFM)

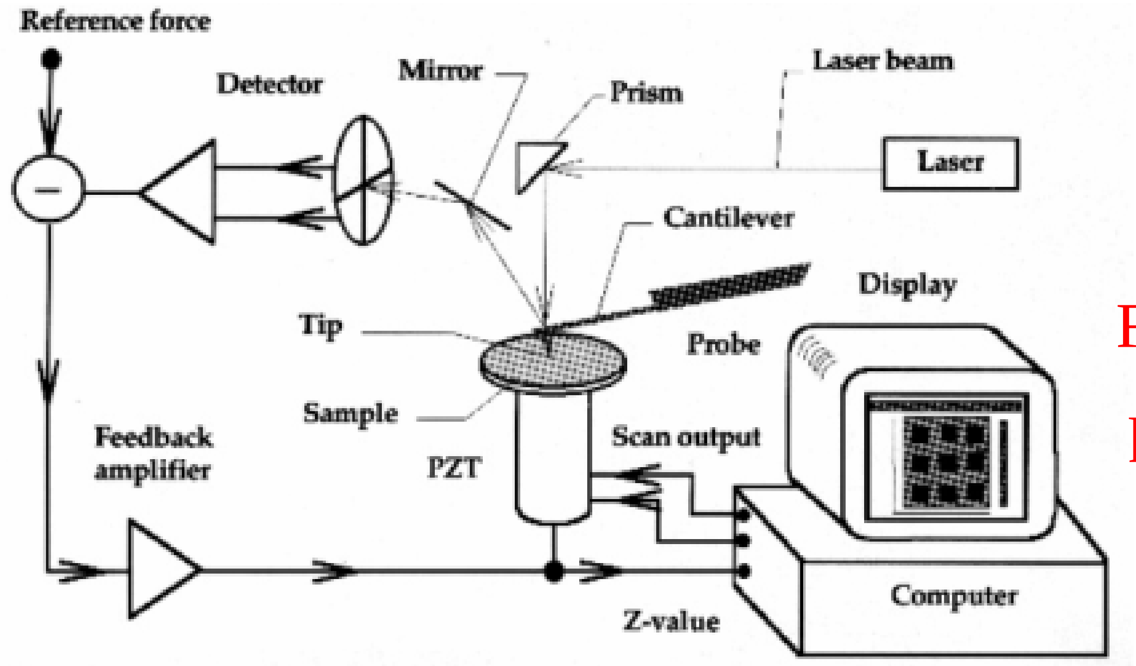

$$F = k\Delta z$$

$$F = 10^{-9} - 10^{-6}\ \mathrm{N}$$

$$k = 0.1 - 1\ \mathrm{N/m}$$

<u>References:</u>

- G. Binnig, C. F. Quate, and C. Gerber, Phys. Rev. Lett. 56, 930 (1986).
- C. Bustamante and D. Keller, Physics Today, 32, December (1995).
- R. Wiesendanger and H.J. Güntherodt, *Scanning Tunneling Microscopy II* , Springer-Verlag, (1992).

Interaction between the probe and sample

Short-range:

1) Bonding

2) Repulsion

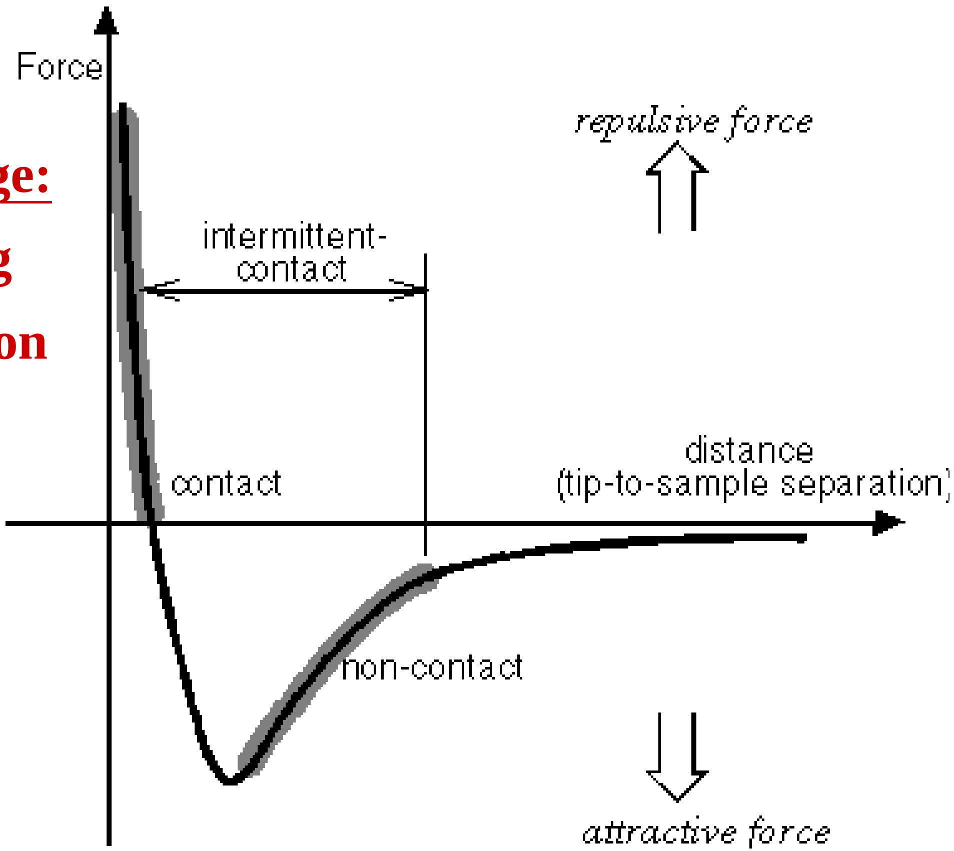

Long-range:

1) Van der Waal

2) Capillary

3) Magnetic

4) Electrostatic

Lennard-Jones potential $\phi(r) = - A/r^6 + B/r^{12}$

Deflection of Cantilever vs Piezo displacement

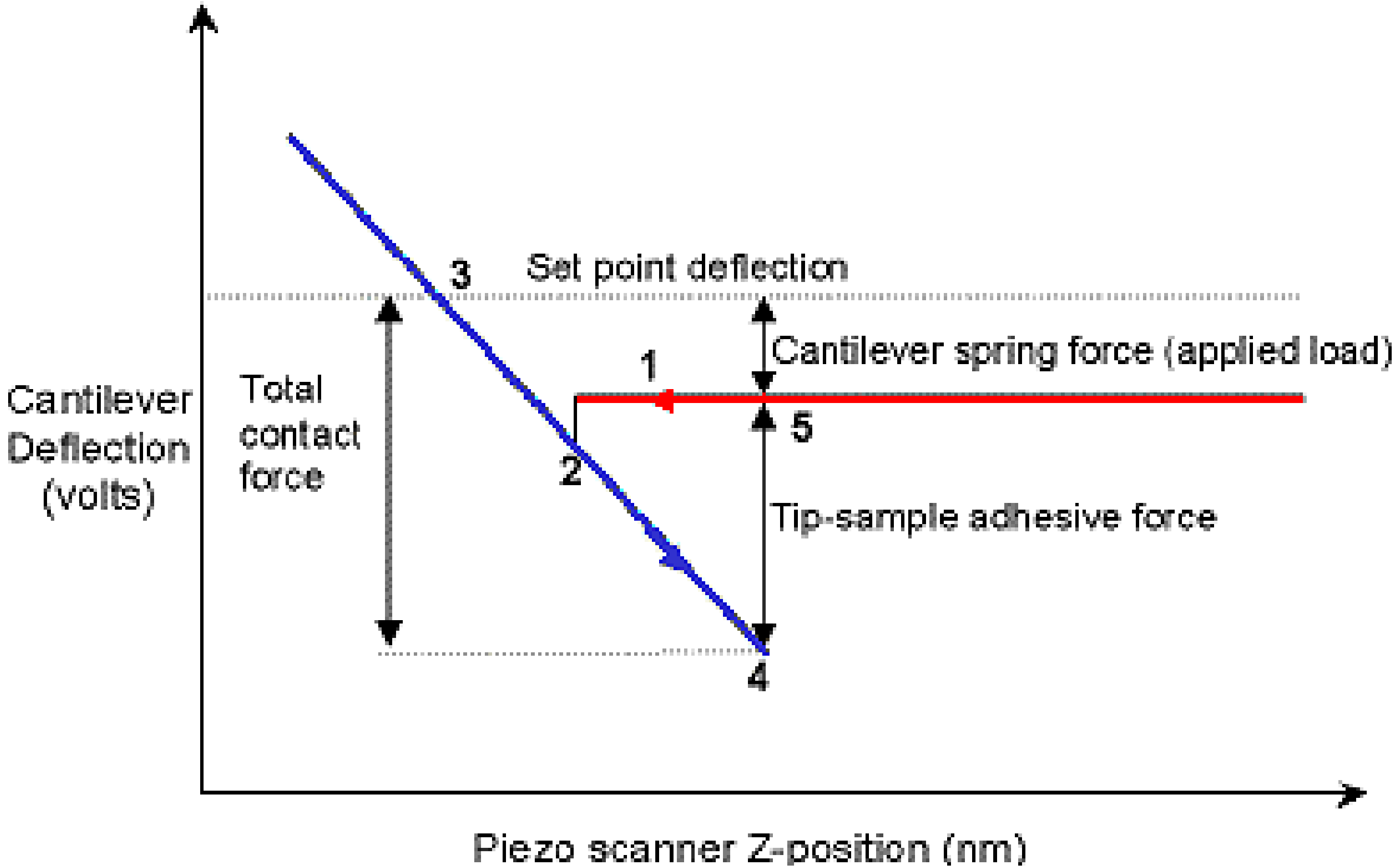

Reaction of the probe to the force

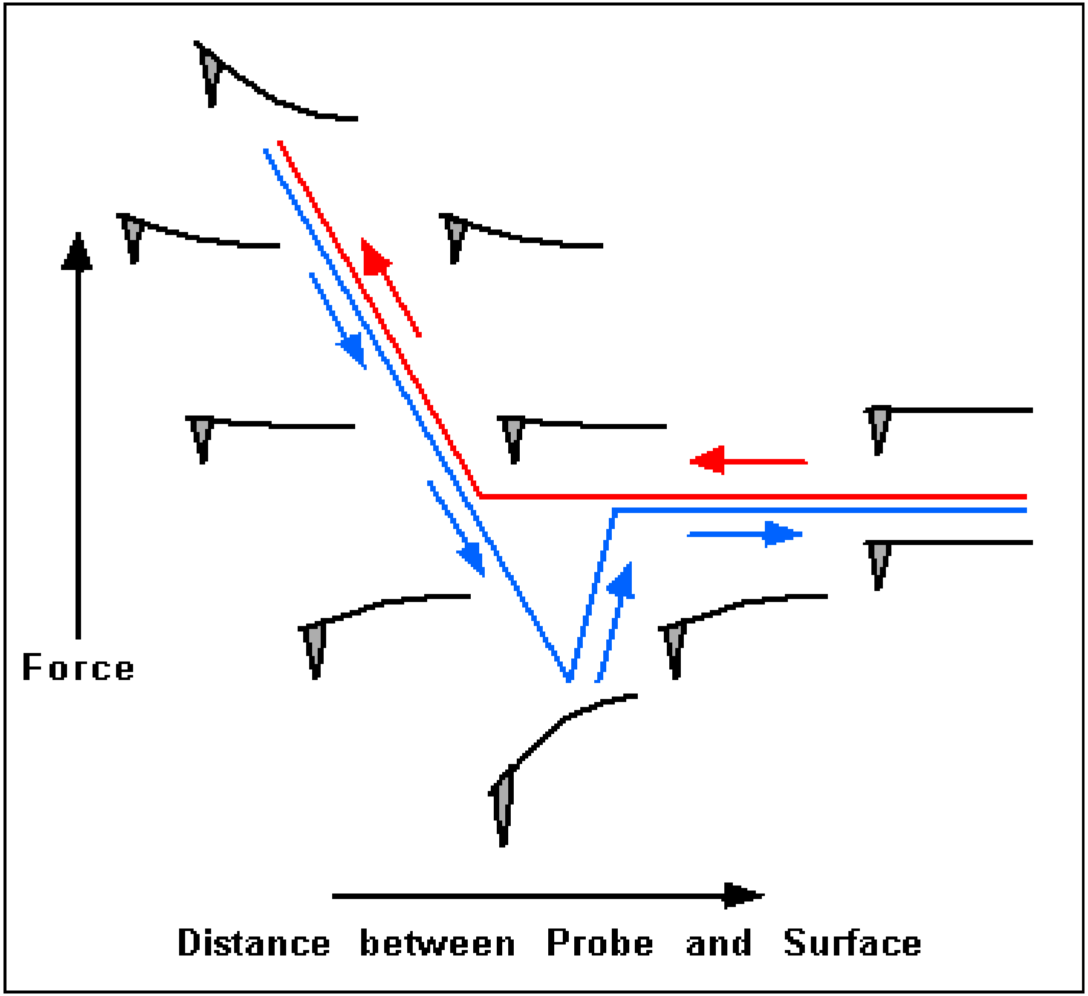

Structure of AFM

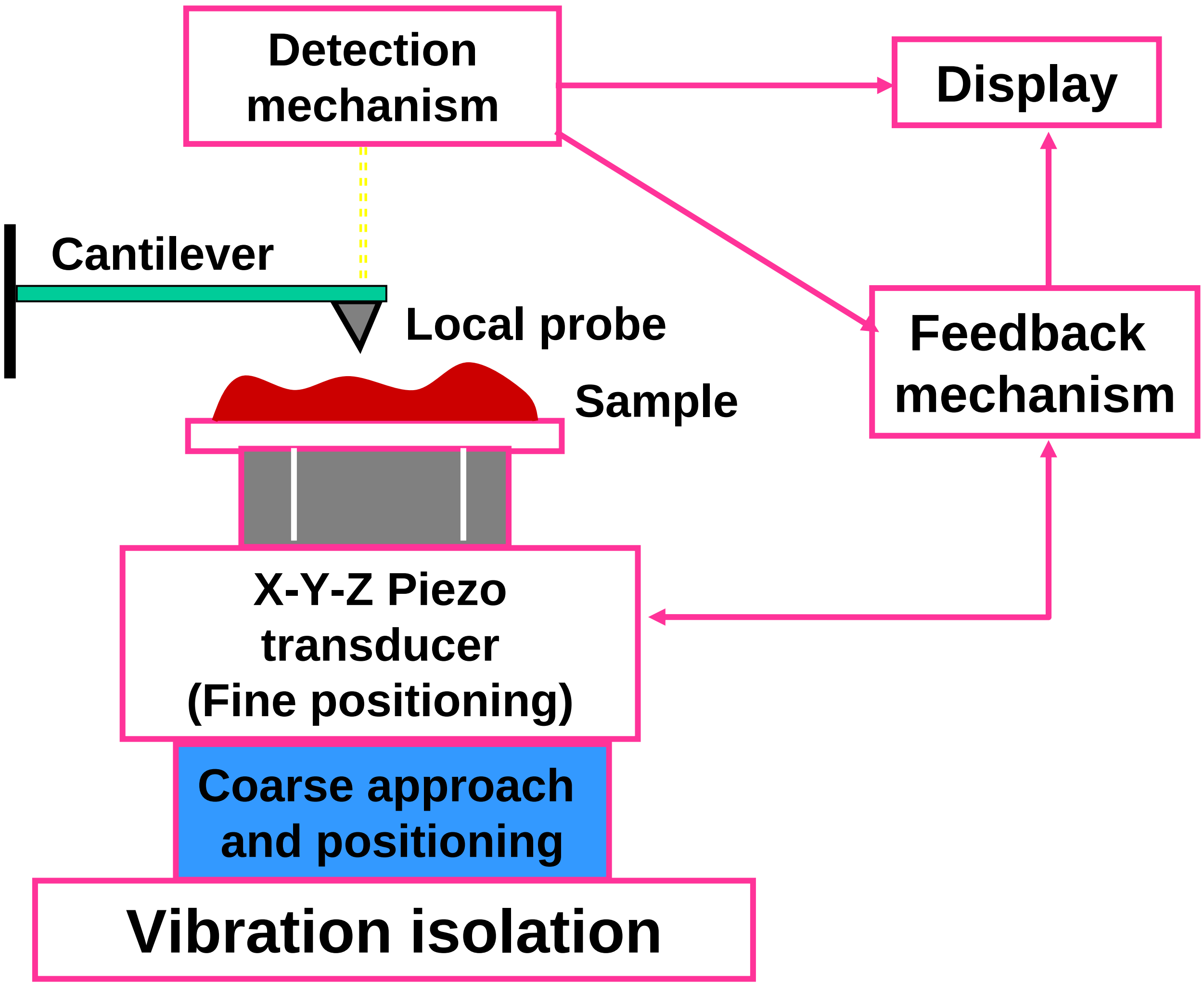

Core components of AFM

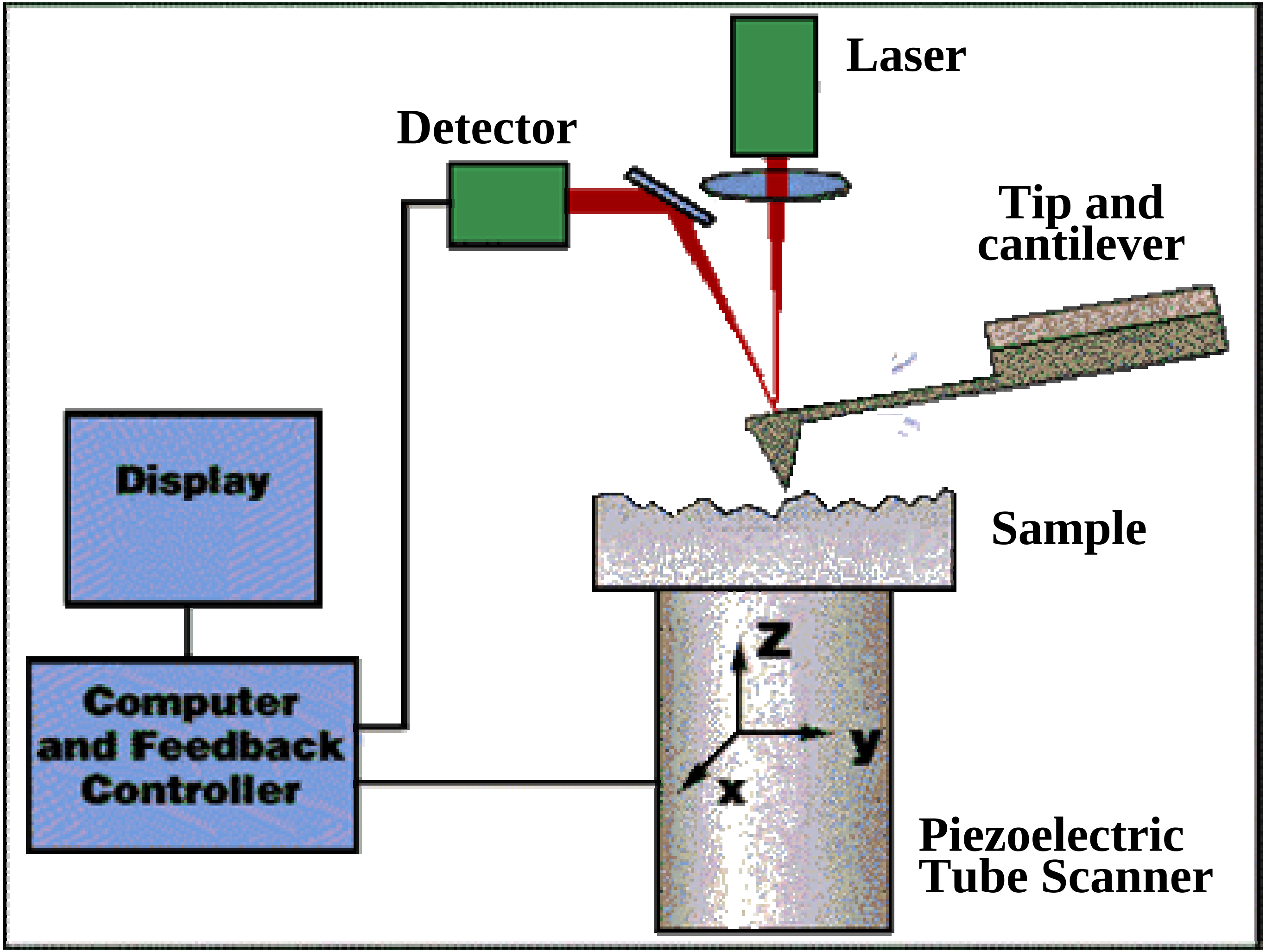

Three scanning modes of AFM

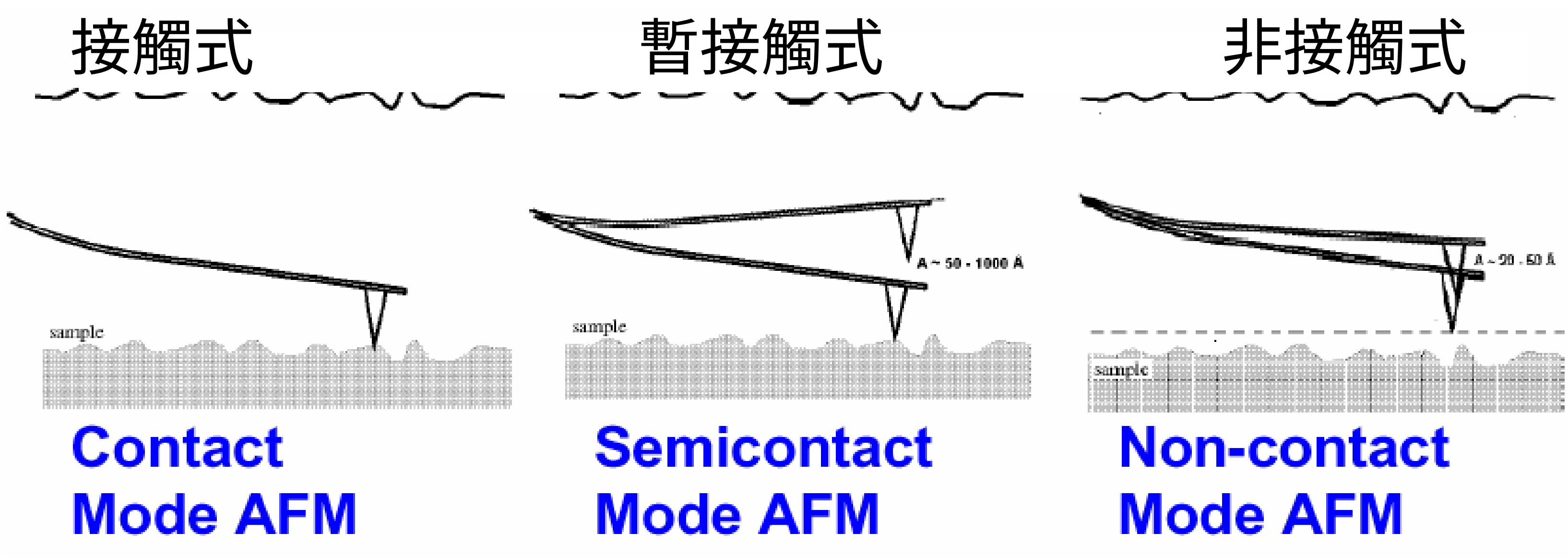

Comparison of three scanning modes

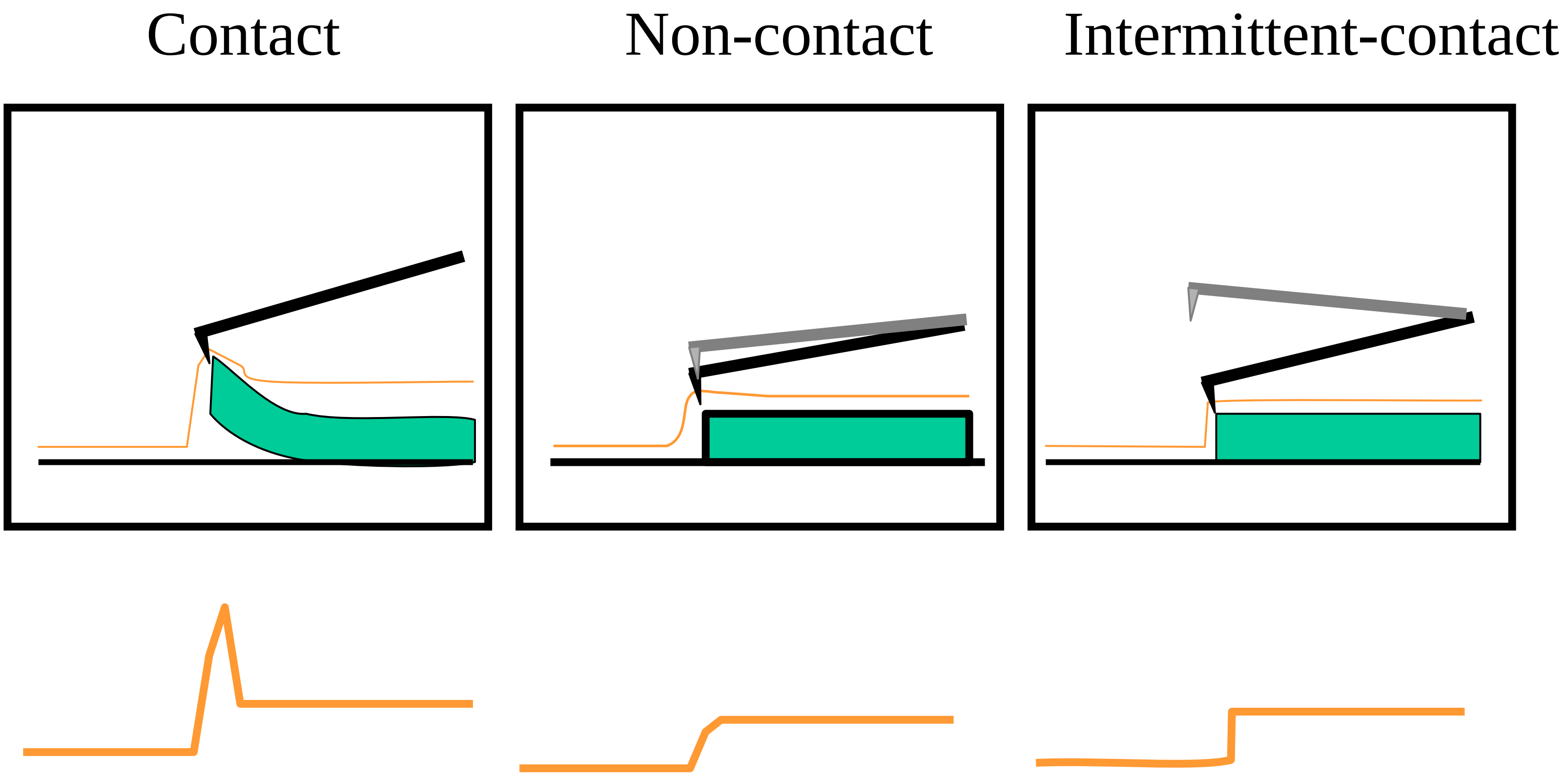

Tapping Mode (10-300 kHz)

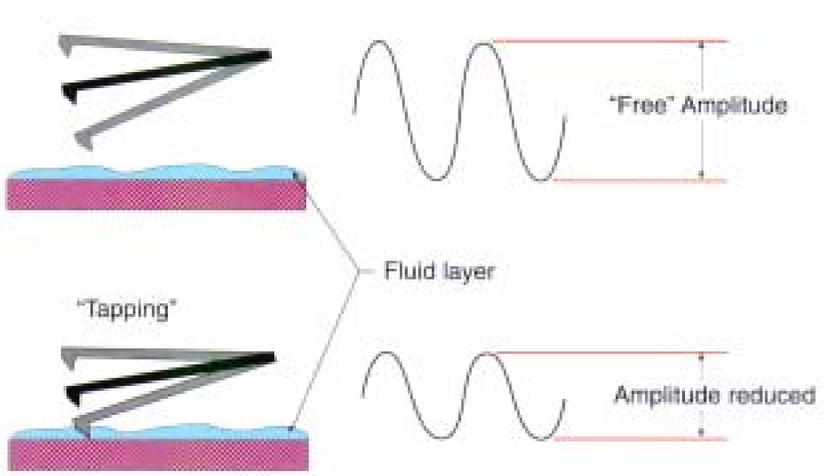

Phase image

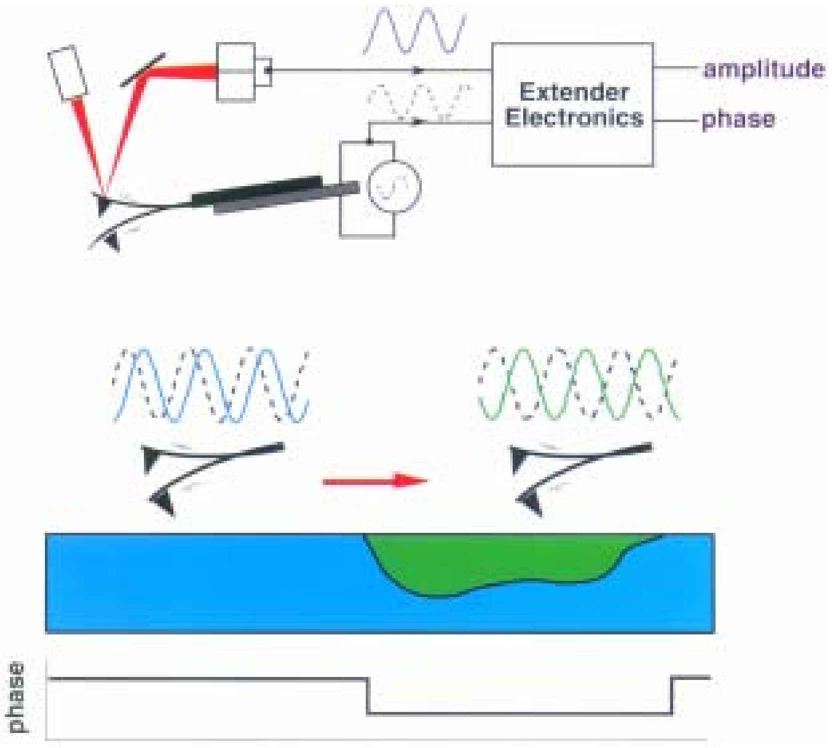

Fabrication of AFM probes

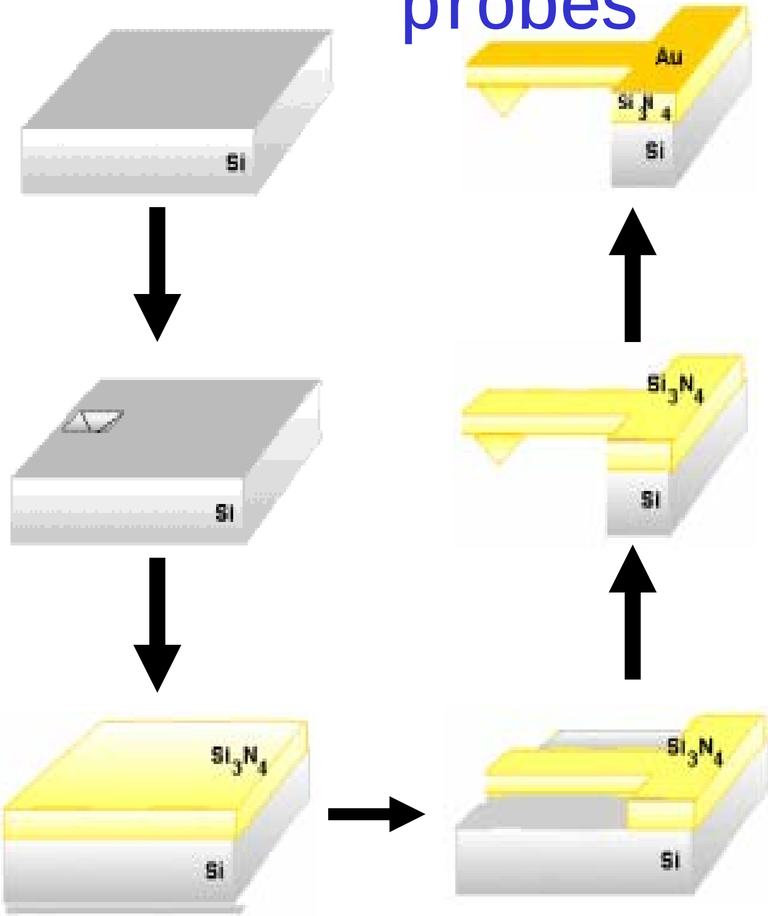

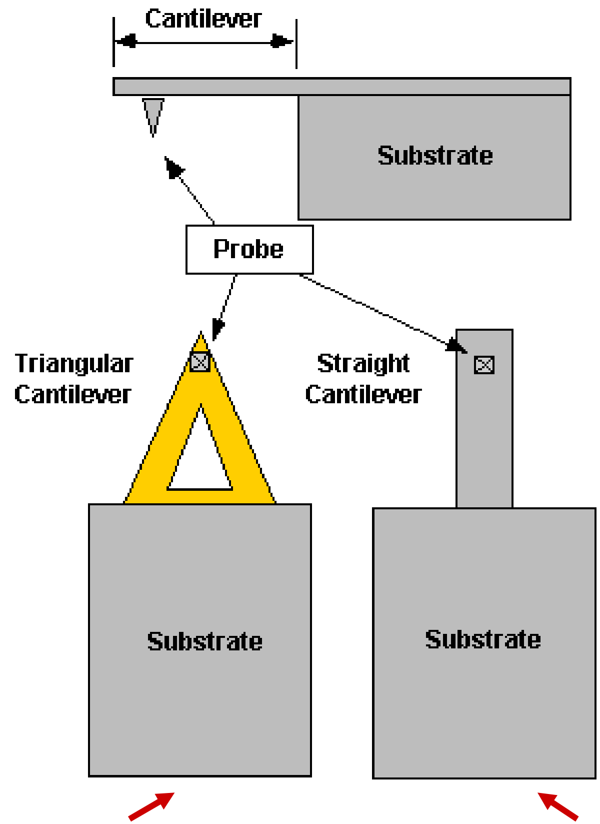

Typical Tip Dimensio	Typical Tip Dimension:
150μm x 30μm x 0.5μ	150μm x 30μm x 3μm
k ~ 0.1 N/m	f_r ~ 100 kHz
Materials: Si_3N_4	Materials: Si

V-shaped

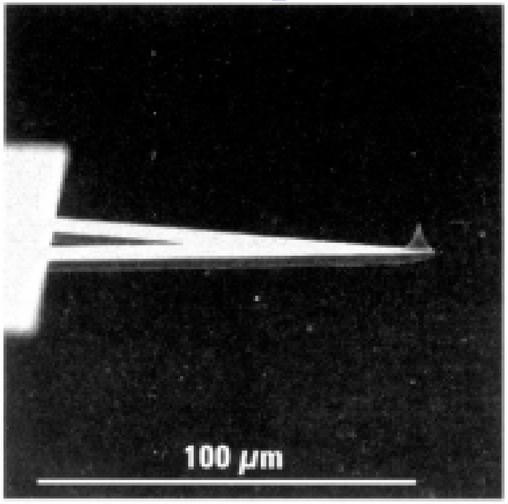

Materials: Si, SiO_2, Si_3N_4
Ideal Tips: hard, small radius of curvature, high aspect ratio

Pyramid Tip

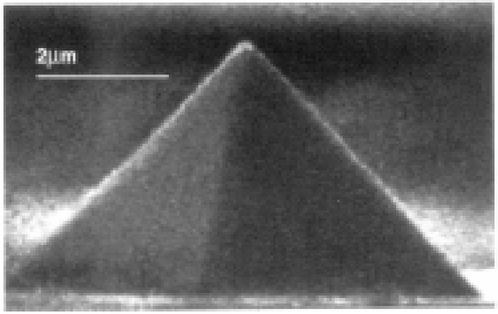

Ultrasharp Tip

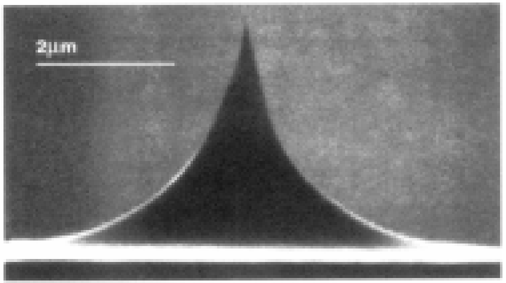

Rectangular-shaped

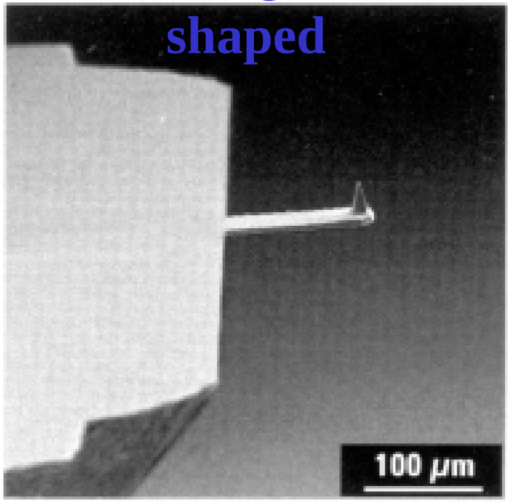

Diamond-coated Tip

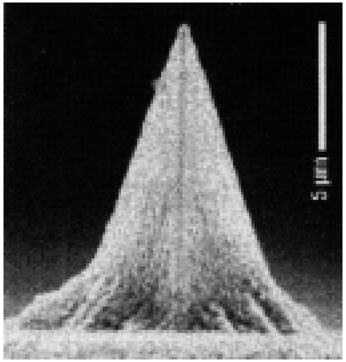

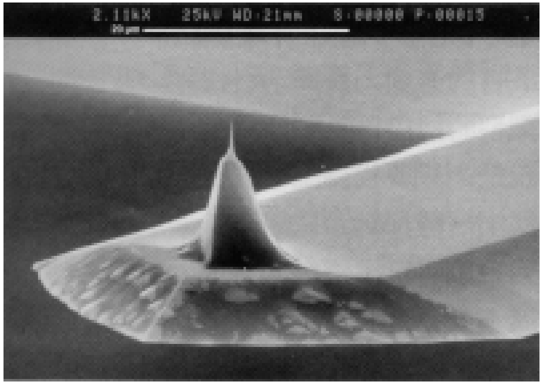

Effects of the Tip Shape

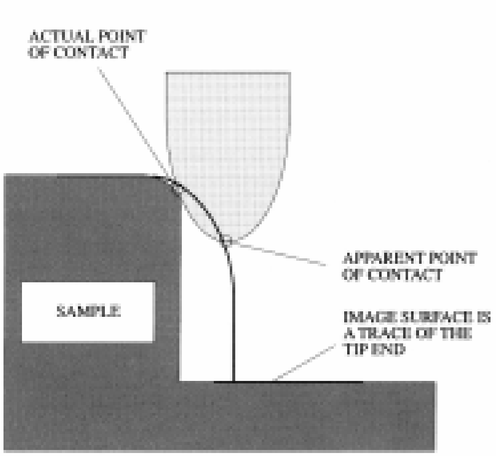

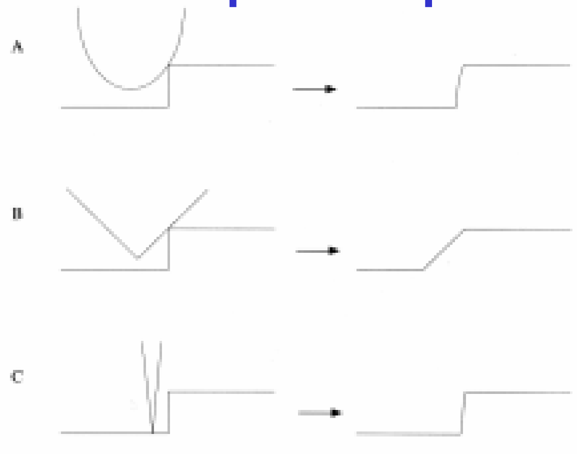

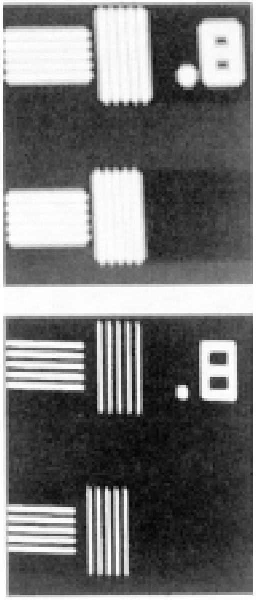

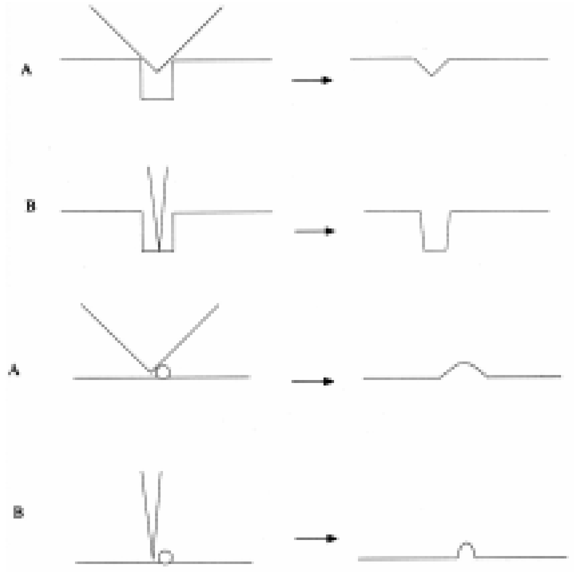

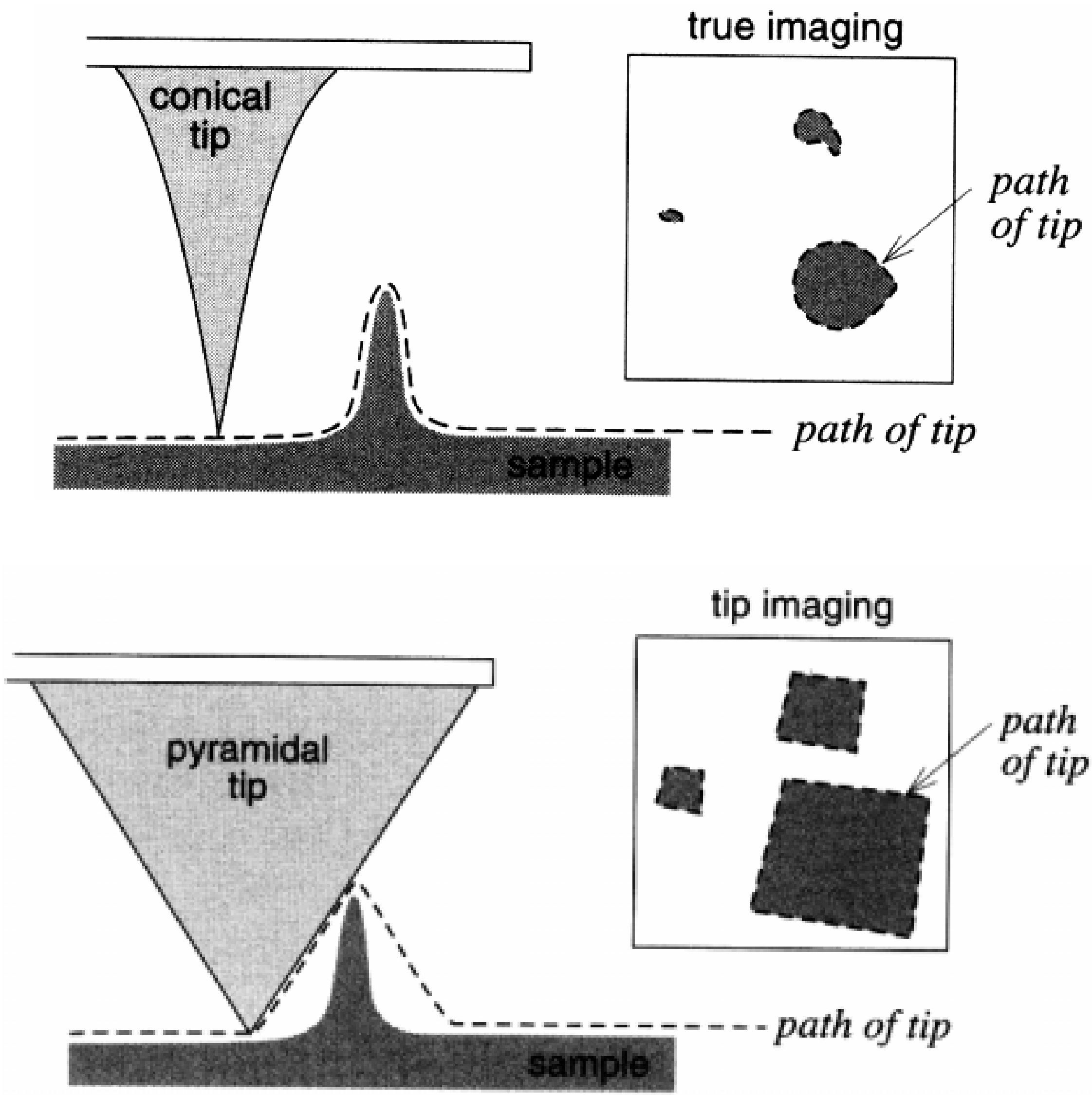
true imaging
conical tip
path of tip
path of tip
sample
tip imaging
pyramidal tip
path of tip
path of tip
sample

AFM Tip + Carbon Nanotube

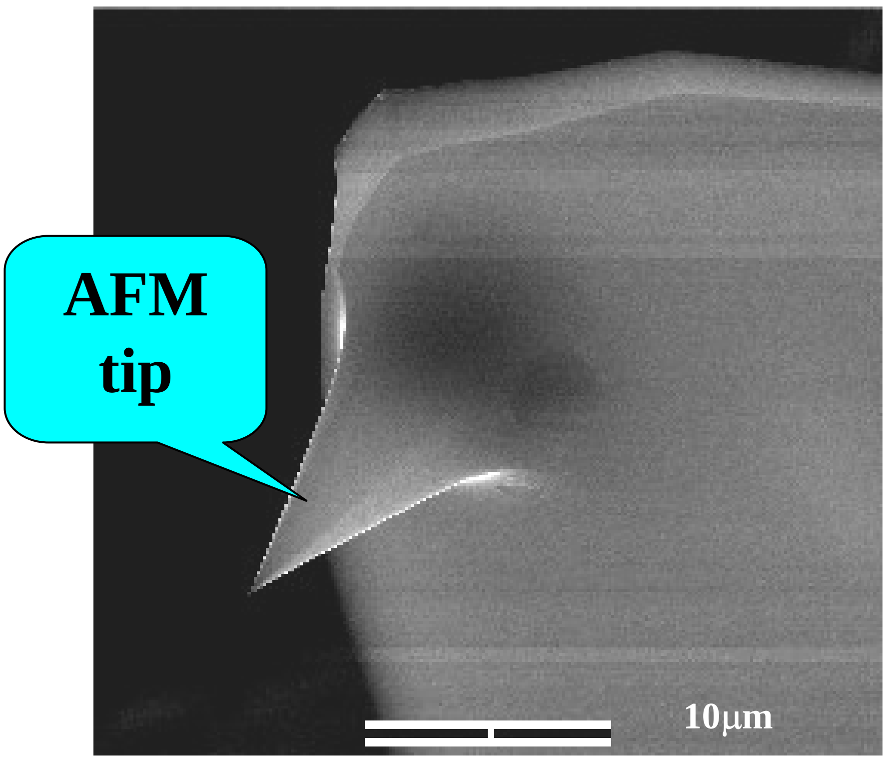

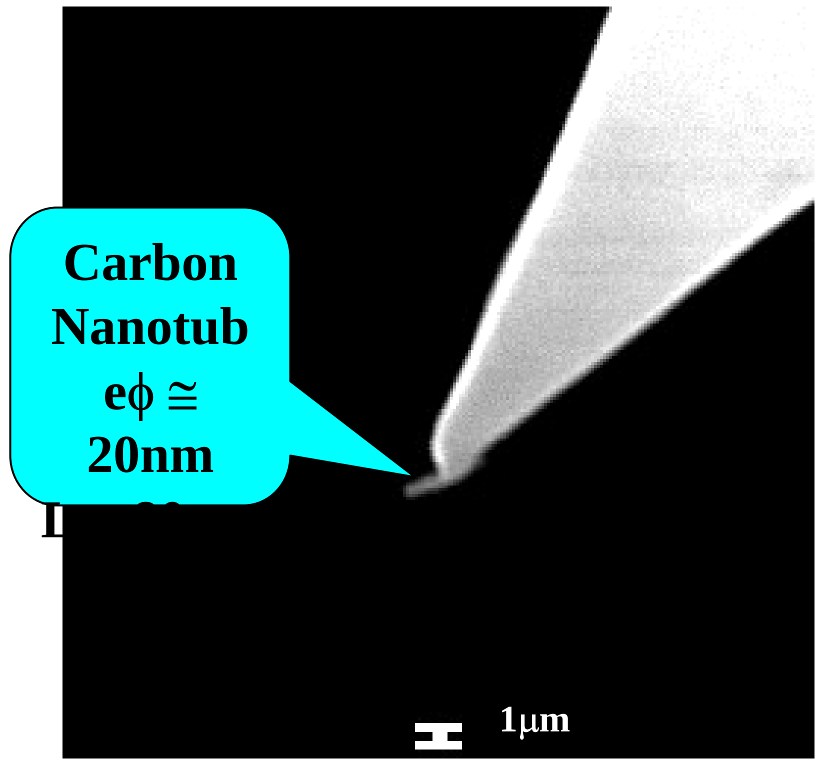

AFM images

CD pits

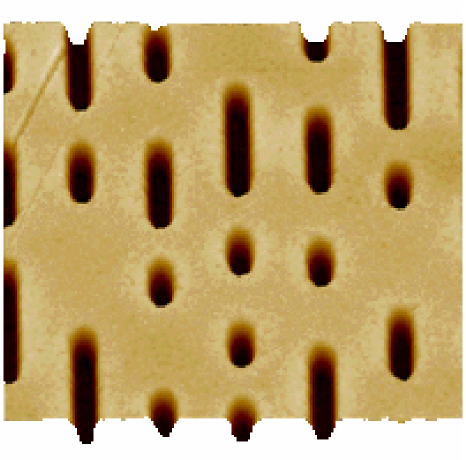

Integrated circuit

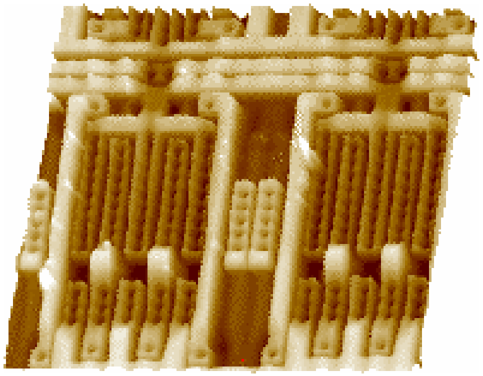

Chromosomes

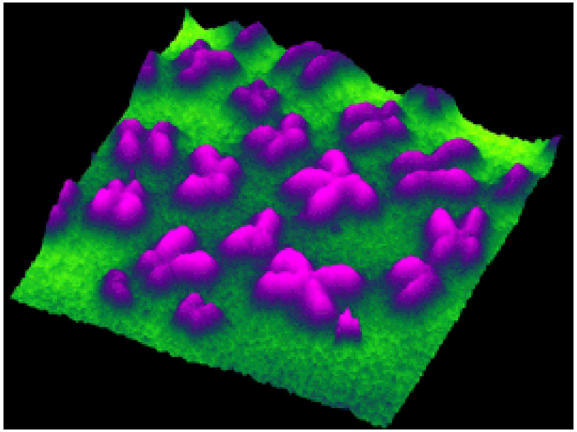

DVD pits

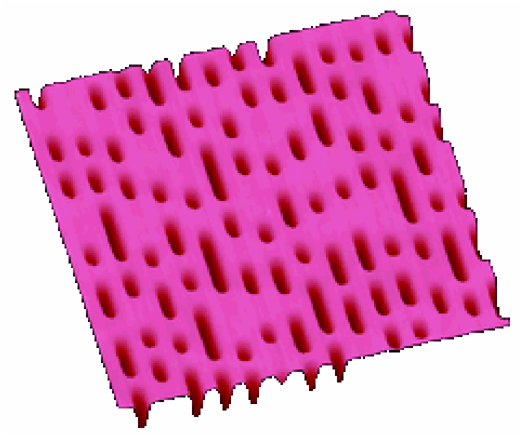

Bacteria

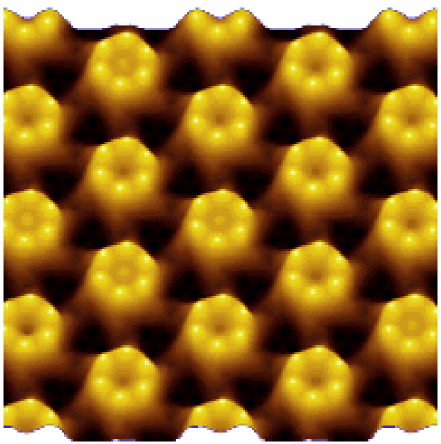

DNA

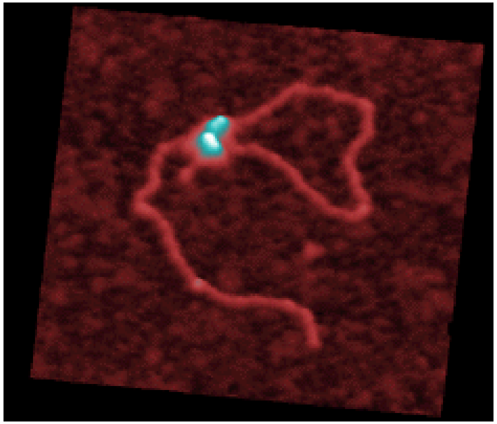

Height image **Phase**

Image

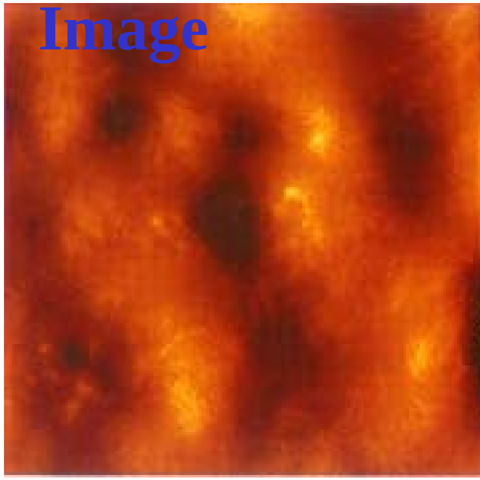

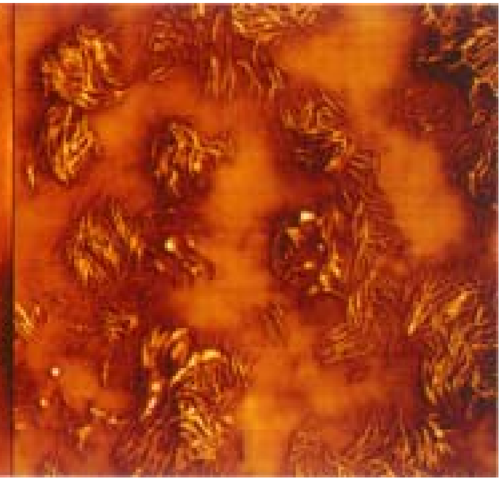

Phase image **Lateral force Image**

MoO_3 on MoS_2

Lateral Force Microscopy

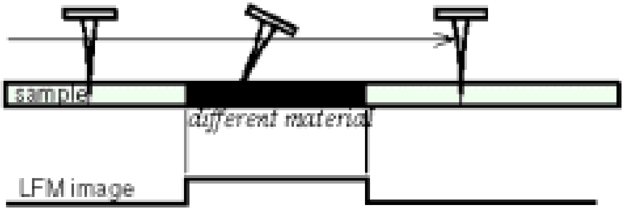

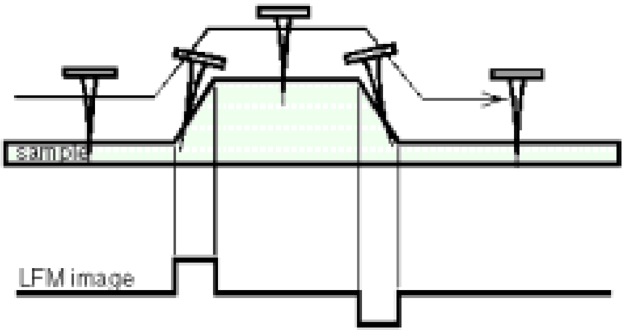

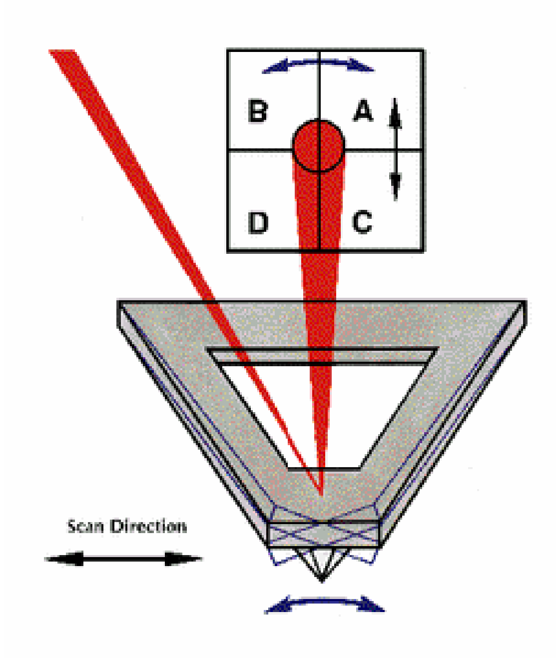

(A+C) – (B+D)

Topography

12 μm

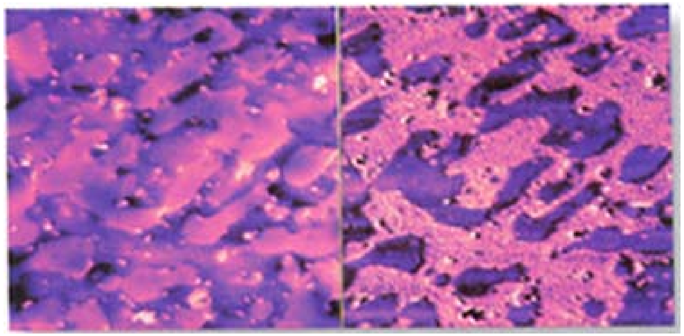

LFM image

Nature rubber/EDPM blend

Atomic Image of Si(111)-(7X7) Taken with AFM

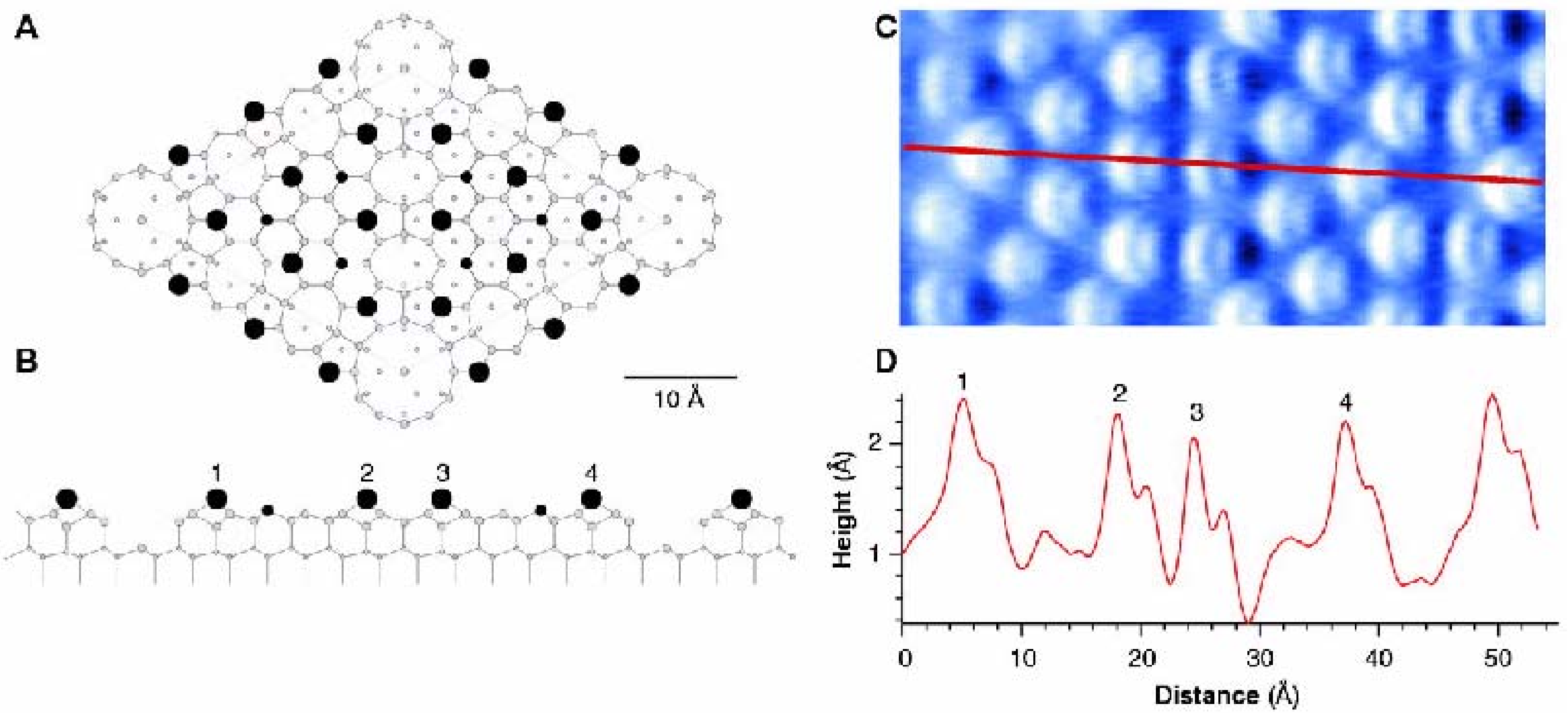

F.J. Giessibl *et al.*, Science <u>289</u>, 422 (2000)

Force-Distance Curve

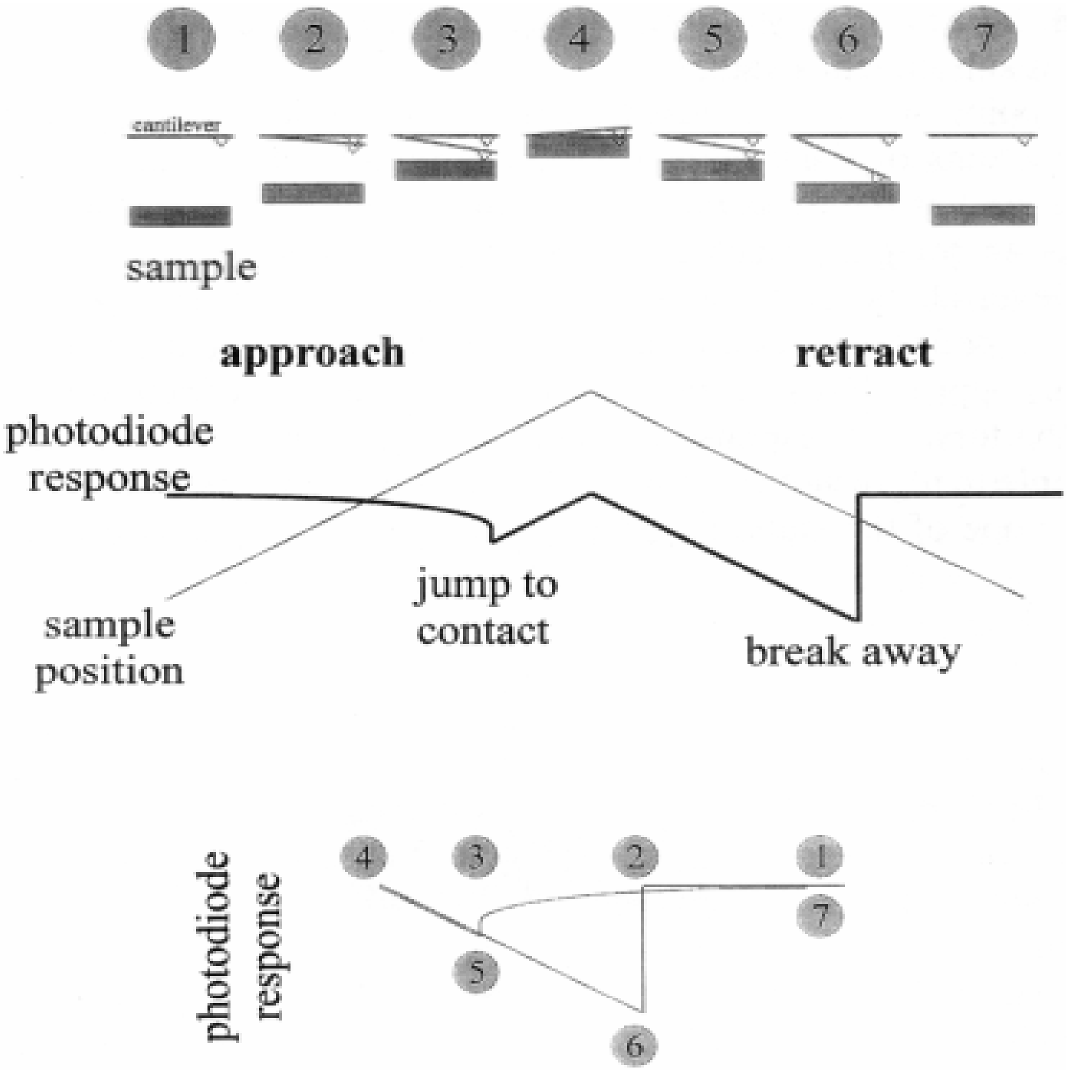

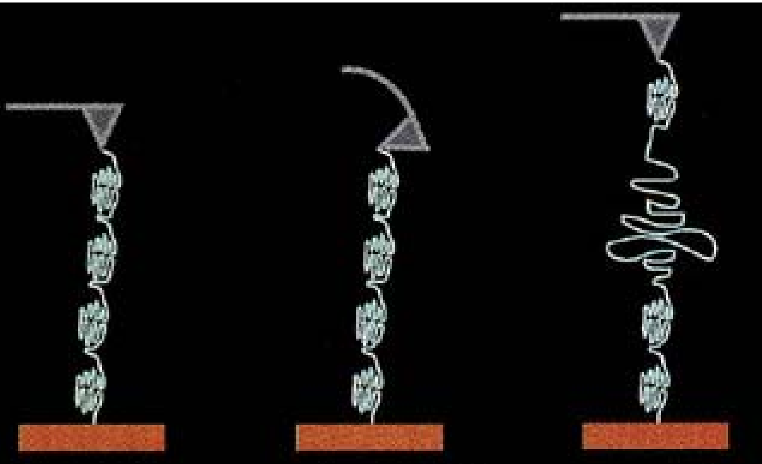

Force measurement of an unfolding complex molecule.

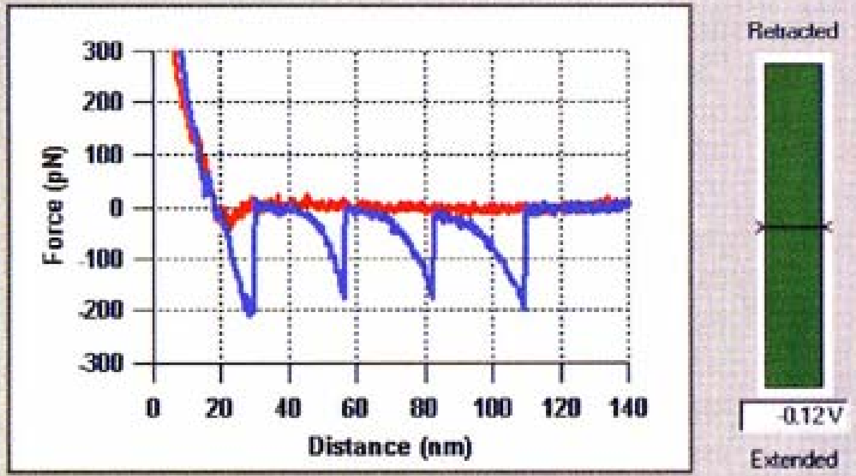

Advanced graphical user interface shows titin muscle molecule force curve.

Measurement of Mechanical Properties

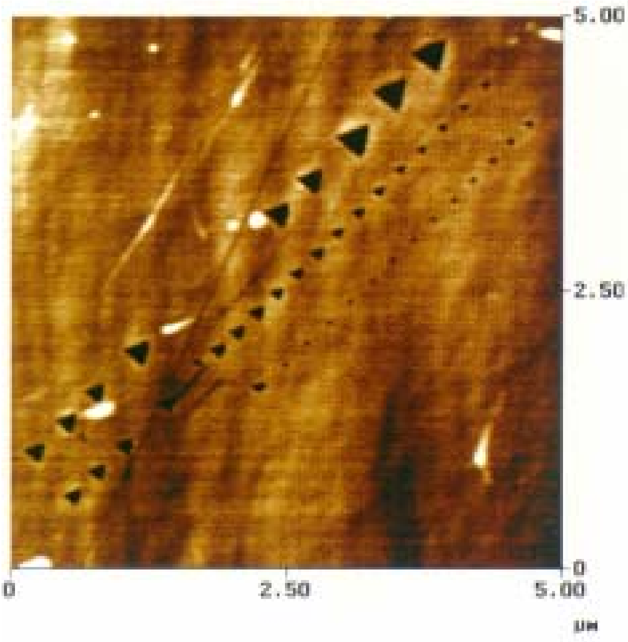

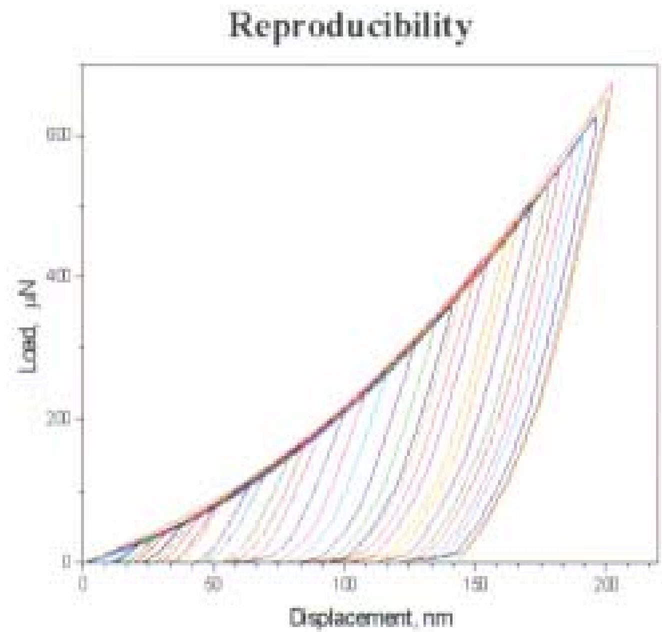

1. The load-displacement curves provide a “mechanical fingerprint” of material’s response to deformation, from which parameters such as hardness and young’s modulus of elasticity can be determined.

2. In measuring the mechanical properties of thin coated system, the size of contact impression should be kept small relative to the film thickness.

Nanolithography of Tapping-Mode AFM

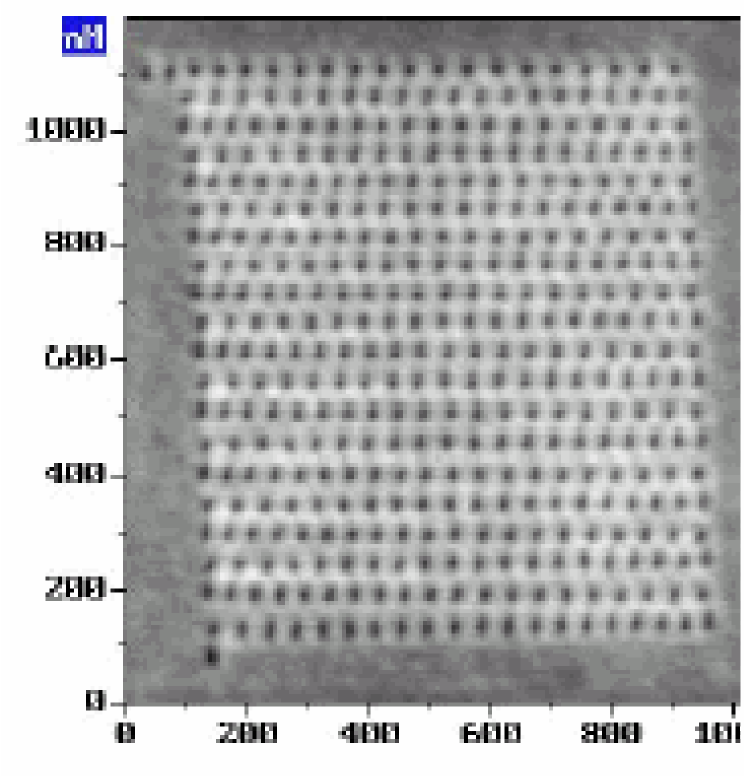

(1.2 μ m╳ 1.2 μ m)

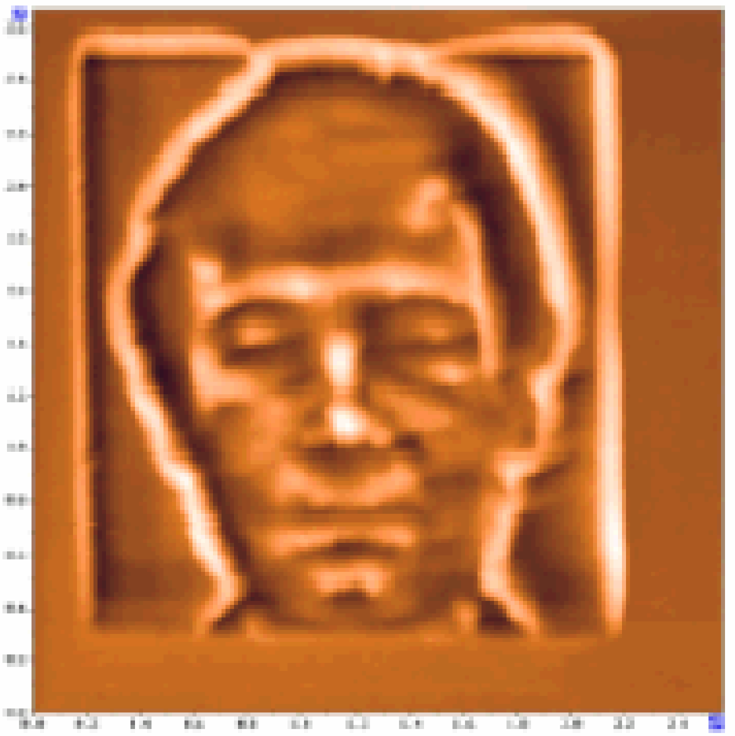

(2.5 μ m╳ 2.5 μ m)

Image of polycarbonate film on silicon surface

Nano-Lithography with an AFM tip

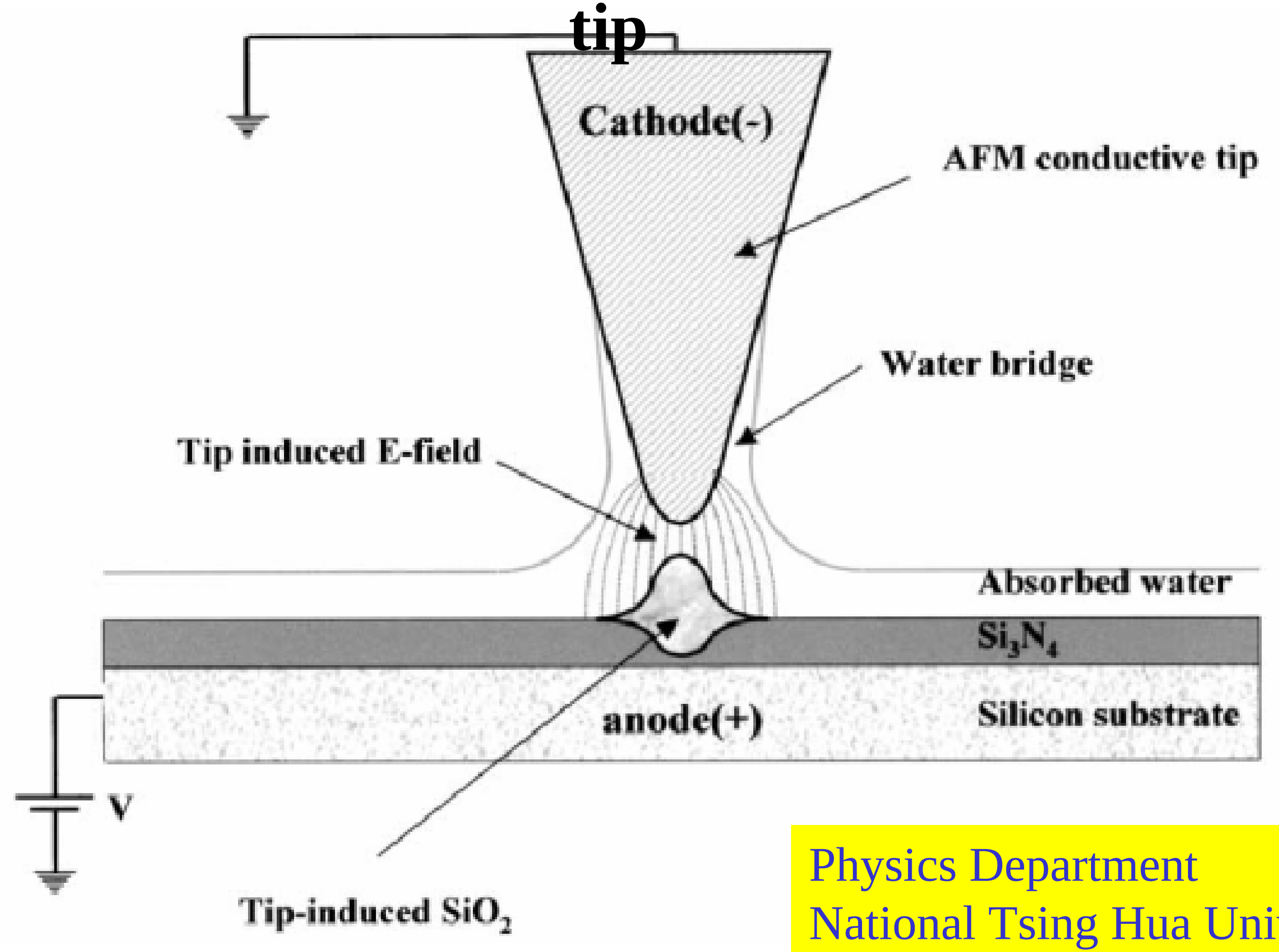

Physics Department
National Tsing Hua University

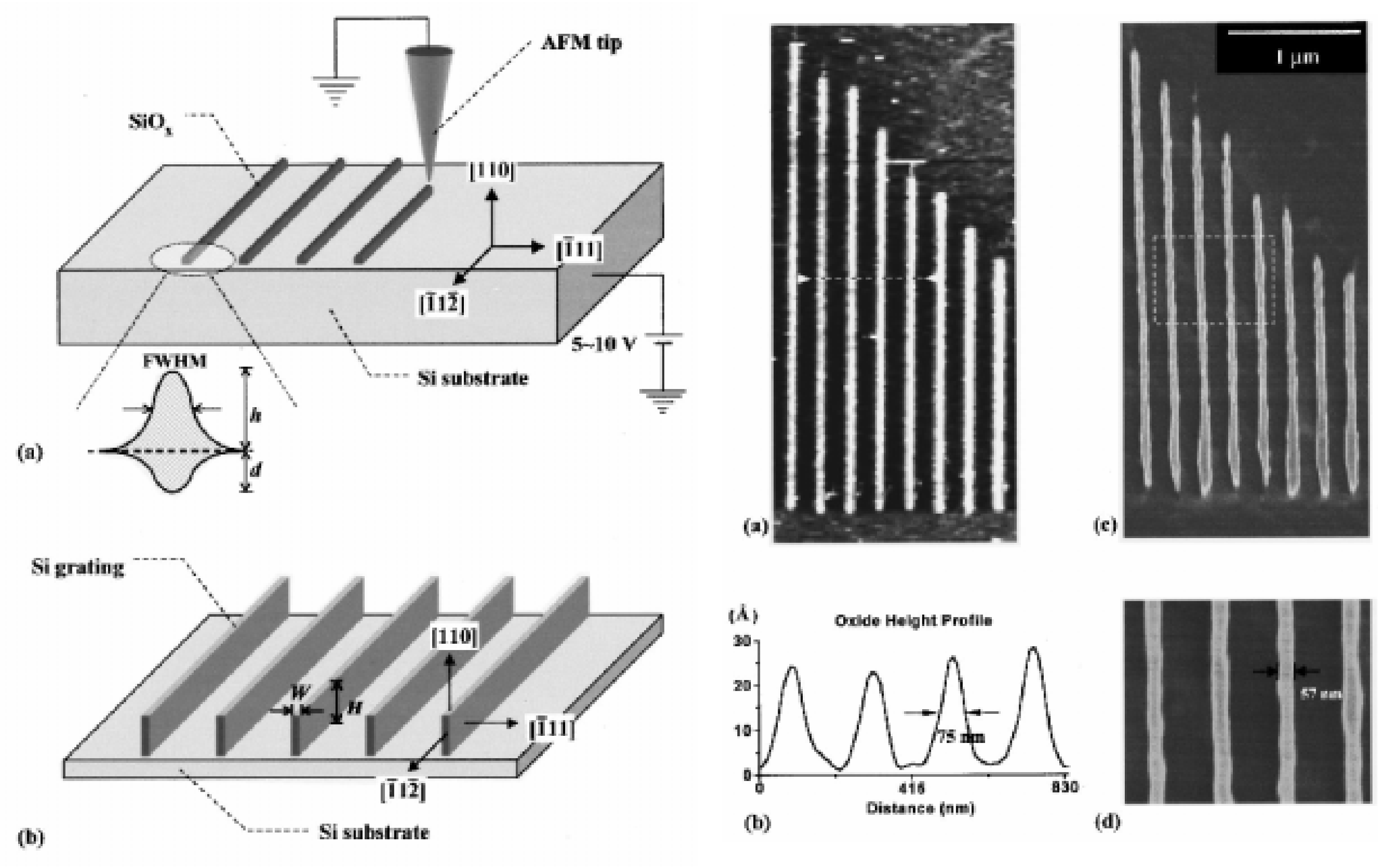

F.S.-S. Chien *et al*., APL <u>75</u>, 2429 (1999)

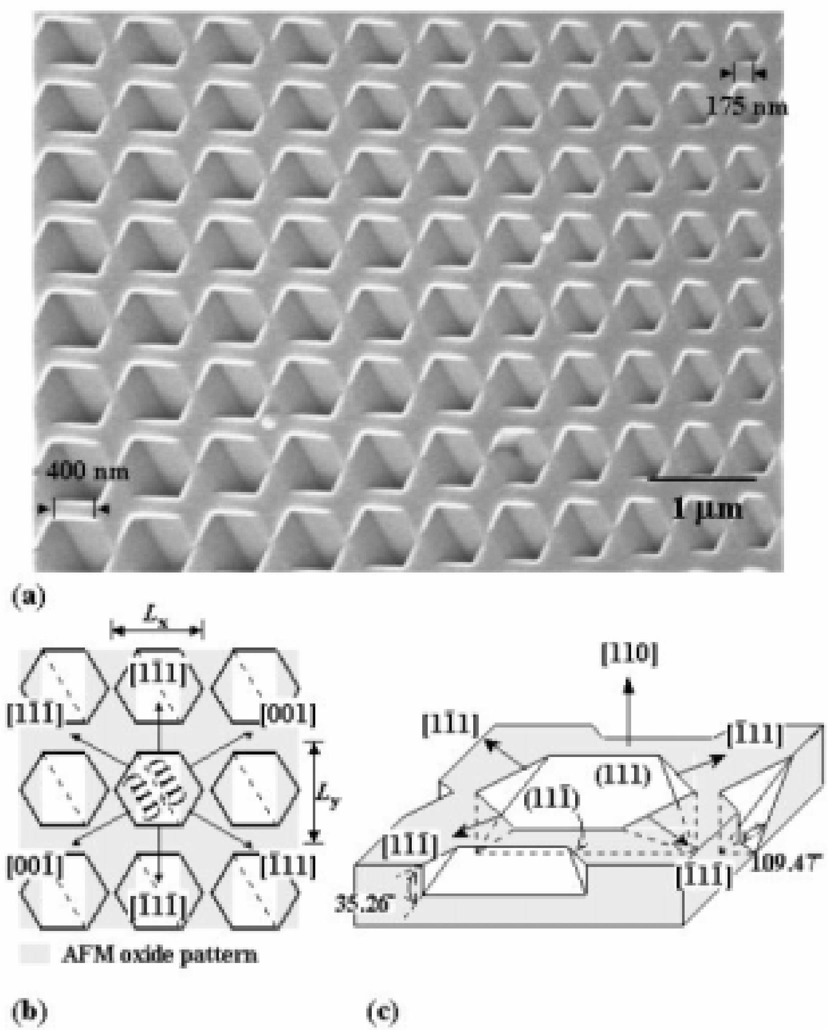

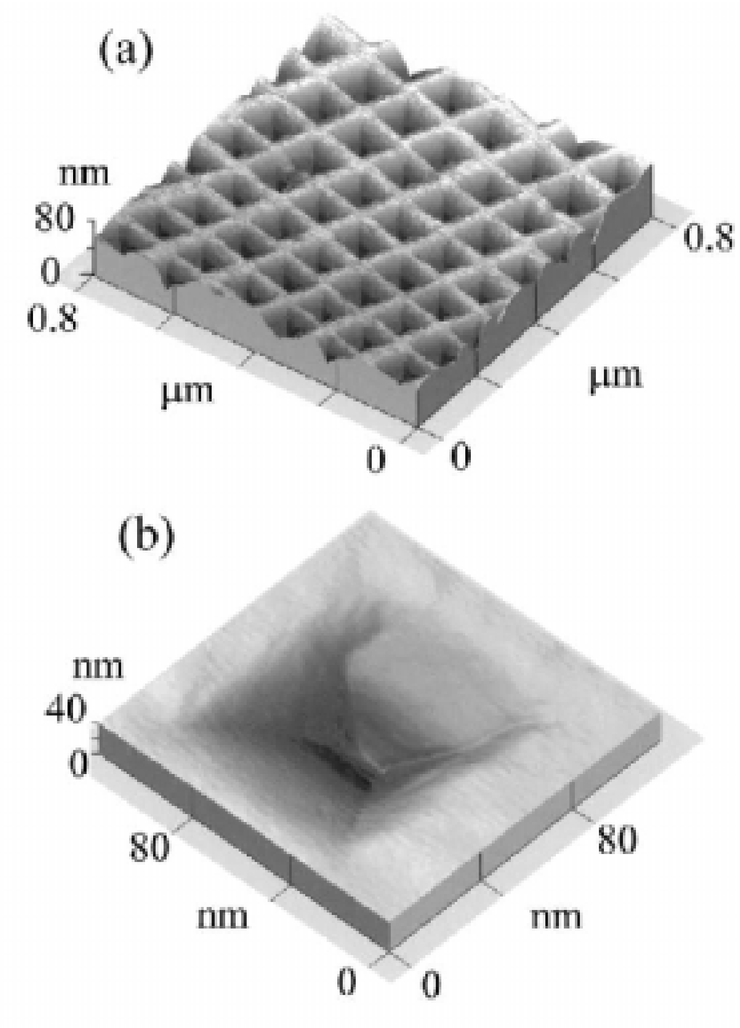

果尚志 , Physics Dept., National Tsing Hua University

Magnetic Force Microscopy (MFM)

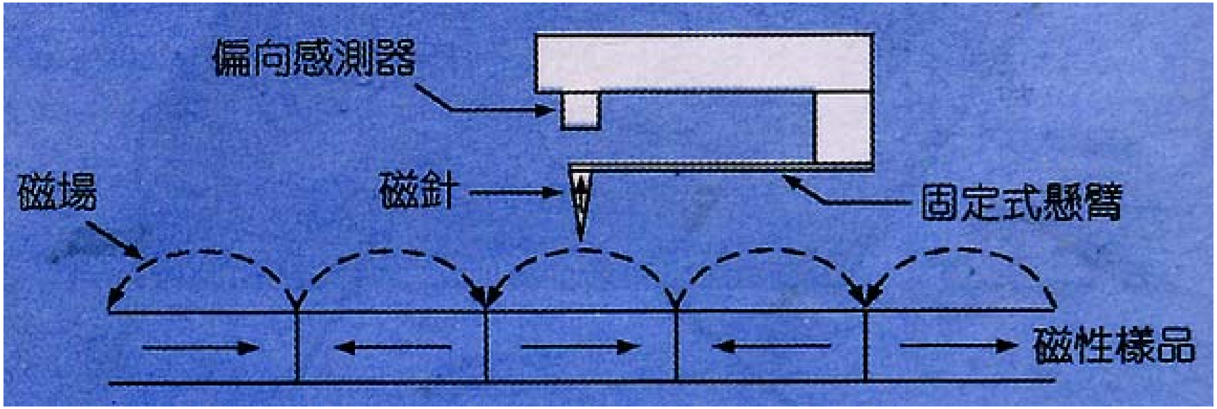

$$F = (m \cdot \nabla)H$$

Tips: silicon probes are magnetically sensitized by sputter coating with a ferromagnetic material.

Resolution: 10 ~ 25 nm.

Applications: hard disks, magnetic thin film materials, micromagnetism.

MFM Images

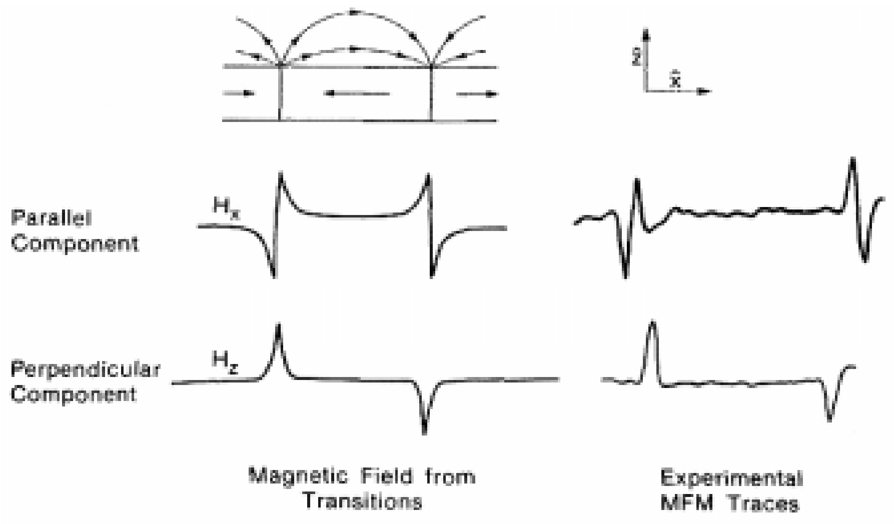

z
x
Parallel Component
H_x
Perpendicular Component
H_z
Magnetic Field from Transitions
Experimental MFM Traces

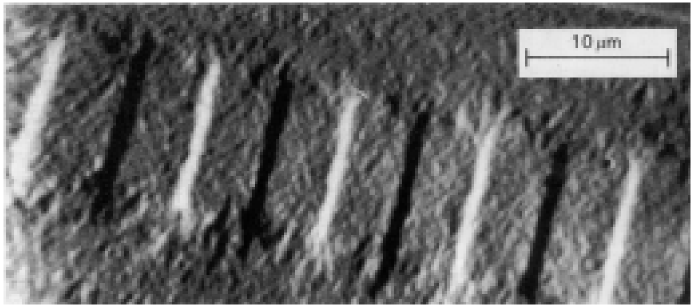

10 μm

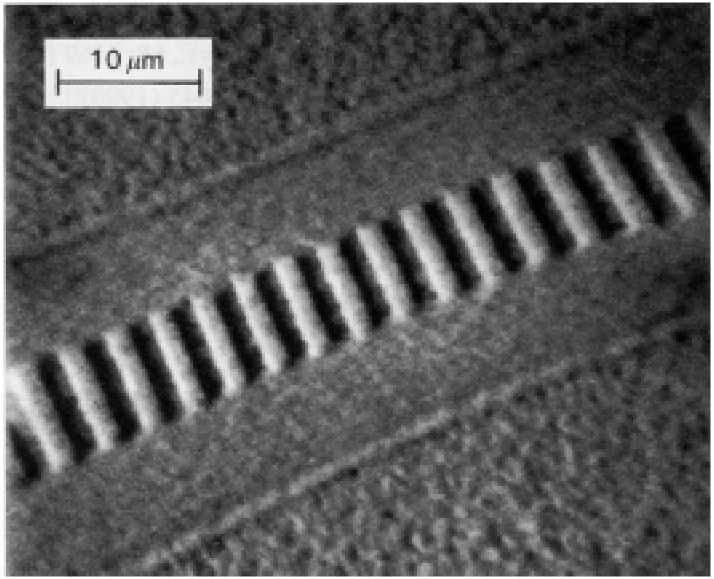

10 μm

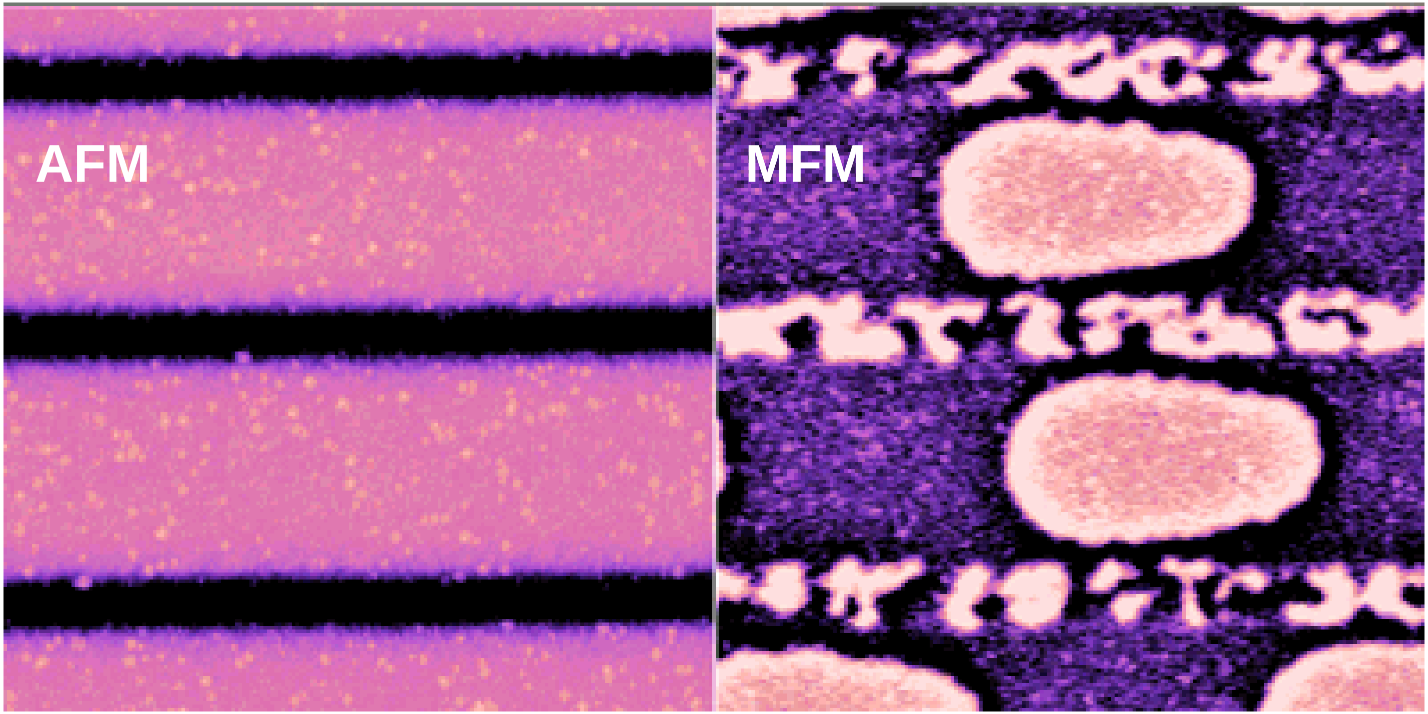

Bits (50 nm) on a magneto-optical disk

Scan area (5 μm× 5 μm)

Scanning Thermal Microscopy (SThM)

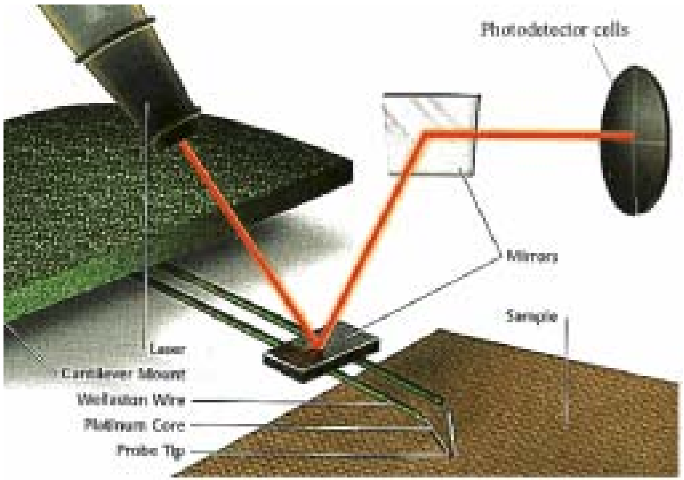

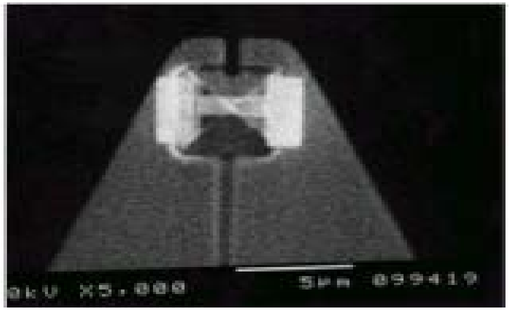

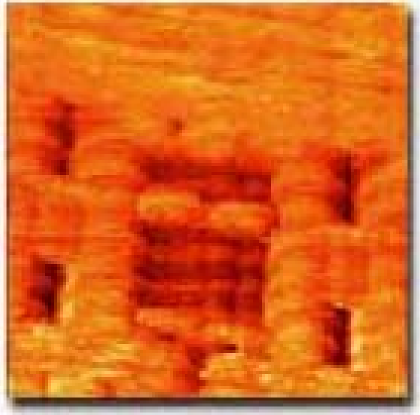

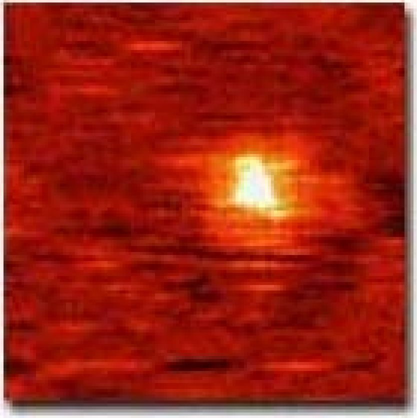

Near-field Scanning Optical Microscopy (NSOM)

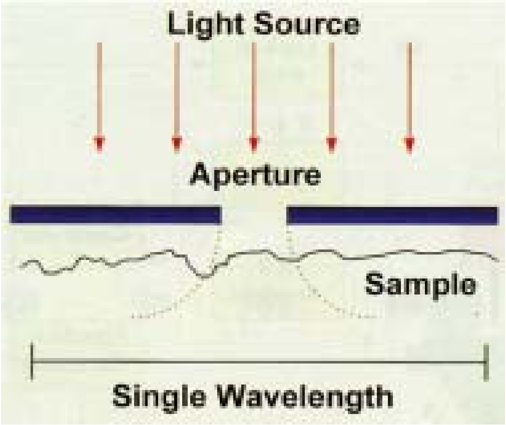

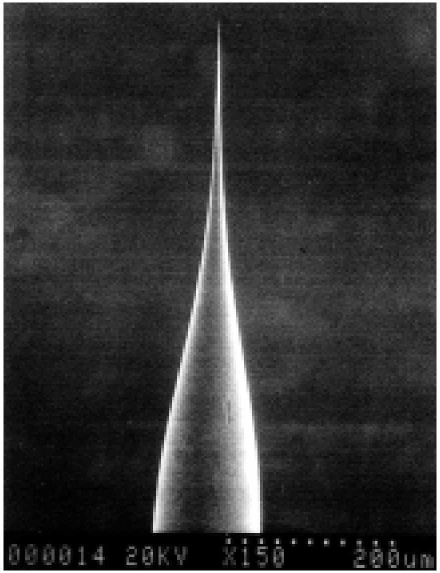

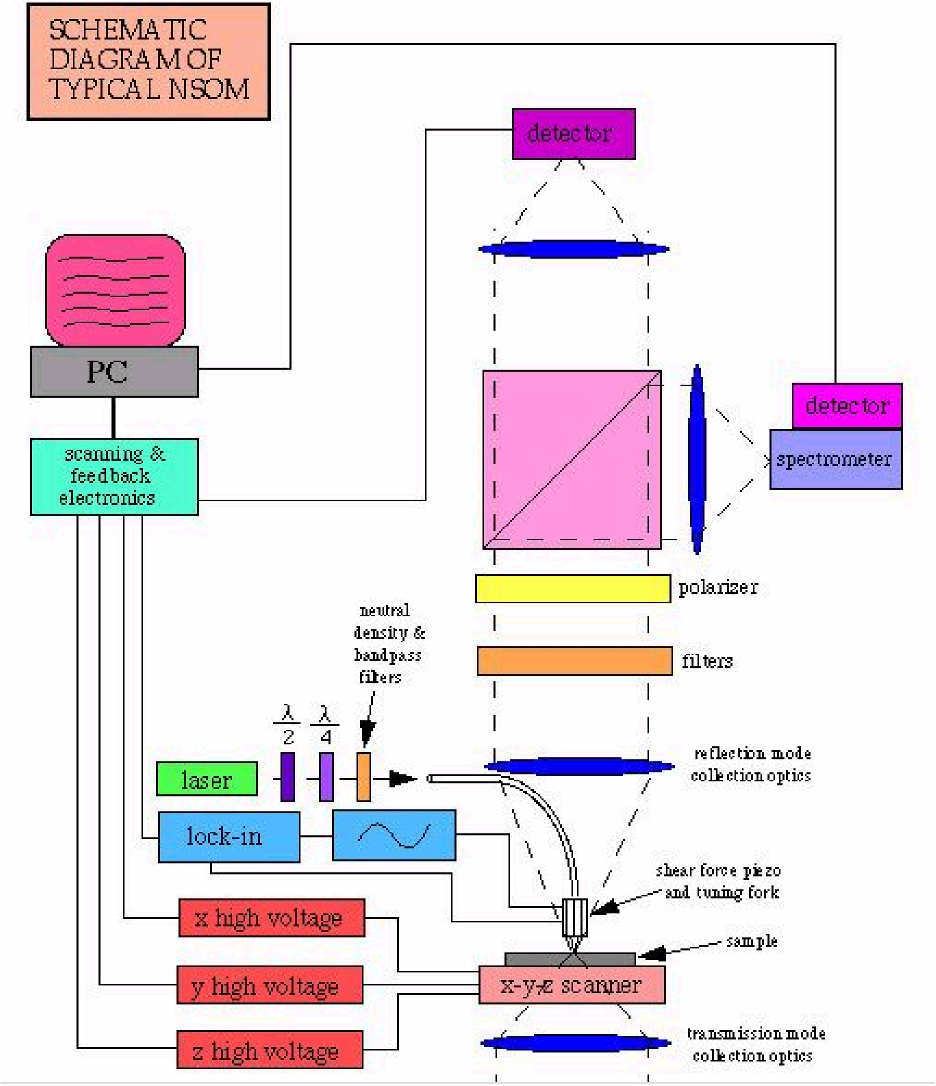

Topography **NSOM Image**

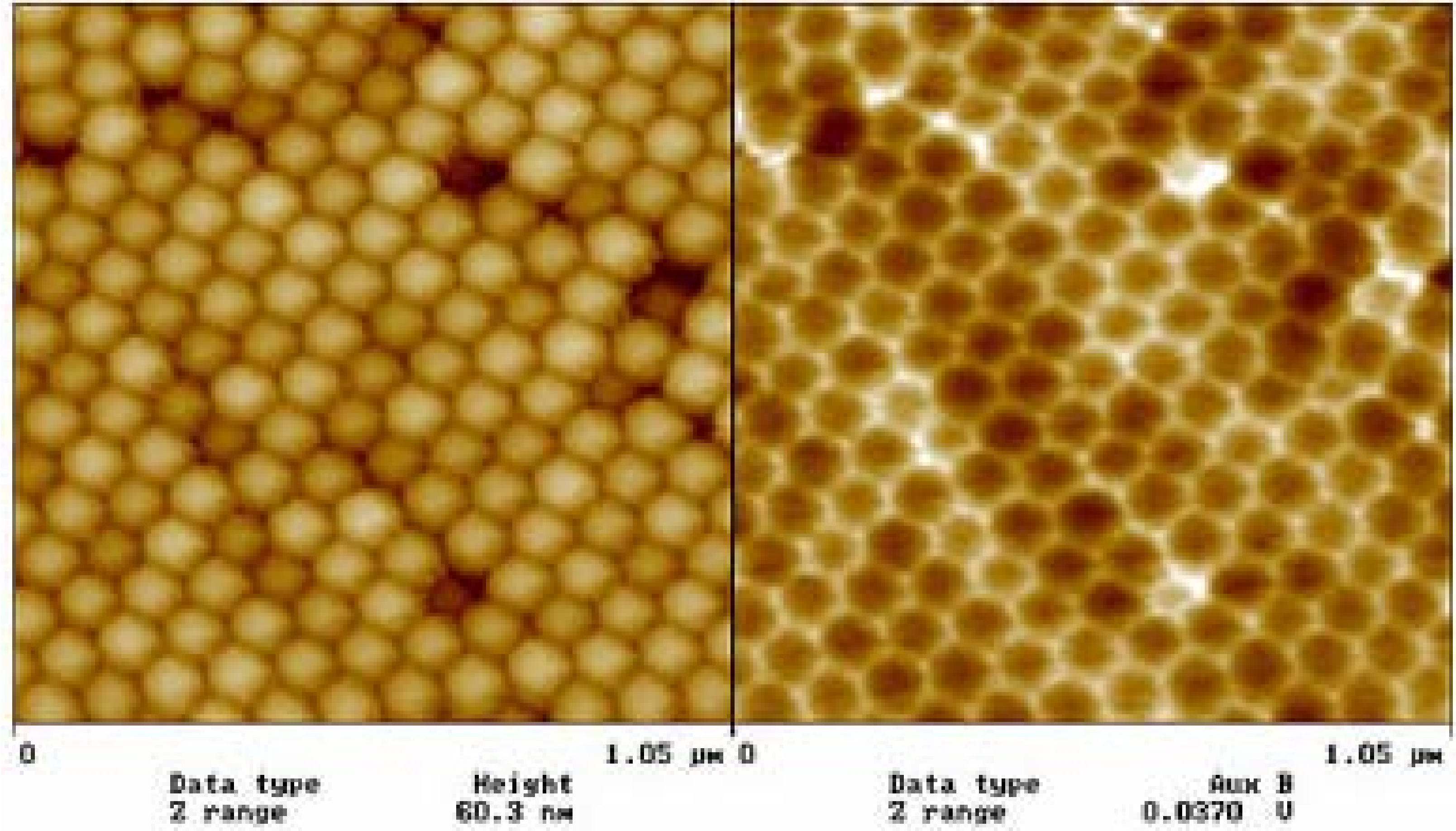

Polystyrenes of 100 nm on glass

Scanning Capacitance Microscopy (SCM)

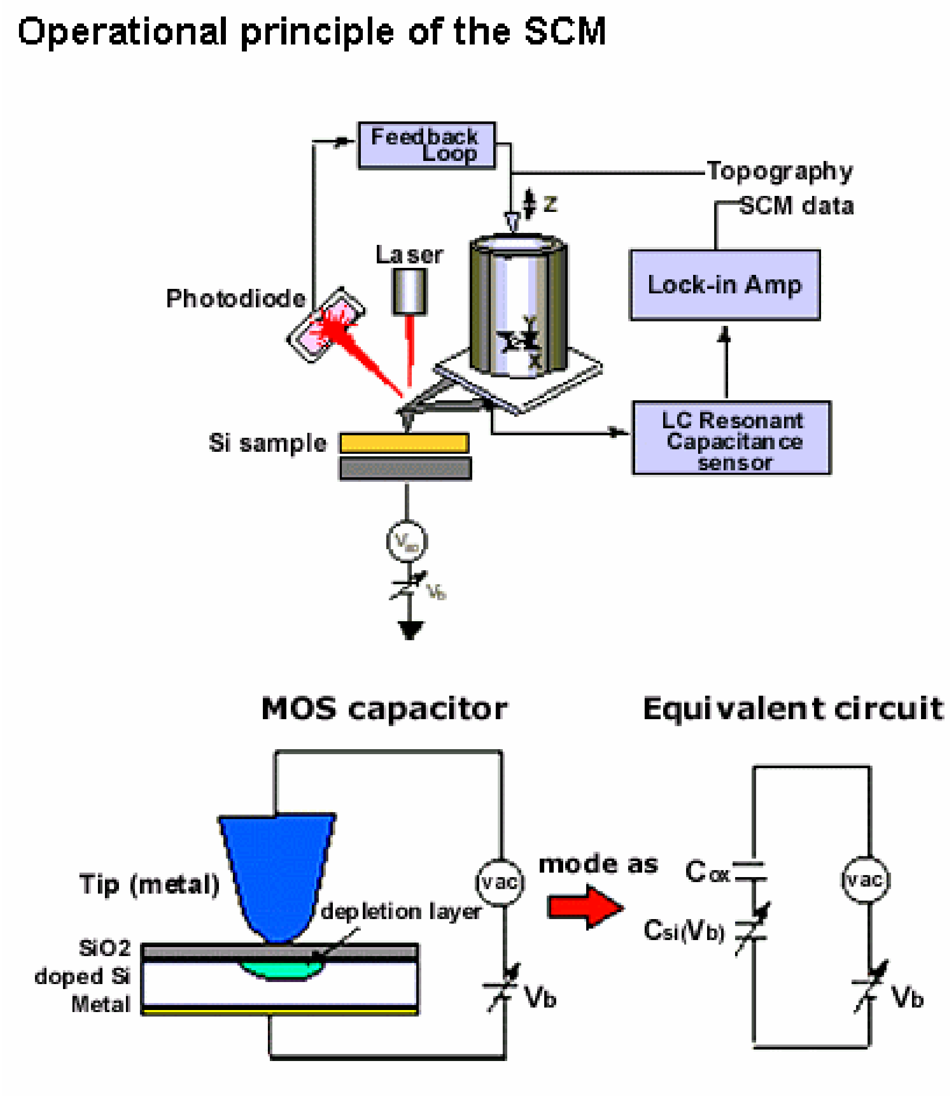

1. **Most SCMs are based on contact-mode AFM with a conducting tip.**
2. **In SCM, the sample (or the metallic tip) is covered with a thin dielectric layer, such that the tip-sample contact forms a MIS capacitor, whose C-V behavior is determined by the local carrier concentration of the semiconductor sample.**
3. **By monitoring the capacitance variations as the probe scans across the sample surface, one can measure a 2D carrier concentration profile.**
4. **One usually measures the capacitance variations (dC/dV), not the absolute capacitance values.**
5. **No signal is measured if the probe is positioned over a dielectric or metallic region since these regions cannot be depleted.**

References:

1. C.C. Williams, Annu. Rev. Mater. Sci. **29**, 471 (1999).
2. P.D. Wolf et al., J. Vac. Sci. Technol. B **18**, 361 (2000).
3. R.N. Kleiman et al., J. Vac. Sci. Technol. B **18**, 2034 (2000).
4. H. Edwards, et al., J. Appl. Phys. **87**, 1485 (2000).
5. J. Isenbart et al., Appl. Phys. A **72**, S243 (2001).

SCM CV Curve

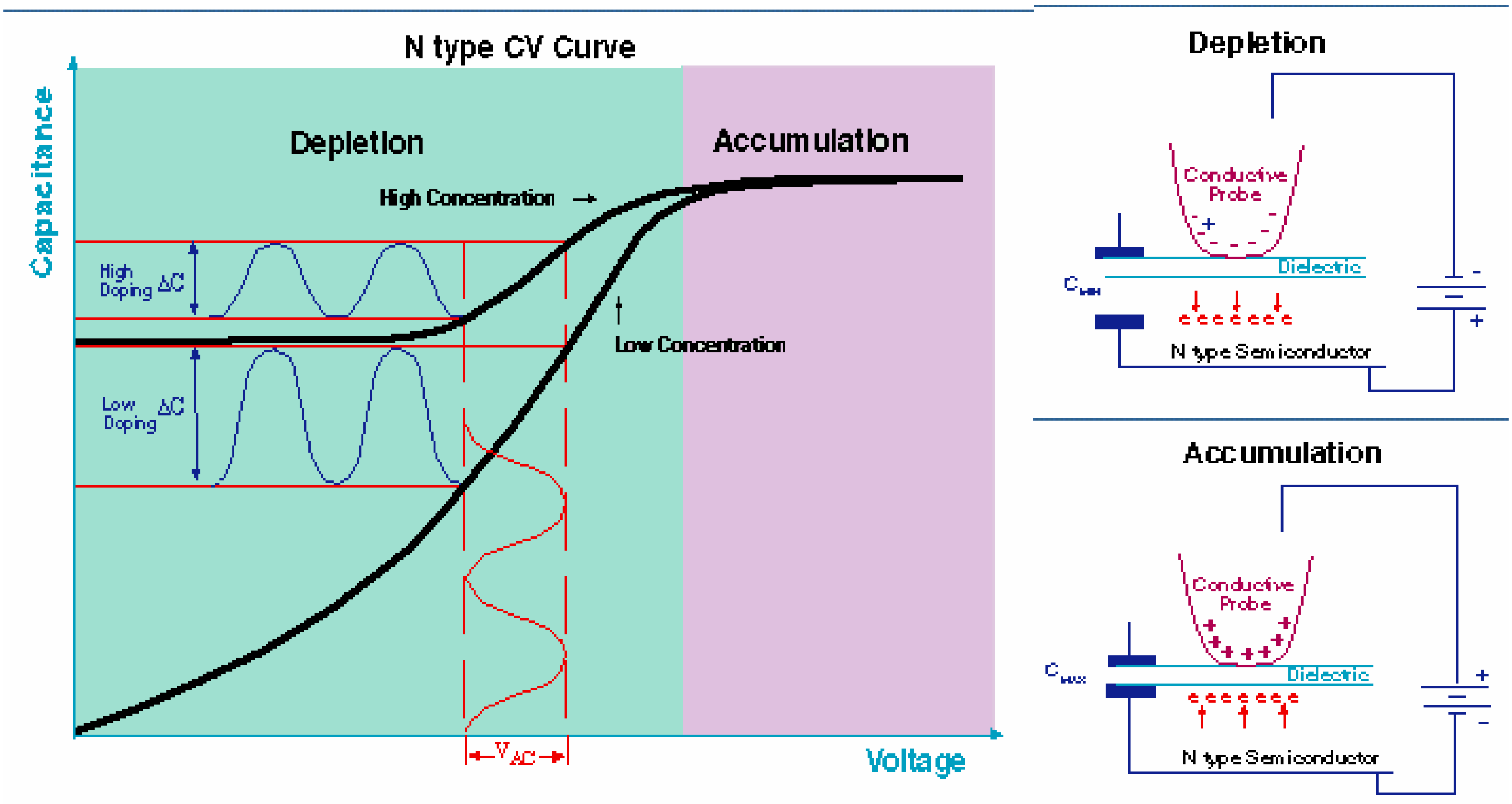

N type CV Curve
Capacitance
Depletion
Accumulation
High Concentration
High Doping ΔC
Low Doping ΔC
Low Concentration
V_AC
Voltage
Depletion
Conductive Probe
Dielectric
C_min
N type Semiconductor
Accumulation
Conductive Probe
Dielectric
C_max
N type Semiconductor

Scanning Capacitance Microscopy

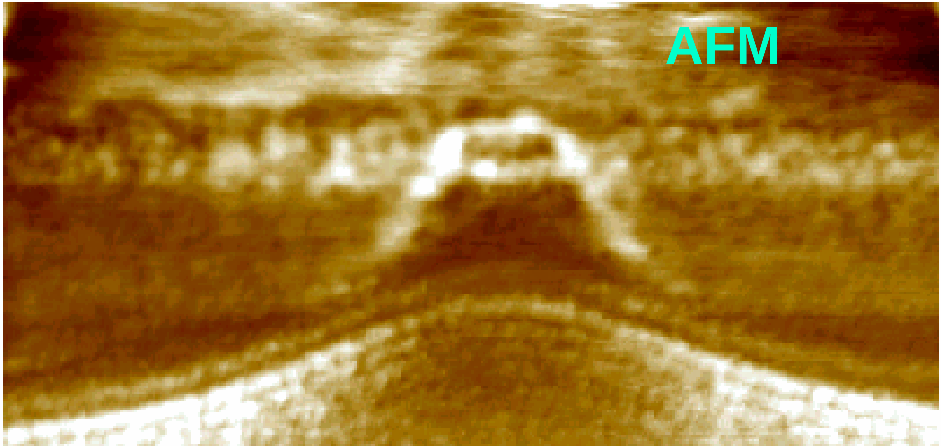

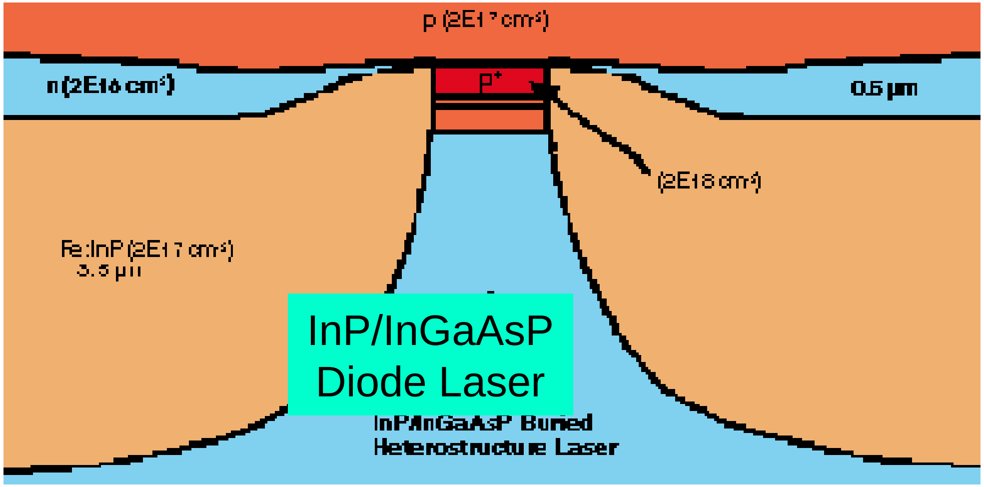

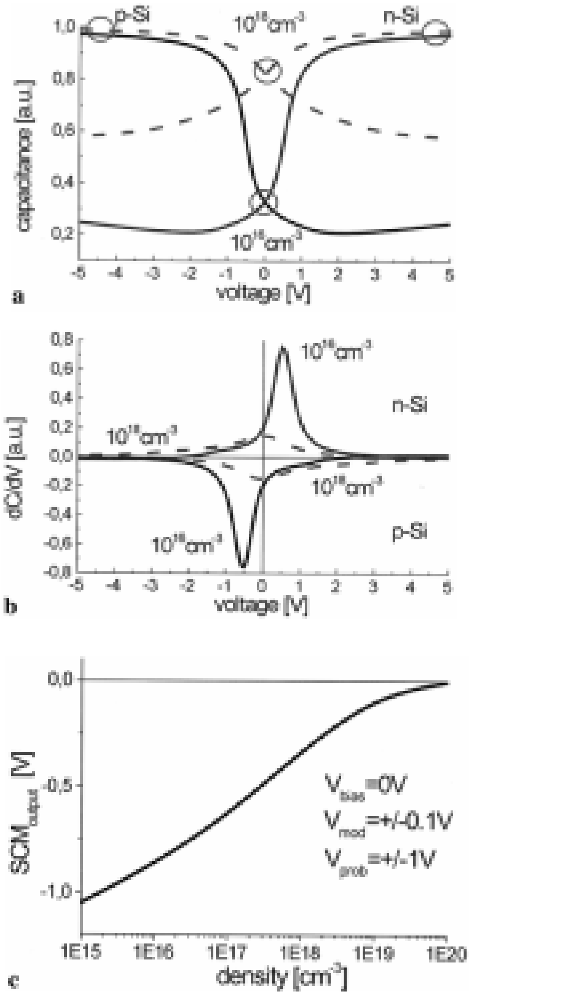

Fig. 2a–c. 3D simulations of SCM on homogeneously doped samples. The tip ($r_a = 25$ nm, $r_i = 25$ nm, $\alpha = 20°$) is modelled in cylindrical coordinates; $d_{Ox} = 10$ nm. **a** $C(V)$ curves on *p*- and *n*-doped silicon with dopant concentrations of 10^{16} cm^{-3} and 10^{18} cm^{-3}, respectively. **b** The corresponding $dC/dV(V)$ curves are calculated analytically. **c** The calibration curve is calculated from $C(V)$-curve simulations. The SCM output is calculated as $\Delta C/\Delta V(V)$ at $V_{bias} = 0$ V taking $V_{mod} = \pm 0.1$ V and $V_{prob} = \pm 1$ V into account

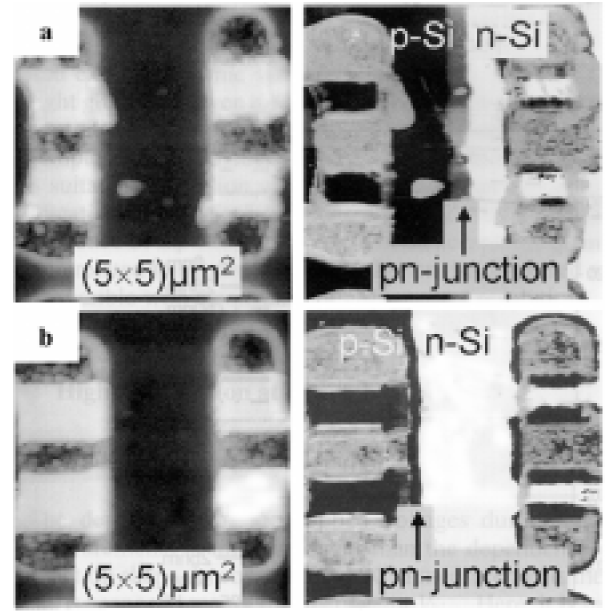

Fig. 3a,b. Failure analysis of an industrial device by means of SCM. Topography (*left-hand side*) and SCM image (*right-hand side*) are taken simultaneously. **a** Well-operating device with the *pn* junction implanted in the middle between the poly-silicon contacts. **b** Defective device with the *pn* junction shifted to the left-hand contacts. Both devices were measured at the same V_{bias} corresponding to the "zero voltage" (see text)

J. Isenbart et al., Appl. Phys. A **72**,

S243 (2001).

1. **The SCM has proven its potential for the analysis of 2D dopant profiles on a scale down to less than 50 nm.**
2. **The quantification of a measured dopant profile is still difficult due to the influence of parameters of the sample, the tip shape, and the capacitance sensor including the applied voltages.**
3. **The properties of the sample, e.g. the roughness of the surface (fluctuation of the oxide thickness), the density of charged impurities and traps in the oxide layer and mobile surface charges, are mainly determined by the sample-preparation procedure.**
4. **The most important influence on the measurements is due to the probing voltage of the capacitance sensor and the applied bias voltage.**
5. **In SCM, not the dopant concentration, but rather the local charge-carrier concentration is measured because only the mobile carriers can contribute to C(V) and thus only the local charge-carrier distribution can be detected.**

Probes of various functions

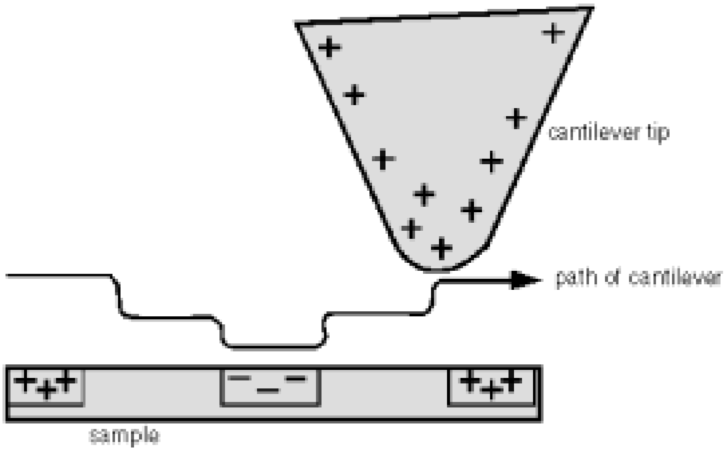

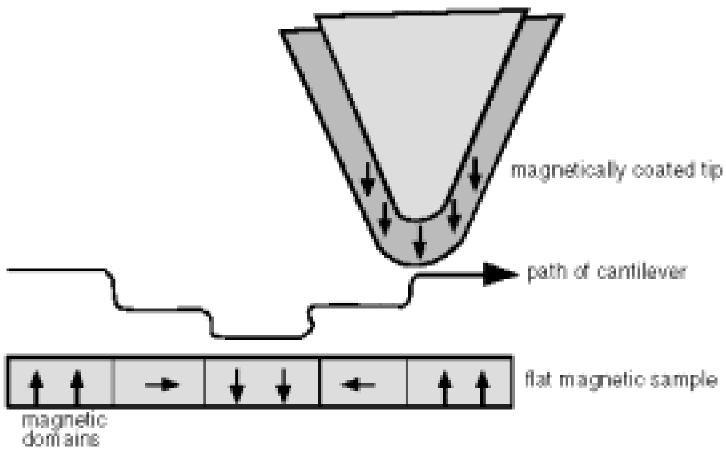

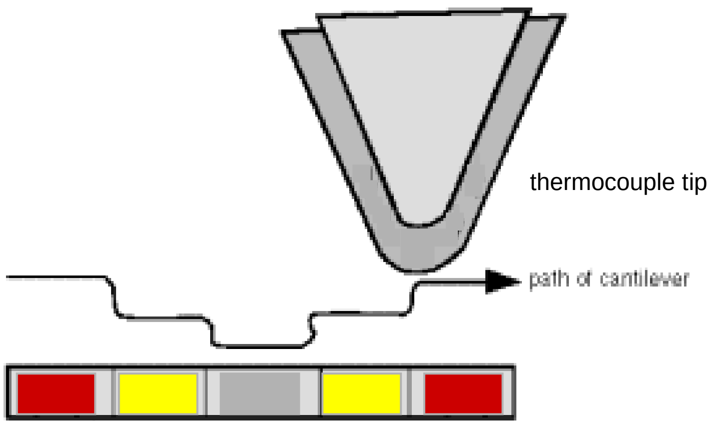

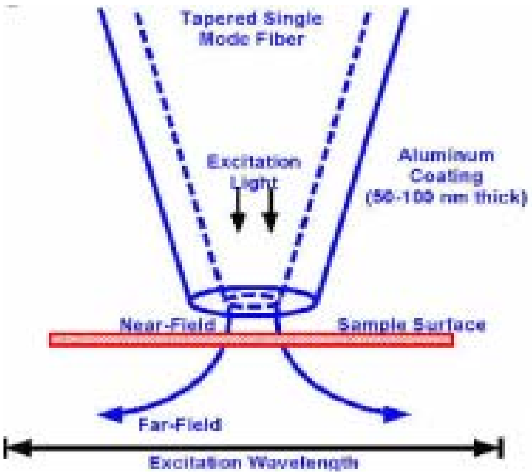

TABLE II. Summary of the different scanning probe microscopy techniques which can be used for 2D carrier profiling of semiconductor devices. The "mode" reflects the scanning mode which is being used to control the movement of the probe (NC=noncontact; C=contact).

Technique	Mode	Probe	Measured quantity
Scanning tunneling microscopy/ spectroscopy (STM/STS)	STM	Metallic needle	No. doping atoms $I-V$ spectra
Selective etching+atomic force microscopy	NC-AFM	Ultrasharp Si	Topography after chemical etch
Scanning capacitance microscopy/ spectroscopy (SCM/STS)	C-AFM	Metal-coated Si or metallic	Depletion capacitance $C-V$ spectra
Scanning spreading resistance microscopy (SSRM)	C-AFM	Diamond-coated Si or diamond	Electrical resistance $I-V$ spectra
Kelvin probe force microscopy (KPM)	NC-AFM	Metal-coated Si or metallic	Electrostatic potential (electric field)
Scanning surface harmonic microscopy (SSHM)	STM	Metallic needle with microwave cavity	Depletion capacitance

TABLE III. Intercomparison of two-dimensional doping (D) and carrier (C) profiling methods (NA=not available).

Method	Ref.	Resol. (nm)	Range (cm^{-3})	Conc. resol.	D/C	Quantifiable	Comments and problems
				SPM techniques			
SCM	(43–59)	10	1e15–1e20	Power	C	Limited	Uncertainties at junctions, poor quantification procedure
SSHM	(60–62)	5	NA	Power	C	No	No quantification procedure
STM-atom counting	(20–23)	Atomic	1e18–1e20	Linear	D	Yes	Only on GaAs, not on Si
STM-STS/ CITS	(24–26) (31,32)	10	NA	Log.	C	Limited	Only junction delineation and type (n or p) identification
STM-STP	(27–30)	10	NA	Limited	C	Limited	Only junction delineation
KPM	(66,67)	100	1e15–1e20	Limited	C	Limited	Poor quantification procedure, stray-fields limit the resolution
SSRM	(68–73)	20	1e15–1e20	Linear	C	Yes	Availability diamond probes
Chemical etch +AFM/STM	(37–39)	10–20	1e17–1e20	Limited	C	Limited	Difficult to quantify, poor reproducibility

P.D. Wolf et al., J. Vac. Sci. Technol. B **18**, 361 (2000).

Scanning Probe Microscopy (SPM)

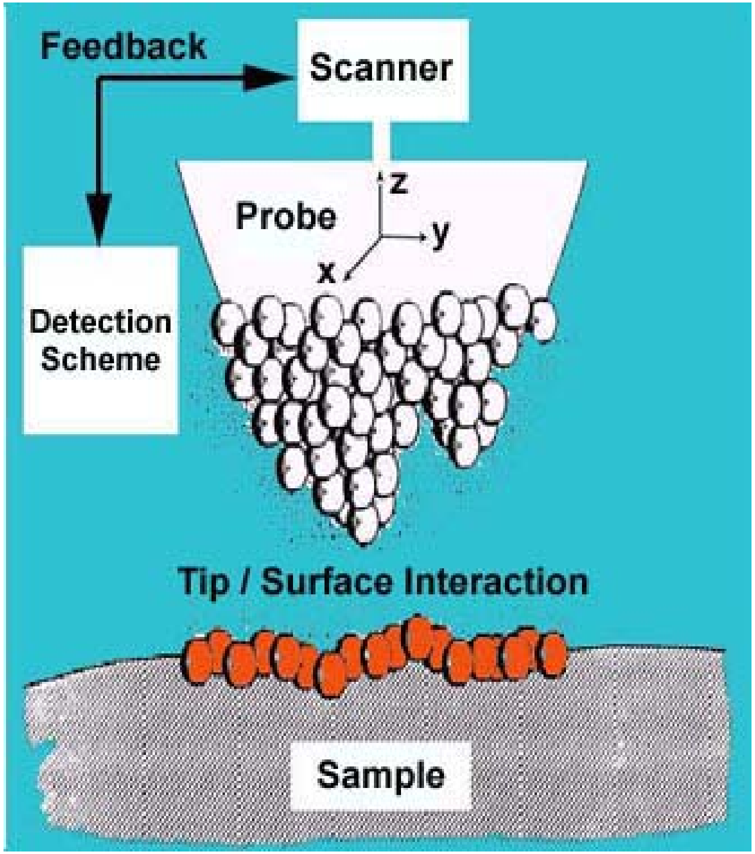

Scanning Tunneling Microscopy (STM)

--- G. Binnig, H. Rohrer et al, (1982)

Near-Field Scanning Optical Microscopy (NSOM)

--- D. W. Pohl (1982)

Atomic Force Microscopy (AFM)

--- G. Binnig, C. F. Quate, C. Gerber (1986)

Scanning Thermal Microscopy (SThM)

--- C. C. Williams, H. Wickramasinghe (1986))

Magnetic Force Microscopy (MFM)

--- Y. Martin, H. K. Wickramasinghe (1987)

Friction Force Microscopy (FFM or LFM)

--- C. M. Mate et al (1987)

Electrostatic Force Microscopy (EFM)

--- Y. Martin, D. W. Abraham et al (1988)

Scanning Capacitance Microscopy (SCM)

--- C. C. Williams, J. Slinkman et al (1989)

Force Modulation Microscopy (FMM)

--- P. Maivald et al (1991)

1. **All SPMs are based on the ability to position various types of probes in very close proximity with extremely high precision to the sample under investigation.**
2. **These probes can detect electrical current, atomic and molecular forces, electrostatic forces, or other types of interactions with the sample.**
3. **By scanning the probe laterally over the sample surface and performing measurements at different locations, detailed maps of surface topography, electronic properties, magnetic or electrostatic forces, optical characteristics, thermal properties, or other properties can be obtained.**
4. **The spatial resolution is limited by the sharpness of the probe tip, the accuracy with which the probe can be positioned, the condition of the surface under study, and the nature of the force being detected.**